# Power Control in Wireless Cellular Networks

# Power Control in Wireless Cellular Networks

**Mung Chiang**

*Electrical Engineering Department, Princeton University*

**Prashanth Hande**

*Electrical Engineering Department, Princeton University*

**Tian Lan**

*Electrical Engineering Department, Princeton University*

**Chee Wei Tan**

*Electrical Engineering Department, Princeton University*

Boston – Delft

**Foundations and Trends® in Networking sample**

*Published, sold and distributed by:*
now Publishers Inc.
PO Box 1024
Hanover, MA 02339
USA
Tel. +1-781-985-4510
www.nowpublishers.com
sales@nowpublishers.com

*Outside North America:*
now Publishers Inc.
PO Box 179
2600 AD Delft
The Netherlands
Tel. +31-6-51115274

A Cataloging-in-Publication record is available from the Library of Congress

The preferred citation for this publication is , Power Control in Wireless Cellular Networks, Foundation and Trends® in sample, vol x, no y, pp 1–156, 2008

*Printed on acid-free paper*

ISBN: 1-933019-09-3

**Foundations and Trends® in Networking sample**
Volume x Issue y, 2008

# Editorial Scope

**Foundations and Trends® in Networking sample** will publish survey and tutorial articles in the following topics:

- Protocols and Cross-Layer Design


### Information for Librarians

Foundations and Trends® in Networking, 2008, Volume 2, 4 issues. ISSN paper version 1931-7883. ISSN online version 1931-7891. Also available as a combined paper and online subscription.

Foundations and Trends® in Networking
sample
Vol. x, No y (2008) 1–156


# Power Control in Wireless Cellular Networks

Mung Chiang[1], Prashanth Hande[2], Tian Lan[3] and Chee Wei Tan[4]

1
2
3
4

## Abstract

Transmit power in wireless cellular networks is a key degree of freedom in the management of interference, energy, and connectivity. Power control in both uplink and downlink of a cellular network has been extensively studied, especially over the last 15 years, and some of the results have enabled the continuous evolution and significant impact of the digital cellular technology.

This monograph provides a comprehensive survey of the models, algorithms, analysis, and methodologies in this vast and growing literature. It starts with a taxonomy of the wide range of power control problem formulations, and progresses from the basic formulation to more sophisticated ones. When transmit power is the only set of optimization variables, algorithms for fixed SIR are presented first, before turning to their robust versions and joint SIR and power optimization. This is followed by opportunistic and non-cooperative power control. Then joint control of power together with beamforming pattern, base station assignment, spectrum allocation, and transmit schedule is surveyed one by one.

Throughout the monograph, we highlight the use of mathematical language and tools in the study of power control, including optimization theory, control theory, game theory, and linear algebra. Practical implementations of some of the algorithms in operational networks are discussed in the concluding chapter. As illustrated by the open problems presented at the end of most chapters, in the area of power control in cellular networks, there are still many under-explored directions and unresolved issues that remain theoretically challenging and practically important.

# Contents

# Contents

# 1

# Introduction

## 1.1 Overview

Transmission powers represent a key degree of freedom in the design of wireless networks. In both cellular and ad hoc networks, power control helps with several functionalities:

- *Interference management*: Due to the broadcast nature of wireless communication, signals interfere with each other. This problem is particularly acute in interference-limited systems, such as CDMA systems where perfect orthogonality among users are difficult to maintain. Power control helps ensure efficient spectral reuse and desirable user experience.
- *Energy management*: Due to limited battery power in mobile stations, handheld devices, or any "nodes" operating on small energy budget, energy conservation is important for the lifetime of the nodes and even the network. Power control helps minimize a key component of the overall energy expenditure.
- *Connectivity management*: Due to uncertainty and time-variation of wireless channels, even when there is neither

signal interference nor energy limitation, the receiver needs to be able to maintain a minimum level of received signal so that it can stay connected with the transmitter and estimate the channel state. Power control helps maintain logical connectivity for a given signal processing scheme.

To define a scope that allows an in-depth treatment within 150 pages, we will focus on power control in cellular networks in this monograph, emphasizing primarily its use in interference management while occasionally touching upon energy and connectivity management. Most of the treatment is devoted to uplink transmission from mobile station (MS) to base station (BS), although extensions to downlink transmission from a BS to MSs are sometimes discussed as well. In many formulations uplink problems are more difficult to solve, although there are exceptions like joint power control and beamforming, and in other formulations uplink and downlink problems present interesting duality relationships. Uplink power control is also often more important in systems engineering of cellular networks [1].

Within the functionality of interference management, there are several types of problem statements, including optimizing Quality of Service (QoS) metrics such as utility functions based on throughput and delay, achieving network capacity in the information-theoretic sense with technology-agnostic converse theorems, or maintaining network stability in queueing-theoretic sense when there are dynamic arrival and departure of users. This monograph focuses on the first type of problems, which is already rich enough that a detailed taxonomy of problem formulations is warranted and will be provided later in this section.

Given the specialization stated above and the range of power control problems in wireline systems like DSL, it is clear that this monograph only covers part of the broad set of problems in interference man-

[1] First, BS power consumption is of less importance in comparison to MS power consumption. Second, the downlink intra-cell interference is much smaller in comparison to uplink intra-cell interference, because maintaining orthogonality of resource allocation (e.g., code allocation in CDMA, tone allocation in OFDM, or frequency and time slot allocation in GSM) to MSs within a cell on the downlink is easily accomplished by the BS. Third, BS locations are fixed and inter-cell interference is less bursty.

agement. Yet within this scope, there is already a wide and growing range of results that are mathematically interesting and practically important. After surveying the key formulations, their relationships with each other, and the key properties of convexity and decomposability in this opening chapter, we organize the core materials in eight chapters. Chapters 2-4 present the basic formulations, starting with the simplest case of power control with fixed equilibrium SIR targets in Chapter 2, and progressing to the case of controlling transient behaviors and admission in Chapter 3, and that of jointly controlling power and SIR assignment in Chapter 4. Chapters 5 and 6 then present extensions to opportunistic and non-cooperative power control, respectively. Power control is often conducted jointly with other resource allocation when spatial, spectral, and temporal degrees of freedom are offered. In Chapters 7-9, we discuss joint power control and beamforming, base station assignment, frequency allocation, and scheduling, for both fixed SIR and variable SIR cases. Each of Chapters 2-9 starts with an overall introduction and concludes with a discussion of open problems. The mathematical techniques of optimization theory, control theory, game theory, and linear algebra will also be highlighted across these eight chapters. Practical impacts of the theory of power control in the wireless industry have been substantial over the years, and some of these engineering implications in operational networks are summarized in Chapter 10.

Power control in wireless networks has been systematically studied since the 1970s. Over the last 15 years, thanks to the tremendous growth of cellular networks and its transformative impacts on society, extensive research on cellular network power control has produced a wide and deep set of results in terms of modeling, analysis, and design. We have tried to include as many contributions in the bibliography as possible, to survey the key results and methodologies in a balanced manner, and to strike a tradeoff between a detailed treatment of each problem and a comprehensive coverage of all major issues. While these lofty goals may not have been attained to perfection, we hope this monograph will serve both as an an imperfect summary of the state-of-the-art and a sketchy illustration of the exciting open problems in the area of power control in cellular networks.

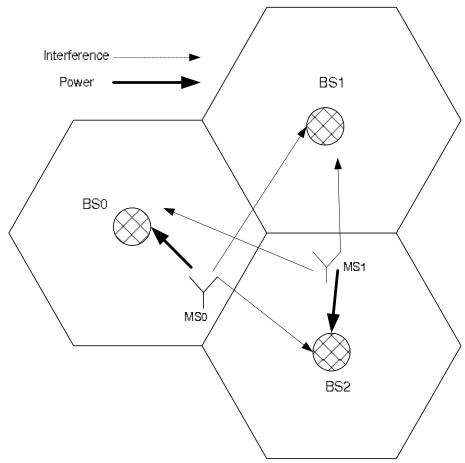


Fig. 1.1 An example of a multi-cellular network and uplink transmission.

## 1.2 Notation

The following notation are used throughout this monograph. Vectors are denoted in bold small letter, e.g., $\mathbf{z}$, with their $i$th component denoted by $z_i$. Matrices are denoted by bold capitalized letters, e.g., $\mathbf{Z}$, with $Z_{ij}$ denoting the $\{i, j\}$th component. Vector division $\mathbf{x}/\mathbf{y}$ and multiplication $\mathbf{xy}$ are considered component-wise, and vector inequalities denoted by $\succeq$ and $\preceq$ are component-wise inequalities. We use $\mathbf{D}(\mathbf{x})$ to denote a diagonal matrix whose diagonal elements are the corresponding components from vector $\mathbf{x}$. A summary of key notation is provided in tables at the end of this chapter.

## 1.3 Taxonomy of Problem Formulations

### 1.3.1 Basic system model

Consider a general multi-cell network where $N$ MSs establish links to $K$ BSs, as illustrated in Fig 1.1. We assume that each MS is served by one of the $K$ BSs, thereby establishing $N$ logical links. Let $\sigma_i$ denote the receiving BS for link $i$.

Let $C_i$ denote the set of links whose transmitted power appear as interference to link $i$. This definition allows us to consider both orthogonal and non-orthogonal uplinks. In a non-orthogonal uplink, such as CDMA, transmitted power from all links appear as interference, so we set $C_i = \{j \mid j \neq i\}$. For an orthogonal uplink, such as OFDM, links terminating on the same BS are orthogonal and do not contribute interference to one another. In this case, we set $C_i = \{j \mid \sigma_j \neq \sigma_i\}$.

Let $h_{kj}$ denote the amplitude gain from MS $j$ to BS $k$. Define the $N \times N$ power-gain matrix $\mathbf{G}$ by

$$G_{ij} = \|h_{\sigma_i j}\|^2, \tag{1.1}$$

which represents the power gain from MS on link $j$ to the receiving BS on link $i$. Correspondingly define a normalized gain matrix $\mathbf{F}$ where

$$F_{ij} = \begin{cases} G_{ij}/G_{ii} & \text{if } j \in C_i, \\ 0 & \text{if } j \notin C_i. \end{cases} \tag{1.2}$$

Let $\mathbf{D_h} = \mathrm{diag}(G_{11}, \ldots, G_{NN})$ be the diagonal matrix representing direct link channel gains, which depend on $\mathbf{h}$.

Let $p_j$ be the transmit signal power on link $j$ at its serving BS $\sigma_j$. Since $h_{\sigma_j j}$ is the path gain from MS on link $j$ to its serving BS, the receiver on link $j$ receives the signal at the power of $p_j \|h_{\sigma_j j}\|^2 = G_{jj} p_j$. If $j \in C_i$, this transmission will appear as interference to link $i$ with a power of $\|h_{\sigma_i j}\|^2 p_j = G_{ij} p_j$. The total interference and noise at the BS serving MS $i$ is given by

$$q_i = \sum_{j \in C_i} G_{ij} p_j + n_i = \sum_{j=1}^{M} F_{ij} G_{jj} p_j + n_i, \tag{1.3}$$

where $n_i \geq 0$ is the power of noise other than interference from other links. In matrix notation, (1.3) can be written as

$$\mathbf{q} = \mathbf{F D_h p} + \mathbf{n}. \tag{1.4}$$

Let $\gamma_i$ be the SIR achieved by link $i$. With the above notation, $\gamma_i = G_{ii} p_i / q_i$, or equivalently,

$$\mathbf{D_h p} = \mathbf{D}(\boldsymbol{\gamma}) \mathbf{q}, \tag{1.5}$$

where $\mathbf{D}(\boldsymbol{\gamma}) = \text{diag}(\gamma_1, \ldots, \gamma_M)$ [2]. Combining (1.4) and (1.5), we get the following basic equations relating the key quantities:

$$\mathbf{q} = \mathbf{F}\mathbf{D}(\boldsymbol{\gamma})\mathbf{q} + \mathbf{n}, \tag{1.6}$$

and

$$\mathbf{D_h}\mathbf{p} = \mathbf{D}(\boldsymbol{\gamma})\mathbf{F}\mathbf{D_h}\mathbf{p} + \mathbf{D}(\boldsymbol{\gamma})\mathbf{n}. \tag{1.7}$$

An important factor that determines the total uplink capacity in commercial networks today is the interference limit $\mathbf{q}^m$, often stated in the form $\mathbf{q}^m = \kappa\mathbf{n}$ for some constant $\kappa \geq 1$. With this definition, the interference, $q_i$, at each BS $i$, is not allowed to be larger than a factor $\kappa$ greater than the thermal noise $n_i$. The factor, $\kappa$, is called the Interference over Thermal (IOT), and typically quoted in dB,

$$\text{IOT} = 10\log_{10}(\kappa).$$

An related measure is the Raise over Thermal (ROT), the ratio of the interference and the signal power to the thermal noise. The IOT limits bound the interference to the cell and limits the power required for new MSs to access the network. Typical IOT values in commercial networks range from 3 to 10 dB.

### 1.3.2 Optimization Variables

Whether a power control problem is formulated as cooperative or non-cooperative, over a period of time or for a target equilibrium, it often involves an optimization formulation. An optimization can be described by four tuples: optimization variables, objective function, constraint set, and constant parameters.

Obviously transmit power vector $\mathbf{p}$ is an optimization variable in all formulations in this monograph. In Chapters 7-9, beamforming pattern, BS assignment, bandwidth allocation, and time schedules also become variables. In addition to these primary variables, there are also secondary variables that are functions of them. An important example is that, in Chapter 4, SIR vector $\boldsymbol{\gamma}$ also becomes a variable.

[2] The difference between the $\mathbf{D}(\boldsymbol{\gamma})$ and $\mathbf{D_h}$ notation is that the diagonal entries of $\mathbf{D}(\boldsymbol{\gamma})$ is exactly $\boldsymbol{\gamma}$ while those of $\mathbf{D_h}$ are functions of $\mathbf{h}$.

### 1.3.3 Objectives

There are two types of terms in the objective function: QoS-based utility and resource cost. Cost function for resource usage is relatively simple. It is often an increasing, convex function $V$ of the underlying resource, e.g., linear function of transmit power.

Utility functions require more discussion. The most general utility function assumes the form of $U(\boldsymbol{\beta})$ where $\boldsymbol{\beta}$ is a vector of metrics. Often it is assumed to be additive across MSs indexed by $i$: $U(\boldsymbol{\beta}) = \sum_i U_i(\boldsymbol{\beta})$, and locally dependent: $U(\boldsymbol{\beta}) = \sum_i U_i(\beta_i)$.

Metric $\beta_i$ may be the achieved throughput or goodput (and $U$ would be an increasing function), or delay, jittering, or distortion (and $U$ would be a decreasing function). These metrics are in turn functions of transmit power and other optimization variables in a given power control problem formulation.

For example, one QoS metric of interest is throughput, which is a function of SIR, which is in turn a function of transmit powers. There are several expressions of this metric. One is in terms of the capacity formula:

$$\beta_i(\gamma_i) = d \log(1 + c\gamma_i) \tag{1.8}$$

where $c$ and $d$ are constants that depend on modulation scheme, symbol period, and target Bit Error Rate (BER). In high-SIR regime, the above expression can be approximated by log function: $\beta_i(\gamma_i) = d \log c\gamma_i$. In low-SIR regime, it can be approximated by linear function: $\beta_i(\gamma_i) = dc\gamma_i$. It turns out both approximations help with formulating a convex optimization problem as discussed later. When other degrees of freedom such as schedules and beamforming patterns are involved, the expression becomes more complicated. Another expression for throughput is through the packet success rate function $f$ that maps SIR to the probability of successfully decoding a packet:

$$\beta_i(\gamma_i) = R_i f(\gamma_i) \tag{1.9}$$

where $R_i$ is the transmission rate.

There are also other QoS metrics such as delay that depend on SIR, and they will be introduced as the chapters progress.

Back to the utility function $U_i$ itself, it is often modeled as a monotonic, smooth, and concave function, but in more general form as required by different applications, it may not be smooth or concave. It can capture any of the following: happiness of users, elasticity of traffic, efficiency of resource allocation, and even the notion of fairness. Consider is a family of utility functions parameterized by $\alpha \geq 0$ [121]:

$$U_i(\beta_i) = \begin{cases} \log(\beta_i) & \text{if } \alpha = 1, \\ (1-\alpha)^{-1}\beta_i^{1-\alpha} & \text{if } \alpha \neq 1. \end{cases} \tag{1.10}$$

Maximizing such an "$\alpha$-fair utility function" leads to an optimizer that satisfies the definition of $\alpha$-fairness in economics literature. For example, proportional fairness is attained for $\alpha = 1$ and maxmin fairness for $\alpha \to \infty$. It is also often believed that larger $\alpha$ means more fairness.

A utility function that will help provide convexity of problem formulation while approximating linear utility function is the following pseudo-linear utility function:

$$U_i(\beta_i) = \log(\exp(\beta_i/c) - 1) \tag{1.11}$$

where $c > 0$ is a constant. This utility function is fairer than the linear utility function but approximates the linear utility at high QoS values. In particular, we have

$$\begin{aligned} \log(\exp(\beta_i/c) - 1) &\to \beta_i/c \quad \text{as} \quad \beta_i \to \infty, \\ \log(\exp(\beta_i/c) - 1) &\to -\infty \quad \text{as} \quad \beta_i \to 0. \end{aligned}$$

Sometimes, QoS-based utility and resource cost are combined into a single objective function for each user, either additively as in utility minus power, or multiplicatively as in throughput over power.

### 1.3.4 Constraints

There are three major types of constraints in power control problems. First is the set of constraints reflecting technological and regulatory limitations, e.g., total transmit power, maximum transmit power for each user, and IOT or ROT. These are usually simple constraints mathematically.

Second are constraints based on inelastic, individual users' requirements, e.g., two MSs' received SIR at a BS need to be the same, or one

MS's rate cannot be smaller than a threshold. It is not always possible to meet these constraints simultaneously. In these cases, the power control problem is infeasible.

The third type of constraints, called feasibility constraints, is most complicated. In information-theoretic sense, it would be the capacity region of an interference channel, which remains unknown. In queueing-theoretic sense, it would be the stochastic stability region. In this monograph, we focus instead on constraints that are defined with respect to QoS feasibility region, which is closely related to SIR feasibility region.

An SIR vector $\boldsymbol{\gamma} \succeq 0$ is called feasible if there exists an interference vector, $\mathbf{q} \succeq 0$, and power vector $\mathbf{p} \succeq 0$, satisfying (1.6) and (1.7), respectively. It is reasonable to assume that the network of BSs and MSs represented by the channel matrix $\mathbf{F}$ in Section 1.3.1 is connected, implying that $\mathbf{F}$ is a primitive matrix. Let $\rho(\cdot)$ denote the spectral radius function [3] of such a positive, primitive matrix. The following lemma from [198] is one of the fundamental results that characterizes SIR feasibility based on spectral radius of system matrices $\mathbf{F}$ and $\mathbf{D}(\boldsymbol{\gamma})$:

---

**Lemma 1.1.** An SIR vector $\boldsymbol{\gamma} \succeq 0$ is feasible if and only if $\rho(\mathbf{FD}(\boldsymbol{\gamma})) < 1$, when $\mathbf{n} \neq 0$, and $\rho(\mathbf{FD}(\boldsymbol{\gamma})) = 1$, when $\mathbf{n} = 0$.

---

Further discussions on SIR and QoS feasibility regions will be provided in Chapters 2 and 4.

### 1.3.5 Problem Formulations

We are ready to provide a quick preview of some representative problem formulations in the rest of the monograph. Given the vast landscape of power control problems covered, a "problem tree" in Figure 1.2 serves as a high-level guide to the relationships among these problems. Meanings of each level of branching off are as follows:

- Level 1: Optimization vs. game theory approach.
- Level 2: Deterministic optimization within each time slot vs. opportunistic approach.

[3] Spectral radius is the maximum of the absolute value of the eigenvalues of a matrix.

- Level 3: Variable SIR vs. fixed SIR approach.
- Level 4 and below: Joint power control and a subset of the following: beamforming, BS assignment, bandwidth allocation, and scheduling.

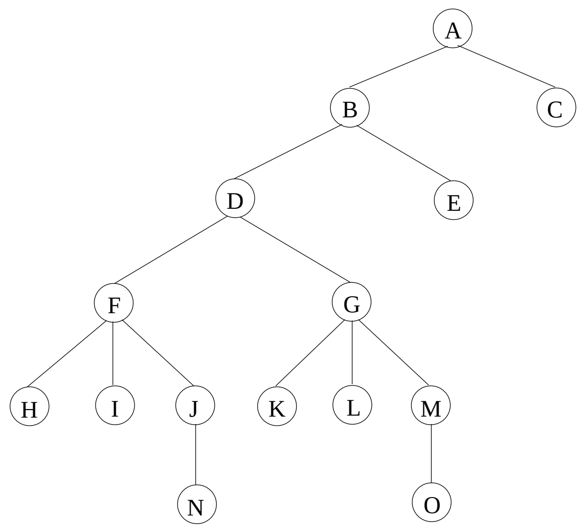


Fig. 1.2 A tree of representative problem formulations. Obviously, only part of the tree is shown here.

Next, we present one or two representative problems in each of the nodes in the problem tree. Symbols are defined in the Table of Notation. The meanings, justifications, solutions, and implications of these problems are not discussed here, since they will be extensively studied in the following 8 chapters. This preview puts the following chapters in the appropriate corners of the problem landscape.

Problem (O), distributed power control, discussed in Chapter 2:

$$\begin{array}{ll} \text{minimize} & \sum_i p_i \\ \text{subject to} & \mathsf{SIR}_i(\mathbf{p}) \geq \gamma_i, \ \forall i \\ \text{variables} & \mathbf{p} \end{array} \tag{1.12}$$

Problem (M), robust distributed power control, discussed in Chapter 3:

$$\begin{array}{ll} \text{minimize} & \sum_i p_i + \phi(\epsilon) \\ \text{subject to} & \mathsf{SIR}_i(\mathbf{p}) \geq \gamma_i(1+\epsilon),\ \forall i \\ \text{variables} & \mathbf{p},\ \epsilon \end{array} \tag{1.13}$$

Problem (N), power control for optimal SIR assignment, discussed in Chapter 4:

$$\begin{array}{ll} \text{maximize} & \sum_i U_i(\gamma_i) \\ \text{subject to} & \mathbf{p}(\boldsymbol{\gamma}) \preceq \mathbf{p}^m \\ \text{variables} & \boldsymbol{\gamma},\ \mathbf{p} \end{array} \tag{1.14}$$

Problem (E), opportunistic power control, discussed in Chapter 5:

$$\begin{array}{ll} \text{maximize} & \sum_s \pi_s \sum_i U_{s,i}(p_{s,i}) \\ \text{subject to} & \sum_s \pi_s g_{s,i}(\mathbf{p}_s) \geq c_i,\ \forall i \\ & \sum_i p_{s,i} \leq P_T,\ \ \forall s \\ \text{variables} & \mathbf{p}_s,\ \ \forall s \end{array} \tag{1.15}$$

Problem (C), Non-cooperative power control, discussed in Chapter 6:

$$\begin{array}{ll} \text{maximize} & U_i(\gamma_i) - V_i(p_i) \\ \text{subject to} & \mathsf{SIR}_i(p_i, \sigma_i, \mathbf{p}_{-i}) \geq \gamma_i,\ \forall i \\ & \mathbf{p} \preceq \mathbf{p}^m \\ & \sigma_i \in \mathcal{S}_i,\ \forall\ i \\ \text{variables} & \mathbf{p},\ \boldsymbol{\gamma},\ \boldsymbol{\sigma} \end{array} \tag{1.16}$$

Problem (K), Joint PC and beamforming power minimization, discussed in Chapter 7:

$$\begin{array}{ll} \text{minimize} & \sum_i p_i \\ \text{subject to} & \mathsf{SIR}_i(\mathbf{W}, \mathbf{p}) \geq \gamma_i,\ \forall i \\ \text{variables} & \mathbf{p},\ \mathbf{W} \end{array} \tag{1.17}$$

Problem (J), Joint PC and beamforming for utility maximization, discussed in Chapter 7:

$$\begin{array}{ll} \text{maximize} & \sum_i U_i(\gamma_i) \\ \text{subject to} & \mathsf{SIR}_i(\mathbf{W}, \mathbf{p}) \geq \gamma_i,\ \forall i \\ & \mathbf{p} \preceq \mathbf{p}^m \\ \text{variables} & \mathbf{p},\ \boldsymbol{\gamma},\ \mathbf{W} \end{array} \tag{1.18}$$

Problem (L), Joint PC and BS assignment, discussed in Chapter 8:

$$\begin{array}{ll} \text{minimize} & \sum_i p_i \\ \text{subject to} & \mathsf{SIR}_i(\mathbf{p}, \boldsymbol{\sigma}) \geq \gamma_i, \ \forall i \\ & \sigma_i \in \mathcal{S}_i, \ \forall i \\ \text{variables} & \mathbf{p}, \ \boldsymbol{\sigma} \end{array} \tag{1.19}$$

Problem (H), Joint PC and scheduling in frequency domain, discussed in Chapter 9:

$$\begin{array}{ll} \text{maximize} & \sum_i U_i(r_i) \\ \text{subject to} & r_i = \sum_{l=1}^{L} b_l \log(1 + c\gamma_i^l), \ \forall i \\ & \boldsymbol{\gamma}^l \in \boldsymbol{\Gamma}^l, \ \forall l \\ & \sum_l p_i^l \leq p_i^m, \ \forall i \\ \text{variables} & \mathbf{p}^l, \ \boldsymbol{\gamma}^l, \ \forall l \end{array} \tag{1.20}$$

Problem (I), Joint PC and scheduling in time domain, discussed in Chapter 9:

$$\begin{array}{ll} \text{maximize} & \sum_i U_i(r_i) \\ \text{subject to} & \mathbf{r} \in \mathcal{X} = Conv(\mathcal{R}(\Gamma)) \\ & \boldsymbol{\gamma} \in \Gamma \\ \text{variables} & \mathbf{r}, \ \boldsymbol{\gamma} \end{array} \tag{1.21}$$

Finally, the above list of representative formulations are compared in Table 1.4. The columns represent the fields describing the problem, and each row corresponds to one node in the tree of problems.

Table 1.1 Table of representative problem formulations

| # | Chapters | Objectives | | | Constraints | | | | | Variables | | | | | | | |
|---|---|---|---|---|---|---|---|---|---|---|---|---|---|---|---|---|---|
| | | $\sum_i U_i(\gamma_i)$ | $-\sum_i V_i(p_i)$ | $\mathbb{E}\left[\sum_i U_i(\gamma_i)\right]$ | SIR | Power | $\mathbb{E}$[Power] | Band | Time | $r_i$ | $\gamma_i$ | $p_i$ | $\sigma_i$ | $\mathbf{w}_i$ | $\epsilon$ | $w_i$ | $t$ |
| C | 6 | ✓ | ✓ | | | ✓ | | | | ✓ | ✓ | ✓ | ✓ | | | | |
| E | 5 | | | ✓ | | ✓ | ✓ | | | ✓ | ✓ | ✓ | | | | | |
| F | 4,7,9 | ✓ | | ✓ | | ✓ | ✓ | ✓ | ✓ | ✓ | ✓ | ✓ | | ✓ | | ✓ | ✓ |
| G | 2,3,7,9 | | ✓ | | ✓ | | | | | | | ✓ | ✓ | ✓ | ✓ | | |
| H | 9 | | | ✓ | | | ✓ | ✓ | | ✓ | ✓ | ✓ | | | | ✓ | |
| I | 9 | | | ✓ | | | ✓ | | ✓ | ✓ | ✓ | ✓ | | | | | ✓ |
| J | 7 | ✓ | | | | ✓ | | | | | ✓ | ✓ | | ✓ | | | |
| N | 4 | ✓ | | | | ✓ | | | | | ✓ | ✓ | | | | | |
| K | 7 | | ✓ | | ✓ | | | | | | | ✓ | | ✓ | | | |
| L | 8 | | ✓ | | ✓ | | | | | | | ✓ | ✓ | | | | |
| M | 3 | | ✓ | | ✓ | | | | | | | ✓ | | | ✓ | | |
| O | 2 | | ✓ | | ✓ | | | | | | ✓ | | | | | | |

## 1.4 Convexity and Decomposability Structures

### 1.4.1 Convexity

Convexity is long recognized as the watershed between easy and hard optimization problems. Convex optimization refers to minimization of a convex objective function over a convex constraint set. For convex optimization, a local optimum is also a global optimum (and unique if the objective function is strictly convex), duality gap is zero under mild conditions, and a rich understanding of its theoretical and numerical properties is available. For example, solving a convex optimization is highly efficient in theory and in practice, as long as the constraint set is represented efficiently, e.g., by a set of upper bound inequality constraints on other convex functions. Zero duality gap further enables distributed solutions through dual decomposition.

To check if a power control problem is convex optimization, we need to check both its objective and constraints. We want the objective function being maximized (e.g., utility function of rate) to be concave, and the one being minimized (e.g., cost function of power consumption) to be convex in the optimization variables. As will be discussed in many chapters later, concavity of utility function may not always hold. In non-cooperative power control formulations, quasi-concavity property of selfish utility functions plays a similarly important role for proving the existence of Nash equilibrium. We also want the constraint set to be convex, and in an efficient representation. Sometimes, a log change of variables turn an apparently non-convex problem into a convex one as in the Geometric Programming approach that has been shown to solve a wide range of constrained power control problems in high-SIR regime and a smaller set of problems in general-SIR regime [39]. More sufficient conditions for such convexity will be discussed in later chapters.

Sometimes discrete optimization variables need to be introduced, thus turning the problem into a nonconvex one. Three important examples include BS assignment among a finite set of BS choices, scheduling an MS to transmit or not, and a discrete set of available power levels.

### 1.4.2 Decomposability

While convexity is the key to global optimality and efficient computation, decomposability is the key to distributed solutions of an optimization problem. Unlike convex optimization, however, there is no definition of a decomposable problem. Rather decomposability comes in different degrees. If a problem can be decomposed into subproblems whose coordination does not involve communication overhead, its solution algorithm can be distributed without any message passing. In other instances, subproblems being solved by different network elements (e.g., MS and BS) need to be coordinated by passing messages among these elements. Counting such communication overhead is not always easy either, it often depends on how far and how often are messages passed and how many bits each message contains. In general, message passing across multiple BS is difficult, whereas between a BS and the MS in its cell is more feasible. Frequency and length of these control messages will be further discussed in Chapter 10.

There are various decomposition techniques from optimization theory, such as dual decomposition, primal decomposition, and penalty function method. However, one of the key constraints in power control problems, the SIR feasibility constraint, turns out to be coupled in a way that is not readily decomposed by these techniques. In Chapter 4, we will show how a reparametrization of this set reveals decomposability structures and leads to a distributed algorithm.

In contrast to the global optimization formulations, distributed algorithms are, by definition, already provided in non-cooperative game formulations of power control, as surveyed in Chapter 6. The challenge then becomes showing that such distributed interactions among selfish network elements will lead to a desirable equilibrium, e.g., they also maximize the global utility function for the whole network. The following two approaches are complementary: modeling as global optimization and searching for decomposition method, or modeling as selfish local optimization and characterizing loss of social welfare optimality.

Table 1.2 Summary of Key Notation

| **Symbol** | **Meaning** |
|---|---|
| $\mathcal{C}$,$\mathcal{D}$,$\mathcal{X}$,$\mathcal{Y}$, $\mathcal{K}$ | Sets in $\mathbb{R}^N$ ($\bar{\mathcal{X}}$ denotes the closure of $\mathcal{X}$) |
| $g(\cdot)$, $\phi(\cdot)$ | Scalar-valued function |
| $c$, $d$ | Scalar constants |
| $\mathcal{L}(\cdot)$ | Lagrangian |
| $\lambda_i$, $\mu_i$, $\nu_i$ | Lagrangian multipliers (or prices) |
| $\mathbf{x}, \mathbf{y}, \mathbf{z}$ | Auxiliary vectors |
| $\mathbf{x}^*$ | Optimizer or stationary point of a problem |
| $\mathbf{x}[t]$ | Variable at the $t$th iteration |
| $\delta$ | Step size for an iterative algorithm |
| $N$ (indexed by $i$ or $j$) | Number of links (MS) |
| $K$ (indexed by $k$) | Number of base-stations (BS) |
| $M$ (indexed by $m$) | Number of BS antennas |
| $C_i$ | A set of links interfering with link $i$ |
| $h_{ki}$ or $\mathbf{h}_{ki}$ | Complex channel amplitude from MS $i$ to BS $k$ |
| $\mathbf{G}$ | Absolute link gain matrix,<br>$G_{ij} = \|h_{\sigma_i j}\|^2$ or $G_{ij} = \left\|\mathbf{w}_i^T \mathbf{h}_{\sigma_i j}\right\|^2$ (for multi-antennas) |
| $\mathbf{F}$ | Normalized link gain matrix,<br>$F_{ij} = G_{ij}/G_{ii}$ if $j \in C_i$ and $F_{ij} = 0$ o.w. |
| $\mathbf{D_h}$ | Direct link gain matrix $\mathbf{D_h}$ =diag$\{G_{11}, \ldots, G_{NN}\}$ |
| $\mathbf{D}(\cdot)$ | Diagonal matrix operator |
| $n_i = \mathbb{E}[z_i]$ (in vector $\mathbf{n}$) | Thermal noise for link $i$ |
| $v_i = \gamma_i n_i / G_{ii}$ | Product of normalized noise with SIR target for link $i$ |
| $\eta_i = n_i/G_{ii}$ (in vector $\boldsymbol{\eta}$) | Normalized noise for link $i$ |
| $\kappa$ | Rise-Over-Thermal |
| $p_i$ (in vector $\mathbf{p}$) | Transmission power of MS $i$ |
| $p_i^m$ (in vector $\mathbf{p}^m$) | Transmit power constraint for link $i$ |

Table 1.3 Summary of Key Notation.

| | |
|---|---|
| $q_i$ (in vector $\mathbf{q}$) | Interference plus noise power for MS $i$ |
| $q_i^m$ (in vector $\mathbf{q}^m$) | Transmit interference constraint for link $i$ |
| $\gamma_i$ (in vector $\boldsymbol{\gamma}$) | SIR value of link $i$ |
| $\mathbf{\Gamma}$, $\mathbf{B}$ | A set of feasible SIRs |
| $\mathsf{SIR}_i(\mathbf{p})$ | SIR function for MS $i$ |
| $\rho(\cdot)$ | Spectral radius operator |
| $\mathbf{I}(\mathbf{p})$ | Standard interference function |
| $R_I$ | Feasibility index of a standard interference function |
| $\lambda_{\mathbf{F}}$ | Lyapunov exponent associated with matrix $\mathbf{F}$ |
| $\mathcal{V}$ | Lyapunov function of power control algorithm |
| $\epsilon$ | Robustness parameter |
| $\mathcal{K}_{1+\epsilon}$ | Invariant cone parameterized by robustness parameter |
| $\tilde{p}_i = \log p_i$ | Log transformation of power |
| $\xi$ | Energy consumption budget (percentage over total power) |
| $U_i(\cdot)$ (with parameter $\alpha$) | Utility function (for $\alpha$ fairness) |
| $s_i$ | Spillage factor |
| $\ell_i$ | Load factor |
| $\theta$ | Convex combination weight |
| $S$ (indexed by $s$) | Number of states |
| $\pi_s$ | Probability that the system is in state $s$ |
| $p_{s,i}$ | Transmit power of user $i$ in state $s$ |
| $G_{s,i}$ | Path gain from base station to user $i$ in state $s$ |
| $g_{s,i}$ | Performance measure of user $i$ in state $s$ |
| $a_{i,j}$ | Fixed weight on each $g_{s,i}^j(p_{s,j})$ to reflect priority |
| $\upsilon_i$ | minimum fraction of the total transmit power by user $i$ |
| $\tilde{\upsilon}_i$ | minimum fraction of the expected total system utility by user $i$ |

Table 1.4 Summary of Key Notation.

| | |
|---|---|
| $\varrho_i$ | Stochastic gradient of Lagrangian |
| $P_T$ | Total transmit power in downlink transmission |
| $\zeta_i$ | Signal-interference product of user $i$ |
| $\vartheta$ | Non-orthogonality factor in CDMA spreading code |
| $E_b/I_0$ | The bit energy to interference density ratio |
| $L$ (indexed by $l$) | Number of (orthogonal) carriers |
| $D_i$ | Multiplexing gain for MS $i$ in a CDMA network |
| $D_t$ and $D_f$ | Number of total information bits and bits in a packet |
| $\mathsf{BER}(\gamma_i)$ | Bit error rate function |
| $f(\cdot)$ | Packet success rate function |
| $\mathcal{A}_i$ | A set of feasible power allocation policies for MS $i$ |
| $\mathbf{w}_i$ (in matrix $\mathbf{W}$) | Uplink beamforming vector for MS $i$ |
| $\hat{\mathbf{w}}_i$ | Downlink beamforming vector for MS $i$ |
| $u_i$ | Information symbol of unit power for MS $i$ |
| $\mathbf{G}_{\text{ex}}$ | Extended coupling matrix for beamforming |
| $\mathbf{1}$ | A vector whose components are 1's |
| $\hat{p}_i$ | Downlink transmission power of MS $i$ |
| $\sigma_i$ | The BS that serves MS $i$ |
| $\mathcal{S}_i$ | A set of allowable BSs that MS $i$ can connect to |
| $b_i$, $B^m$ | Bandwidth for MS $i$ and total bandwidth allowed |
| $r_i(\gamma_i)$ | Rate function of link $i$ |
| $\mathcal{R}$ | Instantaneous rate region |
| $\mathcal{X}$ | The stable arrival rate region |
| Conv($\mathcal{R}$) | Convex hull of $\mathcal{R}$ |
| $T$ | Length of time resource |

# 2

# Power Control with Fixed SIR

## 2.1 Introduction

Much of the study on cellular network power control started in 1992-1993 with a series of results that solve the basic problem formulation, where transmit power is the only variable, constrained by fixed target SIR, and optimized to minimize the total power. In this chapter, we consider the system model in Chapter 1 and first review the Distributed Power Control (DPC) algorithm proposed by Foschini and Miljanic [57]. There are several nice interpretations that motivate this simple yet powerful algorithm from different angles. Then we review an elegant generalization of DPC to the framework of standard interference function and canonical power control algorithms. These generalizations reveal the connection between structures of the basic power control problem and properties of its solution algorithms. They also characterize the link between power control problems and Perron Frobenius theory of nonnegative matrix. Rate of convergence and robustness to stochastic dynamics are mentioned before we conclude this chapter that lays the foundation to the rest of the monograph.

## 2.2 Distributed Power Control

Consider the problem of varying transmit power to satisfy fixed target SIR constraints $\boldsymbol{\gamma}$ and minimize the total power [57, 17, 16]:

$$\begin{array}{ll} \text{minimize} & \sum_i p_i \\ \text{subject to} & \mathsf{SIR}_i(\mathbf{p}) \geq \gamma_i, \ \ \forall i, \\ \text{variables} & \mathbf{p}. \end{array} \tag{2.1}$$

In the above and all of the following optimization problems, we omit non-negativity constraints on variables.

Problem (2.1) can be rewritten as a linear program:

$$\begin{array}{rl} \text{minimize} & \mathbf{1}^T\mathbf{p} \\ \text{subject to} & (\mathbf{I} - \mathbf{D}(\boldsymbol{\gamma})\mathbf{F})\mathbf{p} \succeq \mathbf{v}, \end{array} \tag{2.2}$$

where $\mathbf{I}$ is the identity matrix, and

$$\mathbf{v} = \mathbf{D}(\boldsymbol{\gamma})\boldsymbol{\eta} = \left(\frac{\gamma_1 n_1}{G_{11}}, \frac{\gamma_2 n_2}{G_{22}}, \ldots, \frac{\gamma_N n_N}{G_{NN}}\right)^T.$$

To compute an optimal solution to (2.1), the following algorithm is proposed in [57]:

---

**Algorithm 2.1 (Distributed Power Control [57]).**

$$p_i[t+1] = \frac{\gamma_i}{\mathsf{SIR}_i[t]} p_i[t], \ \ \forall i \tag{2.3}$$

---

where $t = 1, 2, \ldots$, and $\mathsf{SIR}_i[t]$ is the received SIR at the $t$th iteration. In the above and all of the following iterative algorithms, we omit the iteration loop with $t = t + 1$.

The update in (2.3) is distributed as each user only needs to monitor its individual received SIR and can update by (2.3) independently and asynchronously [189]. Intuitively, each user $i$ increases its power when its $\mathsf{SIR}_i[t]$ is below $\gamma_i$ and decreases it otherwise. The optimal power allocation $\mathbf{p}^*$ in (2.1) is achieved in the limit as $t \to \infty$, and satisfies $(\mathbf{I} - \mathbf{D}(\boldsymbol{\gamma})\mathbf{F})\mathbf{p}^* = \mathbf{v}$, i.e., the constraints in (2.2) are tight at optimality.

The above DPC algorithm has been extensively studied, with results on existence of feasible solution and convergence to optimal solution characterized through several approaches.

First is a set of equivalent conditions for SIR feasibility:

---

**Theorem 2.1 (Existence of a feasible power vector).** The following statements are equivalent:

1) There exists a power vector $\mathbf{p} \succeq \mathbf{0}$ such that $(\mathbf{I} - \mathbf{D}(\boldsymbol{\gamma})\mathbf{F})\mathbf{p} \succeq \mathbf{0}$.

2) $\rho(\mathbf{D}(\boldsymbol{\gamma})\mathbf{F}) < 1$.

3) $(\mathbf{I} - \mathbf{D}(\boldsymbol{\gamma})\mathbf{F})^{-1} = \sum_{k=0}^{\infty} \mathbf{D}(\boldsymbol{\gamma})\mathbf{F}^k$ exists and is positive componentwise, with

$$\lim_{k\to\infty} (\mathbf{D}(\boldsymbol{\gamma})\mathbf{F})^k = 0. \tag{2.4}$$

---

Assuming the fixed SIR targets $\boldsymbol{\gamma}$ is feasible, the DPC algorithm converges to a power-minimum solution:

---

**Theorem 2.2 (Convergence and optimality of DPC algorithm).** If the constraints in (2.1) have a feasible solution, then

$$\mathbf{p}^* = (\mathbf{I} - \mathbf{D}(\boldsymbol{\gamma})\mathbf{F})^{-1}\mathbf{v} \tag{2.5}$$

is feasible and power-minimum, i.e., for any solution $\hat{\mathbf{p}}$ satisfying the constraints of (2.1),

$$\hat{\mathbf{p}} \succeq \mathbf{p}^*. \tag{2.6}$$

---

One way to view the DPC algorithm is through the power update to solve the matrix inversion $\mathbf{p} = (\mathbf{I} - \mathbf{D}(\boldsymbol{\gamma})\mathbf{F})^{-1}\mathbf{v}$. If condition 3 in Theorem 2.1 is satisfied, the expansion of this matrix inversion as a power series becomes

$$\mathbf{p}[t+1] = \mathbf{D}(\boldsymbol{\gamma})\mathbf{F}\mathbf{p}[t] + \mathbf{v}, \tag{2.7}$$

which in scalar form is indeed (2.3).

Other properties, such as rate of convergence, and interpretations, such as best response strategy of a game, of the DPC algorithm, will be discussed later in the monograph.

**Maximum power constraint.** If we assume a maximum power constraint $p_i^m$, a modified form of the DPC algorithm is given as follows [189]:

$$p_i[t+1] = \min\left\{\frac{\gamma_i}{\mathsf{SIR}_i[t]}p_i[t],\ p_i^m\right\}, \ \ \forall i. \tag{2.8}$$

However, a problem with using (2.8) is that a user may hit its maximum power ceiling at some iteration $\bar{t}$ with $\mathsf{SIR}_i[\bar{t}] < \gamma_i$, and this may result in $\mathsf{SIR}_i[t] < \gamma_i$ for $t \geq \bar{t}$, i.e., the SIR constraint is not satisfied even though the user transmits at the maximum power. In this case, it can be shown that the power of those users in the network that satisfy $\mathsf{SIR}_i[\bar{t}] \geq \gamma_i$ for some $t \geq \bar{t}$ will converge to a feasible solution, whereas the other users that cannot achieve the required SIR threshold will continue to transmit at maximum power.

**Discrete power levels.** In [184], the authors consider solving (2.1) over a discrete set of available power levels. Now (2.1) becomes an integer programming problem, which is in general hard to solve for global optimality. In [184], a Minimum Feasible Value Assignment (MFVA) iterative algorithm is developed to solve this integer programming problem. The MFVA algorithm can be made distributed and solved asynchronously. Furthermore, the MFVA algorithm finds the optimal solution in a finite number of iterations which is polynomial in the number of power levels and the number of users in the network [184]. This algorithm can be interpreted as a relaxed version of the framework proposed in [189], to be discussed in the following section.

## 2.3 Standard Interference Function

A general framework for uplink power control is proposed in [189] by identifying a broad class of iterative power control systems. The SIR of each user can be described by a vector inequality of interference constraints of the form

$$\mathbf{p} \succeq \mathbf{I}(\mathbf{p}). \tag{2.9}$$

Here, $\mathbf{I}(\mathbf{p}) = [I_1(\mathbf{p}), \ldots, I_n(\mathbf{p})]^T$ where $I_i(\mathbf{p})$ denotes the interference experienced by user $i$. A power vector $\mathbf{p} \succeq \mathbf{0}$ is feasible if $\mathbf{p}$ satisfies (2.9), and an interference function $\mathbf{I}(\mathbf{p})$ is feasible if (2.9) is satisfied.

For a system with interference constraint in (2.9), we examine the following iterative algorithm.

---

**Algorithm 2.2 (Standard Interference Function Algorithm [189]).**

$$\mathbf{p}[t+1] = \mathbf{I}(\mathbf{p}[t]). \tag{2.10}$$

Convergence for synchronous and totally asynchronous version of the iteration (2.10) can be proven when $\mathbf{I}(\mathbf{p})$ satisfy the following definition for power vectors $\mathbf{p}$ and $\mathbf{p}'$:

**Definition 2.1 ([189]).** $\mathbf{I}(\mathbf{p})$ is a standard interference function[1] if it satisfies: 1) If $\mathbf{p} > \mathbf{p}'$, then $\mathbf{I}(\mathbf{p}) > \mathbf{I}(\mathbf{p}')$ (monotonicity property). 2) If $c > 1$, then $c\mathbf{I}(\mathbf{p}) > \mathbf{I}(c\mathbf{p})$ (scalability property).

We also assume that for each $i$ and $j \neq i$, $I_j(\mathbf{p}) \to \infty$ as $p_i \to \infty$. Existence of fixed point of iteration 2.10 has been characterized by the following definition and theorems:

**Definition 2.2.** [69] The feasibility index $R_I$ of a standard interference function $\mathbf{I}(\mathbf{p})$ is

$$R_I = \max\{c \in \mathbb{R} \mid \ \mathbf{p} \succeq c\mathbf{I}(\mathbf{p}) \ \text{ for some feasible } \mathbf{p}\}$$

**Theorem 2.3.** [69] A standard interference function $\mathbf{I}(\mathbf{p})$ is feasible if and only if $R_I > 1$.

**Theorem 2.4.** [189] For iteration 2.10, if a fixed point exists, then the it is unique, and the power vector converges to the fixed point from any initial power vector.

It is readily verified that the power update algorithm in (2.7) is a standard interference function where

$$I_i(\mathbf{p}) = \frac{\gamma_i}{G_{ii}} \left( \sum_{j \neq i} G_{lj} p_j + n_i \right), \quad \forall i. \tag{2.11}$$

Hence, the DPC algorithm converges under both synchronous and totally asynchronous condition if there exists a feasible solution, and the feasibility index $R_I$, given by $1/\rho(\mathbf{D}(\boldsymbol{\gamma})\mathbf{F})$, is larger than 1 [69].

[1] The positivity of $\mathbf{I}(\mathbf{p})$, the other condition in [189], can be shown to be implied by monotonicity and scalability.

## 2.4 Canonical Power Control

A more general framework on convergence analysis is given in [103] that builds on the standard interference function in [189]. The authors define a broader class of synchronous and totally asynchronous power control algorithms known as the canonical algorithms.

Before stating the conditions that define the canonical algorithms, we introduce some more notation. Let $\mathcal{T}_i$, a subset of the set of positive real numbers, be the target region of user $i$. The target region is defined as $\mathcal{T} = \mathcal{T}_1 = \mathcal{T}_1 \times \mathcal{T}_2 \times \cdots \times \mathcal{T}_n$. Let $X, Y \subseteq \mathbb{R}^n$, $\bar{X}$ be the closure of $X$ and $\bar{Y}$ be the closure of $Y$, we say that $X$ is separated from $Y$ if $X \cap \bar{Y} = Y \cap \bar{X} = \emptyset$.

---

**Definition 2.3 ([103]).** A power update algorithm is called bounded if it satisfies the bounding condition; it is called reactive if it satisfies the reactive condition.

1) Bounding Condition: There exists a $\gamma$ such that

$$\min_i \{p_i[t], \gamma_i I_i(\mathbf{p}[t])\} \leq p_i[t+1] \leq \max_i \{p_i[t], \gamma_i I_i(\mathbf{p}[t])\} \tag{2.12}$$

for any MS $i$ and iteration $t$.

2) Reactive Condition: For any user $i$ and $X \subseteq \mathbb{R}$ where $X$ is separated from the target region $\mathcal{T}_i$, there exists $\epsilon > 0$ and an infinite subset of nonnegative integers $T^i$ such that

$$\left| \frac{p_i[t]}{p_i[t+1]} - 1 \right| > \epsilon \tag{2.13}$$

whenever $\mathsf{SIR}_i[t] \in X$ and $t \in T^i$.

---

The above conditions can be motivated as follows. First, $p_i[t]$ and $\gamma_i I_i[t+1]$ in the bounding condition forms a lower and an upper bound on the power level at the next update. Consider the case when power is not high enough, i.e., $p_i[t] \leq \gamma_i I_i[t+1]$. If $p_i[t+1]$ is set below $p_i[t]$, the SIR will move away from the SIR threshold. On the other hand, if $p_i[t+1]$ is set above $\gamma_i I_i[t]$, the resulting SIR will overshoot the target [103]. Second, under the reactive condition, the SIR's of the users are not allowed to stay outside the target region indefinitely. The powers keep changing when the target region is not reached. Intuitively, if these conditions are satisfied, the power of each user moves toward the SIR threshold, and it will not stop moving until the target is reached.

---

**Definition 2.4 ([103]).** A power control algorithm is called canonical if it satisfies the following conditions:

1) The interference measure is a standard interference function.
2) The target region $\mathcal{T}$ is closed.
3) The power control update algorithm is bounded and reactive.

---

**Theorem 2.5 (Canonical power control theorem [103]).** If the power control algorithm of user $i$ is canonical, then

$$\lim_{t\to\infty} \mathsf{SIR}_i[t] \in \mathcal{T}_i. \tag{2.14}$$

---

Theorem 2.5 guarantees that a canonical algorithm converges, and the resulting SIR falls within the target region. In [189], the author considers power control algorithm with a unique limit point, i.e., $\mathcal{T}$ consists of only a single point. In general, multiple limit points can exist. The limit point depends on the initial power vector, the power update schedule, and the actual power update algorithm.

Applying Theorem 2.5 to the DPC algorithm, it can be checked that [103]:

1) *Interference function:* The interference function given by (2.11) is standard.

2) *Target region:* The target region $\mathcal{T}_i$ is $[\gamma_i, \gamma_i]$, which is closed in the positive set of $\mathbb{R}$.

3) *Bounding condition:* (2.7) satisfies the bounding condition. *Reactive condition:* Let $A$ be a set in the positive set of $\mathbb{R}$ separated from $\mathcal{T}_i$. Then there exists $\epsilon > 0$ such that $[\gamma_i/(1+\epsilon), \gamma_i/(1-\epsilon)]$ is disjoint from $A$. For any $t \in \mathcal{T}_i$, if $\mathsf{SIR}_i \in A$, then $|p_i[t]/\gamma_i I_i[t] - 1|$. Hence, we have

$$\left|\frac{p_i[t]}{p_i[t+1]} - 1\right| > \epsilon. \tag{2.15}$$

Therefore, the DPC algorithm is canonical and its convergence is implied by Theorem 2.5. In addition, [103] also shows that a discretized DPC algorithm with limited feedback that adjusts the transmit power level by a fixed dB margin [164, 90] is also canonical.

## 2.5 Extensions

### 2.5.1 Rate of convergence

We now turn to the rate of convergence for the DPC algorithm. It was shown in [75] that the DPC algorithm converges to the fixed point at a geometric rate.

---

**Theorem 2.6 ([75]).** Suppose that $\rho(\mathbf{D}(\boldsymbol{\gamma})\mathbf{F}) < 1$ in the DPC algorithm. Starting from any initial power vector $\mathbf{p}[0]$, the sequence $\mathbf{p}[t]$ converges geometrically to the fixed point, such that $\|\mathbf{p}[t] - \mathbf{p}^*\| \leq a^t \|\mathbf{p}[0] - \mathbf{p}^*\|$ for some nonnegative constant $a < 1$.

---

There are various factors that affect how the sequence $\mathbf{p}[t]$ converges. One is the initial power vector, which can reduce the convergence time if it is sufficiently close to the fixed point. In addition, as the number of users in the network increases, i.e., the congestion in the network increases, the speed of convergence may become slower.

Figure 2.1 shows the evolution of the received SIR's for a particular user using DPC, in a cell for the case when there are three, five and ten users, with different initial points (either the maximum power of 1600mW or 0W). In this example, initializing from a maximum power has a smaller convergence time than initializing from zero power. As the number of users increases, the convergence time to the SIR threshold is longer. Power control algorithms that take into account congestion is briefly discussed below and in detail in Chapter 3.

### 2.5.2 Perron-Frobenius eigenvalue as a congestion measure

As shown in Theorem 2.1, $\rho(\mathbf{D}(\boldsymbol{\gamma})\mathbf{F})$ is an important parameter that determines the existence of the optimal power allocation. In addition, $\rho(\mathbf{D}(\boldsymbol{\gamma})\mathbf{F})$ has been proposed as a congestion measure in [67]. Here,

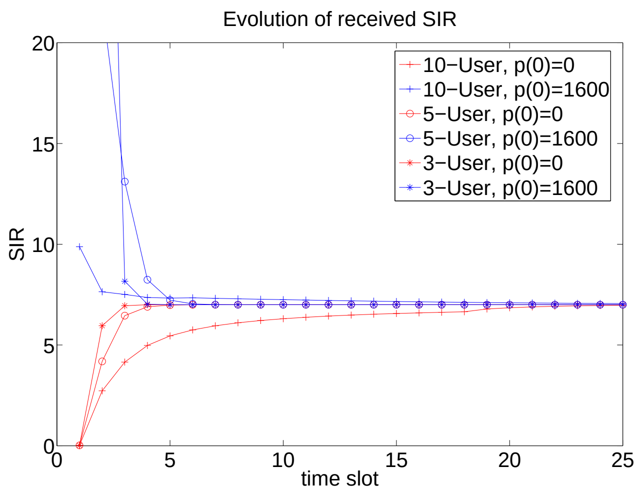


Fig. 2.1 A typical numerical example of using the DPC algorithm for a particular user with different initial points (either at the maximum power of 1600mW or the zero power) and different number of users in a cell. The SIR thresholds for all users are set as $\gamma_i = 7$ for all $i$. The received SIR for the user converges slower with an increasing number of users.

congestion refers to either an increase in the number of users in the cell (thereby increasing the dimension of $\mathbf{p}$ and $\mathbf{D}(\boldsymbol{\gamma})\mathbf{F}$), or an increase in the minimum SIR requirement of any user (thereby increasing some of the elements in $\mathbf{D}(\boldsymbol{\gamma})\mathbf{F}$). In the former case, $\rho(\mathbf{D}(\boldsymbol{\gamma})\mathbf{F})$ increases as shown in [67]. In the latter case, $\rho(\mathbf{D}(\boldsymbol{\gamma})\mathbf{F})$ increases since the spectral radius of an irreducible nonnegative matrix is an increasing function of any of its elements.

The following result characterizes $\rho(\mathbf{D}(\boldsymbol{\gamma})\mathbf{F})$ (and thus the feasible SIR thresholds in (2.1)) by using a classical result on non-negative matrices [59].

---

**Theorem 2.7 ([59]).** For any square nonnegative matrix $\mathbf{F}$, we have

$$\prod_i \gamma_i^{x_i y_i} \rho(\mathbf{F}) \leq \rho(\mathbf{D}(\boldsymbol{\gamma})\mathbf{F}) \leq \max_i \gamma_i \, \rho(\mathbf{F}), \tag{2.16}$$

where $\mathbf{x}$ and $\mathbf{y}$ are the left and right (non-negative) eigenvector of $\mathbf{F}$ corresponding to its spectral radius, respectively.

Equality holds for both the lefthand-side and the righthand-side bounds if and only if $\gamma_i$ is the same constant for all $i$.

---

From Theorem 2.7, it is easy to see that, in order for the DPC algorithm to converge i.e., $\rho(\mathbf{D}(\boldsymbol{\gamma})\mathbf{F}) < 1$, a sufficient condition can be given by $\max_i \gamma_i \; \rho(\mathbf{F}) < 1$. Similarly, a necessary condition can be given by $\prod_i \gamma_i^{x_i y_i} \rho(\mathbf{F}) < 1$, which implies that feasible SIR thresholds have to satisfy

$$\sum_i x_i y_i \log \gamma_i + \log \rho(\mathbf{F}) < 0. \tag{2.17}$$

It is easy to see that a simple choice of $\gamma_i < 1/\rho(\mathbf{F})$ for all $i$ satisfies (2.17).

The author in [56] shows that $\rho(\mathbf{D}(\boldsymbol{\gamma})\mathbf{F})$ can be suitably interpreted as the traffic load on the CDMA network when the congestion is high. Using (2.1), the authors in [168] propose per-link "interference price" for each SIR constraint in (2.1), and the aggregate sum of all the "interference prices" gives a congestion measure, playing a similar role as $\rho(\mathbf{D}(\boldsymbol{\gamma})\mathbf{F})$.

### 2.5.3 Stochastic power control

There are two types of stochastic dynamics often modeled in wireless cellular networks. One is channel variations and the other is user mobility. Robustness against these dynamics has been analyzed and algorithms leveraging them have been designed. Some of these results will be surveyed in various sections of the monograph, starting with this subsection.

The previous sections has focused on power control with fixed channels. The authors in [72, 73] show that the DPC algorithm resulting from such formulations may not accurately capture the dynamics of a time-varying channel. Suppose the channel gains $G_{ij}$ are allowed to vary with time. Let $\{G\} = \{\mathbf{G}(t) : t > 0\}$ be a stationary ergodic sequence of random channel gain matrices. Assume that the sequence $\{G\}$ takes values in a discrete or continuous set of square, nonnegative, and irreducible matrices. Next, we can rewrite (2.7) as

$$\mathbf{p}[t+1] = \mathbf{D}(\boldsymbol{\gamma})\mathbf{F}[t]\mathbf{p}[t] + \mathbf{v}[t]. \tag{2.18}$$

It is shown in [72, 73] that the power $\mathbf{p}[t]$ converges in distribution to a well defined random variable if and only if the Lyapunov exponent $\lambda_F$, defined as

$$\lambda_F = \lim_{t\to\infty} \frac{1}{t} \log ||\mathbf{D}(\boldsymbol{\gamma})\mathbf{F}[1]\mathbf{D}(\boldsymbol{\gamma})\mathbf{F}[2]\ldots\mathbf{D}(\boldsymbol{\gamma})\mathbf{F}[t]||\,|, \tag{2.19}$$

is strictly less than 0 for any norm.

---

**Theorem 2.8 ([72, 73]).** Using iteration (2.18), $\mathbf{p}[t]$ converges weakly to a limit random variable $\mathbf{p}(\infty)$ if $\lambda_F < 0$ and $\mathbb{E}[\log(1 + |||\mathbf{v}[t]|||)] < \infty$. Furthermore, we have

$$\lim_{t\to\infty} \mathbb{E}[\log(\mathsf{SIR}_i[t])] = \log\gamma_i, \quad \forall i. \tag{2.20}$$

Otherwise, $\mathbf{p}[t] \to \infty$ with probability one.

---

Note that in formulations with random channels, the minimum SIR requirements have changed; rather than being constrained by $\mathsf{SIR}_i = \gamma_i$, the stochastic version of the DPC algorithm is constrained by $\mathbb{E}[\log\mathsf{SIR}_i] = \log\gamma_i$. Using the Jensen's inequality, we have $\log\mathbb{E}[\mathsf{SIR}_i] \geq \mathbb{E}[\log\mathsf{SIR}_i]$. Consequently, this may cause overshoot in the minimum SIR requirement [72, 73].

The authors in [72, 73] propose a stochastic approximation based, on-line algorithm for controlling transmitter powers, using a fixed step size that provides weak convergence and faster response to time-varying channel conditions.

Under slow fading channel condition, the interference at a receiver is correlated from one time slot to the next. Based on the interference measurements in the previous time slots, one can apply appropriate methods to predict the interference to be perceived at the receiver. With the predicted interference and estimated channel gains between the transceivers, the transmit power can be adjusted in the next time slot. In [100], the author proposes a state space model and Kalman filter method for this purpose. The advantage of the Kalman filter method is that it is simple, due to its recursive structure, robust over a wide range of parameters, and provides an optimal estimate of the interference in the sense of minimum mean square error (MMSE). Other work that exploit the temporal correlation of interference in power control algorithms include [104, 85, 161, 174, 95, 35].

Aside from the stochastic nature of the channel gains, impairments such as noisy feedback can also result in stochastic uncertainties that lead to power variation. The authors in [156] proposed an adaptive power control algorithm for random channels that predicts channel and other stochastic behaviors based on the past observations and then use these predictions to update the transmit power. Similar to [100], an online implementation of the predictive algorithm in [156] is made possible with a robust Kalman filter used for interference estimation. Other work on stochastic power control include [172, 139, 199, 111, 155, 200, 142, 82, 34, 80, 79, 131, 126].

In Chapter 5, we consider more in details power control algorithms that take advantage of the varying channel condition opportunistically when allocating power to maximize given performance metric in the network.

In the next chapter, we will investigate power control algorithms that specifically take into account robustness against disturbances and provide protection against SIR outage in the next chapter.

## 2.6 Open Problems

The feasibility of (2.1) is determined by $\mathbf{D}(\boldsymbol{\gamma})\mathbf{F}$ (cf. Theorem 2.1). In [58], the authors propose heuristics for joint power control and channel assignment algorithm in order to ensure feasible power allocation in each channel. Optimal power control and channel assignment algorithms are especially important in cognitive radio networks where there are different classes of user priorities [157]. A joint, distributed optimal power control and channel assignment algorithm remains an open problem.

While the equilibrium properties of fixed SIR power control are well understood, both transience properties and extensions to variable SIR are more challenging. These two topics will be addressed in the next two chapters, respectively

# 3

# Transients, Robustness, and Admission

## 3.1 Introduction

While the equilibrium of the DPC algorithm in Chapter 2.2 is well-understood, what happens during the transience is less clear and more challenging to characterize. In particular, the SIR of an active link can dip below the SIR targets when there is a slight perturbation such as the entry of a new user. Consider the following example of a cell originally with two active users. A new user enters using the DPC algorithm, and causes an SIR outage that deviates from the SIR targets by as much as 63% during the transience that lasts for approximately 20 time slots, as shown in Figure 3.1. This simple example illustrates a limitation of the DPC algorithm: the lack of QoS quality in times of congestion.

How to prevent such dips, and in general, how to admit users and manage congestion in cellular network power control becomes an important question. In particular, to guarantee that active links continue to have acceptable received SIR when there are disturbances in the network, an active link protection scheme has to be incorporated with power and user access control [17, 16, 138, 186, 150, 48, 11, 70, 12, 132, 13, 168, 167, 108]. In this chapter, we look at how robust power control

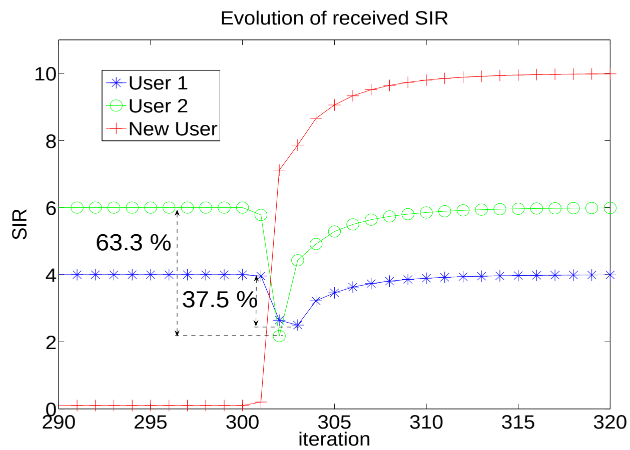


Fig. 3.1 A small numerical example of transient behavior of the DPC algorithm. Originally, there are two users, but a new user enters the same channel at the 300th time slot. The received SIR's of the two active users experience an SIR outage that deviates from the SIR targets by as much as 37% and 63% during the transience period.

in transience and its integration with admission control. In Section 3.2, a characterization of the SIR space that ensures SIR guarantees at all time slots for power control algorithms is presented. In Section 3.3, a robust version of the DPC algorithm in Chapter 2.2 with access control is given. In Section 3.4, the design of a general robust distributed power control scheme is discussed, together with its effectiveness in providing both energy management and interference management and in modulating the energy-robustness tradeoffs.

## 3.2 SIR Invariant Region

In this section, we look at the dynamics and the evolution of the SIR's in the DPC algorithm *before* reaching the equilibrium. Using tools from control theory, the authors in [17, 53] characterize the SIR invariant regions for the DPC algorithm.

Consider an autonomous discrete-time dynamical system $\mathbf{x}[t+1] = f(\mathbf{x}[t])$, $\mathbf{y}[t] = g(\mathbf{x}[t])$, with initial state $\mathbf{x}[0]$. The state of the system and the output at time $t$ are $\mathbf{x}[t] \in \mathbb{R}^n$ and $\mathbf{y}[t] \in \mathbb{R}^m$ respectively.

**Definition 3.1 ([53]).** A subset of the output space is called *invariant* if once the output enters this set, it remains there for all future time steps, i.e., if $\mathbf{y}[t] \in \mathcal{S}$, then $\mathbf{y}[t+1] \in \mathcal{S},\ \forall\, t$.

For the DPC algorithm, let the power $p_i[t]$ be the state of each link $i$ at time $t$, and refer to the corresponding $\mathsf{SIR}_i[t]$ as the output. The state equation is given by (2.3). Assuming that $\rho(\mathbf{D}(\boldsymbol{\gamma})\mathbf{F}) < 1$, i.e., $\gamma_i$'s are feasible, it is next shown how to identify invariant regions in the SIR space and the associated conditions on SIR guarantees [53].

### 3.2.1 SIR guarantees

Assuming all links have already achieved a certain SIR level $\tilde{\gamma}_i$, e.g., the minimum SIR required for link connectivity, under what conditions can we meet the SIR level for all subsequent time steps? The following common ratio condition in [53] characterizes an answer to this question:

**Theorem 3.1.** [53] If there is a constant $\epsilon > 0$ such that $\gamma_i/\tilde{\gamma}_i = 1+\epsilon,\ \forall i$, then $\mathsf{SIR}_i[t] \geq \tilde{\gamma}_i,\ \forall i$, implies $\mathsf{SIR}_i[t+1] \geq \tilde{\gamma}_i,\ \forall i$.

Note that $\gamma_i/\tilde{\gamma}_i = 1+\epsilon$ can be interpreted as the "safety margin" because it allows for each link to be a factor $1+\epsilon$ above its minimum required SIR. Theorem 3.1 states that, for any $\gamma$, $\mathbf{F}$, and $\mathbf{u}$ that satisfy $\rho(\mathbf{D}(\boldsymbol{\gamma})\mathbf{F}) < 1$, particular cones in the SIR space are invariant. These cones are copies of the nonnegative orthant $\mathbb{R}^n_+$, shifted by a constant $1/(1+\epsilon)$ times the vector $\boldsymbol{\gamma}$, which can be parameterized by $\epsilon$ as $\mathcal{K}_{1+\epsilon} = \mathbb{R}^n_+ + 1/(1+\epsilon)\boldsymbol{\gamma}$, for all $\epsilon \geq 0$.

### 3.2.2 Lyapunov function interpretation

The invariant cones discussed above are reminiscent of the level sets of a Lyapunov function. Indeed, the cones $\mathcal{K}_{1+\epsilon}$ can be extended to invariant rectangles, which form the level sets of a Lyapunov function. The following result describes the associated rectangles [53].

**Lemma 1.** For any $\epsilon > 0$, if $|\mathsf{SIR}_i[t] - \gamma_i| \leq \gamma_i\,(1 - 1/(1+\epsilon))\ \forall\, i$, then

$$|\mathsf{SIR}_i[t+1] - \gamma_i| < \gamma_i\,(1 - 1/(1+\epsilon))\ \ \forall i. \tag{3.1}$$

Let $\mathsf{SIR}[t]$ be the vector with entries $\mathsf{SIR}_i[t]$ for all $i$. It is shown in [53] that the rectangular regions shown in Figure 3.2 are invariant, and form the level sets of the following Lyapunov function.

**Theorem 3.2.** [53] The invariant sets given in Lemma 1 are the level sets of the following Lyapunov function

$$\mathcal{V}(\mathsf{SIR}[t]) = \max_i \frac{1}{\gamma_i} |\mathsf{SIR}[t] - \gamma_i| = \|\mathbf{D}(\boldsymbol{\gamma})^{-1}(\mathsf{SIR}[t] - \boldsymbol{\gamma})\|_\infty. \tag{3.2}$$

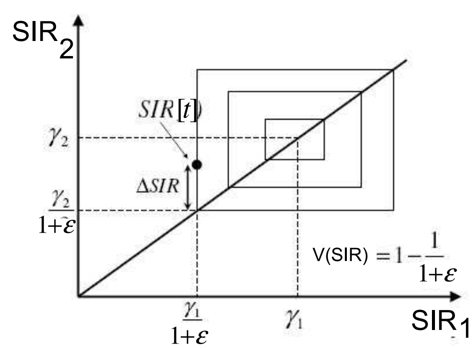


Fig. 3.2 The level sets of the Lyapunov function

The invariant rectangles shown in Figure 3.2 illustrate that, at any time $t$, the possible SIR drops are always bounded by a known value. For example in Figure 3.2, $\mathsf{SIR}[t]$ lies on the boundary of one of the rectangles. Since this rectangle is invariant $\mathsf{SIR}[t+1]$ will also be inside this region. Therefore, drops in the SIR of each link, i.e., components of vector $\mathsf{SIR}[t] - \mathsf{SIR}[t+1]$, can be no larger than the componentwise distance of $\mathsf{SIR}_i[t]$ to the line $\mathsf{SIR}_i[t]/\gamma_i = 1 + \epsilon$; this distance is labeled $\Delta SIR$ in Figure 3.2.

## 3.3 Power Control with Active Link Protection

Turning from analysis of invariant region to design of robust power control, we next summarize a robust DPC algorithm proposed in [17, 16].

### 3.3.1 DPC/ALP Algorithm

By extending the DPC algorithm, the authors in [17, 16] proposed the Distributed Power Control with Active Link Protection (DPC/ALP) algorithm to protect active users from new users that access the same channel. The two key ideas of the DPC/ALP algorithm are: 1) the gradual power-up of new users; and 2) the introduction of an SIR margin $\epsilon$ to cushion the existing users, which is accomplished by modifying the SIR constraint in (2.1) to

$$\mathsf{SIR}_i(\mathbf{p}) \geq \gamma_i(1+\epsilon), \ \ \forall\, i \tag{3.3}$$

where $\epsilon > 0$. Parameter $\epsilon$ serves as a protection margin for users that are running (2.3) and helps keep them from falling below $\boldsymbol{\gamma}$ in a dynamic setting when new users access the same channel.

For a given $\epsilon$, the DPC/ALP algorithm is given by

---

**Algorithm 3.1 (Distributed Power Control/Active Link Protection [17, 16]).**

$$p_i[t+1] = \begin{cases} \frac{(1+\epsilon)\gamma_i}{\mathsf{SIR}_i[t]} p_i[t], & \text{if } \mathsf{SIR}_i[t] \geq \gamma_i \\ (1+\epsilon)p_i[t], & \text{if } \mathsf{SIR}_i[t] < \gamma_i \end{cases} \quad \forall\, i. \tag{3.4}$$

---

Implicitly, the DPC/ALP algorithm solves the following problem of power minimization subject to a robust version of the SIR constraint:

$$\begin{array}{ll} \text{minimize} & \sum_i p_i \\ \text{subject to} & \mathsf{SIR}_i(\mathbf{p}) \geq \gamma_i(1+\epsilon), \ \ \forall\, i, \\ \text{variables} & \mathbf{p}. \end{array} \tag{3.5}$$

Since $\epsilon$ is fixed, (3.5) can still be rewritten as a linear program in a way similar to (2.2), and the DPC/ALP Algorithm converges to the optimal solution of (3.5) if and only if $(1+\epsilon)\rho(\mathbf{D}(\boldsymbol{\gamma})\mathbf{F}) < 1$ [17].

From Theorem 3.1, we immediately see that the DPC/ALP algorithm provides SIR protection for active links, i.e., $\mathsf{SIR}_i[t] \geq \alpha_i \ \forall\, i$, implies $\mathsf{SIR}_i[t+1] \geq \alpha_i \ \forall\, i$. Also, it is shown in [17] that if the $i$th link has $\mathsf{SIR}_i[t] \leq \gamma_i$, then $\mathsf{SIR}_i[t] \leq \mathsf{SIR}_i[t+1]$, i.e., the received SIR of a new user strictly increases. Furthermore, the power overshoots of the DPC/ALP algorithm can be bounded as follows.

---

**Theorem 3.3 (Bounded power overshoot [17]).** In the DPC/ALP algorithm, for any fixed $\epsilon$, we have $p_i[t+1] \leq (1+\epsilon)p_i[t]$ for links with $\mathsf{SIR}_i[t] \geq \gamma_i$.

---

Theorem 3.3 shows that the powers of active links can only increase in a smooth way, in order to accommodate the new links that are powering up [17, 16]. A larger $\epsilon$ obviously provides more protection to existing users, but comes at a price of higher power expenditure and, from Theorem 3.3, possibly a larger power overshoot. Furthermore, a larger $\epsilon$ makes user admission faster, but may cause excessive interference or even infeasibility of the enhanced target SIR. How to control these tradeoffs modulated by $\epsilon$? Intuitively, $\epsilon$ should be time-varying instead of being a constant, controlled possibly by some "interference price" that is updated by inferring the network congestion level from local measurements. This intuition will be made clear in the following section.

## 3.4 Robust Distributed Power Control

We now examine a robust distributed power control (RDPC) algorithm in [168, 167]. It is developed based on the following: sensitivity analysis on the effects of power changes, interference prices obtained from Lagrangian duality theory, congestion measures related to the size of the Perron-Frobenius eigenvalue, and a primal-dual update equation with desirable convergence properties. It turns out that the RDPC algorithm solves an underlying optimization problem, whose objective function can be tuned to influence the behavior of the RDPC algorithm in a predictive way. We conclude this section with the application of the RDPC algorithm in modulating the energy-robustness tradeoff.

First, we consider a general problem formulation in [168] that takes robustness into account. Using the protection margin in (3.3) to enhance the SIR constraints, we consider the minimization of the total power expenditure plus a cost function:

$$\begin{array}{ll} \text{minimize} & \sum_i p_i + \phi(\epsilon) \\ \text{subject to} & \mathsf{SIR}_i(\mathbf{p}) \geq \gamma_i(1+\epsilon) \quad \forall\, i, \\ \text{variables} & \epsilon,\ \mathbf{p}. \end{array} \tag{3.6}$$

Note that now $\epsilon$ is an optimization variable and $\phi(\epsilon)$ is a decreasing, convex cost function that captures the tradeoff in adjusting $\epsilon$. This objective function will be very useful in modulating the tradeoff between robustness and energy both at equilibrium and during transience. The following necessary condition characterizes feasible solutions to (3.6):

---

**Lemma 3.1.** [168] For a feasible $\mathbf{p}$ and $\epsilon$ to (3.6), the following holds:

$$(1+\epsilon)\rho(\mathbf{D}(\boldsymbol{\gamma})\mathbf{F}) < 1. \tag{3.7}$$

---

Note that (3.6) can no longer be written as a linear program as can be done with (2.1) and (3.5), and in fact it is a nonconvex optimization problem. It can nevertheless be rewritten as a convex optimization problem for certain functions $\phi(\epsilon)$ [168]. By applying a log transformation to $p_i$, for all $i$, and $\epsilon$ ($\tilde{p} = \log p$ and $\tilde{\epsilon} = \log \epsilon$), the following equivalent problem is obtained:

$$\begin{array}{rl} \text{minimize} & \sum_i e^{\tilde{p}_i} + \phi(e^{\tilde{\epsilon}}) \\ \text{subject to} & \log(\mathsf{SIR}_i(\tilde{\mathbf{p}})/\gamma_i) \geq \log(1+e^{\tilde{\epsilon}}) \quad \forall\, i, \\ \text{variables:} & \tilde{\mathbf{p}},\ \tilde{\epsilon}. \end{array} \tag{3.8}$$

We will focus on those $\phi$ satisfying the condition in the following lemma.

---

**Lemma 3.2.** [168] The optimization problem in (3.8) is convex if $\frac{\partial^2\phi(z)/\partial z^2}{\partial\phi(z)/\partial z} \geq -1/z$ for $z > 0$.

---

### 3.4.1 RDPC Algorithm

The main algorithm in [168] is given next. The details of its derivation will be given in the next subsection (in particular, (3.10)-(3.11) follow from Theorem 3.4 and (3.12) follows from Theorem 3.4). It will also be shown that $\boldsymbol{\nu}$ is the Lagrange multiplier vector for (3.8).

---

**Algorithm 3.2 (Robust Distributed Power Control [168]).**

- The base station initiates at $\epsilon[0]$. New users power up with sufficiently small $p_i[0]$, e.g., $p_i[0] = n_i$.

**Update by each user $i$:**

(1) Update the transmitter powers $p_i[t+1]$ at the $[t+1]$th step:

$$p_i[t+1] = \begin{cases} \frac{(1+\epsilon[t])\gamma_i}{\mathsf{SIR}_i[t]} p_i[t], & \text{if } \mathsf{SIR}_i[t] \geq \gamma_i \\ (1+\epsilon[t])p_i[t], & \text{if } \mathsf{SIR}_i[t] < \gamma_i. \end{cases} \tag{3.9}$$

**Update by the base station:**

(1) Update $\mathbf{x}[t+1]$:

$$\mathbf{x}[t+1] = (1+\epsilon[t])(\mathbf{D}(\boldsymbol{\gamma})\mathbf{F})^T\mathbf{x}[t] + \mathbf{1}. \tag{3.10}$$

(2) Update $\boldsymbol{\nu}[t+1]$:

$$\nu_i[t+1] = x_i[t+1]p_i[t+1], \ \ \forall i. \tag{3.11}$$

(3) Update $\epsilon[t+1]$ by solving

$$-\frac{\partial \phi(\epsilon)}{\partial \epsilon}\bigg|_{\epsilon=\epsilon[t+1]} (1+\epsilon[t+1]) = \mathbf{1}^T\boldsymbol{\nu}[t+1]. \tag{3.12}$$

---

Both the DPC and DPC/ALP algorithms are *primal algorithms with linear updates*, whereas the RDPC algorithm is a *primal-dual algorithm with nonlinear updates*. Also, the power update (3.9) differs

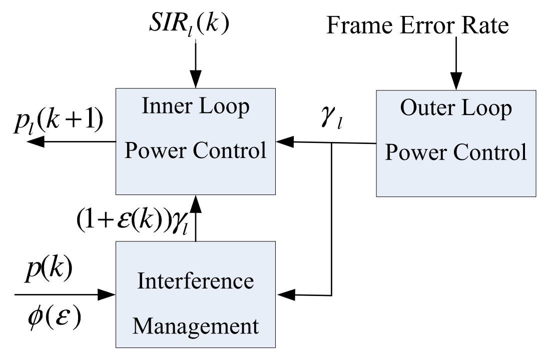


Fig. 3.3 A schematic of the RDPC algorithm for uplink power control.

from the DPC/ALP algorithm in [17, 16] in that $\epsilon$ is not a constant parameter, but is updated at each time slot according to variables $\mathbf{x}$ and $\boldsymbol{\nu}$. Equation (3.12) quantifies the remark on choosing the parameter $\epsilon$ in [17]: "$\epsilon$ should be chosen such that $(1+\epsilon)$ is larger when the network is uncongested, so that links power up fast, and grow smaller as congestion builds up to have links power up more gently".

The following theorem for the RDPC algorithm connects it to the underlying optimization model [168]:

---

**Theorem 3.4.** If $\{\epsilon[t]\}$ converges to a finite value $\epsilon^*$, and $\rho(\mathbf{D}(\boldsymbol{\gamma})\mathbf{F}) < \dfrac{1}{1+\epsilon^*}$, then the RDPC algorithm converges to a global optimum $(\mathbf{p}^*, \epsilon^*)$ of problem (3.6).

---

A general schematic diagram of the RDPC algorithm for an uplink transmission is shown in Figure 3.3. The inner loop power control block consists of a transmit power update for each user based on the measured SIR values (see (3.9)), and the outer loop power control block adjusts the SIR targets $\boldsymbol{\gamma}$ as a function of the frame error rates. The interference management block takes as input the measured power of all users, and, based on a particular cost function $\phi(\epsilon)$, modulates the parameter $\epsilon$, which is then fed to the outer loop block (see (3.10)-(3.12)).

### 3.4.2 Development of RDPC

Intuitively, the amount of congestion in the system and the "price" of maintaining the SIR constraints, should be a factor in determining how robust a power control algorithm needs to be. Following [168], consider the case of $\epsilon = 0$ in (3.6), which corresponds to (2.1). Sensitivity analysis is then used in [168] to show how adjusting $\boldsymbol{\gamma}$ affects the solution for (2.1), which further instructs the network designer on how to choose the right cost function $\phi(\epsilon)$ in (3.6).

Recall that the SIR constraints in (2.1) are tight at optimality, assuming that there is a feasible power allocation for all users. Hence, tightening or loosening this constraint set affects the optimal value of (2.1). For the $i$th SIR constraint in (2.1), define a perturbed SIR target $\gamma_i/u_i$ where $1/u_i$ represents a fractional perturbation of the SIR target $\gamma_i$, and substitute the $i$th SIR constraint in (2.1) by $\gamma_i/\mathsf{SIR}_i(\mathbf{p}) \leq u_i$ for all $i$. Obviously, $0 < u_i < 1$ or $u_i > 1$ if we tighten or loosen the $i$th SIR constraint, respectively. Next, define $f^*(\mathbf{u})$ as the optimal value of (2.1) with these perturbed constraints:

$$\begin{array}{rl} f^*(\mathbf{u}) = \text{minimize} & \sum_i p_i \\ \text{subject to} & \gamma_i/\mathsf{SIR}_i(\mathbf{p}) \leq u_i \quad \forall\, i, \\ \text{variables} & \mathbf{p}. \end{array} \tag{3.13}$$

If $f^*(\mathbf{u})$ does not exist for some $\mathbf{u}$, define $f^*(\mathbf{u}) = \infty$. Let $\tilde{p}_i = \log p_i$ and the parameter $\tilde{u}_i = \log u_i$, and taking the logarithm of the SIR constraints, $f^*(\mathbf{u})$ can be written in the log transformed parameter $\tilde{\mathbf{u}}$ as $\tilde{f}^*(\tilde{\mathbf{u}})$, the optimal value of the objective function in the following problem:

$$\begin{array}{ll} \text{minimize} & \sum_i e^{\tilde{p}_i} \\ \text{subject to} & \log(\gamma_i/\mathsf{SIR}_i(\tilde{\mathbf{p}})) \leq \tilde{u}_i \quad \forall\, i, \\ \text{variables} & \tilde{\mathbf{p}}. \end{array} \tag{3.14}$$

The following result quantifies the tradeoff between power expenditure and robustness [27].

---

**Lemma 3.3.** Let $\nu_i^*$, for all $i$, be the optimal Lagrange multipliers of the unperturbed problem in (3.14), (i.e., for $\tilde{\mathbf{u}} = \mathbf{0}$), then

$$100\frac{\tilde{f}^*(\frac{\beta_i}{100}\mathbf{e}_i) - \tilde{f}^*(\mathbf{0})}{\tilde{f}^*(\mathbf{0})} = -\beta_i \nu_i^*/\tilde{f}^*(\mathbf{0}) + o(\beta_i) \tag{3.15}$$

where $\mathbf{e}_i$ is a vector that has all its entries 0, except the $i$th entry, which is 1.

---

The engineering implication is as follows. Relaxing (or tightening) the $i$th SIR target constraint by $\beta_i$ percent in (2.1) decreases (or increases) the total power by approximately $\beta_i \nu_i^* / \tilde{f}^*(\mathbf{0})$ percent, for a small $\beta_i$. Hence, the total power reduction (or increment) is approximately $\sum_i \beta_i \nu_i^* / \tilde{f}^*(\mathbf{0})$ percent. If users with large $\nu_i^*$ is compromised slightly, all users obtain power saving and lower interference simultaneously.

To complete the development of the iterative updates in the RDPC algorithm, the following result is derived in [168] to compute $\boldsymbol{\nu}$ in Lemma 3.3.

---

**Lemma 3.4.** The optimal power $\mathbf{p}^*$ in (2.1) and the Lagrange multiplier $\boldsymbol{\nu}^*$ in the unperturbed problem in (3.14) satisfy

$$\nu_i^* = p_i^* \left( 1 + \sum_{i \neq i} \frac{G_{il} \nu_i^*}{\sum_{j \neq i} G_{ij} p_j^* + n_i} \right), \quad \forall i. \tag{3.16}$$

Furthermore, the following updates can be used to compute $\boldsymbol{\nu}^*$:

$$\begin{aligned} \mathbf{p}[t+1] &= (\mathbf{D}(\boldsymbol{\gamma})\mathbf{F})\mathbf{p}[t] + \mathbf{v}, && (3.17) \\ \mathbf{x}[t+1] &= (\mathbf{D}(\boldsymbol{\gamma})\mathbf{F})^T \mathbf{x}[t] + \mathbf{1}, && (3.18) \end{aligned}$$

and

$$\nu_i[t+1] = x_i[t+1] p_i[t+1], \quad \forall i. \tag{3.19}$$

As $t \to \infty$, $\nu_i[t]$ converges to $\nu_i^*$ in (3.16) for all $i$ if and only if $\rho(\mathbf{D}(\boldsymbol{\gamma})\mathbf{F}) < 1$.

---

### 3.4.3 Balancing the tradeoffs

We next look at the application of the RDPC algorithm that balances the tradeoff between SIR robustness and energy expenditure. Based on the sensitivity analysis in Lemma 3.3, the extra power needed to provide $\epsilon^*$ amount of SIR margin is

$$100(\mathbf{1}^T \boldsymbol{\nu}^* \epsilon^* / \mathbf{1}^T \mathbf{p}^*) \tag{3.20}$$

percent, or, from (3.12),

$$-\left.\frac{\partial\phi(\epsilon)}{\partial\epsilon}\right|_{\epsilon=\epsilon^*} 100(1+\epsilon^*)\epsilon^*/\mathbf{1}^T\mathbf{p}^* \tag{3.21}$$

percent. Suppose the network can tolerate at most an increase of $100\delta/\mathbf{1}^T\mathbf{p}^*$ percent in total power to limit interference [1]. Now, from (3.21), it is shown in [168] that

$$\frac{\partial\phi(\epsilon)}{\partial\epsilon} = -\frac{\delta}{\epsilon(1+\epsilon)}, \tag{3.22}$$

which upon integration yields

$$\phi(\epsilon) = \delta\log(1+1/\epsilon). \tag{3.23}$$

It is easy to verify that $\phi(\epsilon)$ in (3.23) is strictly convex decreasing and satisfies Lemma 3.2.

Recall that the convergence result in Theorem 3.4 requires an assumption that $\epsilon[t] \to \epsilon^*$ as $t \to \infty$. For the function $\phi(\epsilon)$ in (3.23), further analysis can be carried out to remove this assumption and prove local asymptotically stability of the RDPC algorithm in general.

Let $\mathbf{z}[t] = [\mathbf{p}[t]^T\ \mathbf{x}[t]^T]^T$, $\mathbf{z}^* = [\mathbf{p}^{*T}\ \mathbf{x}^{*T}]^T$, and $\Delta = \delta/\mathbf{1}^T\mathbf{p}^*$.

---

**Theorem 3.5.** [168] Consider the mapping from $\mathbf{z}[t]$ to $\mathbf{z}[t+1]$ and its Jacobian matrix $\mathbf{J} = \left.\frac{\partial f(\mathbf{z})}{\partial \mathbf{z}}\right|_{\mathbf{z}=\mathbf{z}^*}$ where

$$f(\mathbf{z}) = \begin{bmatrix} \left(1+\frac{\Delta}{\mathbf{p}^T\mathbf{x}}\right)(\mathbf{D}(\gamma)\mathbf{F}\mathbf{p} & + & \mathbf{v}) \\ \left(1+\frac{\Delta}{\mathbf{p}^T\mathbf{x}}\right)(\mathbf{D}(\gamma)\mathbf{F})^T\mathbf{x} & + & \mathbf{1} \end{bmatrix}. \tag{3.24}$$

We have $\rho(\mathbf{J}) = \left(1+\frac{\Delta}{\mathbf{p}^{*T}\mathbf{x}^*}\right)\rho(\mathbf{D}(\gamma)\mathbf{F})$.

Furthermore, the RDPC algorithm with $\phi$ in (3.23) is locally asymptotically stable if and only if

$$\rho(\mathbf{J}) = \left(1+\frac{\Delta}{\mathbf{p}^{*T}\mathbf{x}^*}\right)\rho(\mathbf{D}(\gamma)\mathbf{F}) < 1. \tag{3.25}$$

---

[1] This $\delta$ can be obtained from different kinds of models. For example, in [43], the authors propose an in-cell rise-over-thermal (IROT) constraint. Given an IROT constraint, $\delta$ can be configured as the input parameter for the RDPC algorithm.

In addition the tradeoff between robustness and energy, another tradeoff during the transience is between the speed of user admission and the amount of allowed interference. Both tradeoffs can be controlled by changing the curvature of the function $\phi(\epsilon)$, which then changes the dynamic and equilibrium properties of the RDPC algorithm.

In [168], the following family of $\phi_\alpha(\epsilon)$ is considered, parameterized by a nonnegative integer $\beta$, for $\epsilon \in (0, 1]$:

$$\phi_\beta(\epsilon) = \delta \left( \sum_{n=1}^{\beta} (-1)^{\beta-n} \epsilon^{-n}/n + \log(1 + 1/\epsilon) \right). \tag{3.26}$$

This $\phi_\beta(\epsilon)$ given by (3.26) is strictly decreasing and also satisfies Lemma 3.2. Using (3.26), we see that $\partial\phi_\beta(\epsilon)/\partial\epsilon$ provides a way to adjust the curvature of the function $\phi_\beta(\epsilon)$ such that $\epsilon^*$ increases as the control parameter $\beta$, tunable by the network operator, gets larger. This implies that energy expenditure increases, but new user admission rate also increases. Therefore, new users can power up faster with increasing traffic load.

In [167], the RDPC algorithm can be further modified for the time-division duplex network by exploiting the uplink-downlink duality, as discussed in Chapter 7. In this case, the interference price $\boldsymbol{\nu}$ can be interpreted as the product of uplink and downlink power [167].

### 3.4.4 Numerical example

The ability of the RDPC algorithm to balance energy and robustness compared to the DPC algorithm and the DCP/ALP algorithm is illustrated using a numerical example. Using $\phi(\epsilon)$ in (3.23), the RDPC algorithm is configured with $\delta$ to have at most 15 percent total power increment, and the $\epsilon^*$ computed is 0.021. During time slots 0-250, only User 1 and 2 are active. From time 250, User 3 becomes active. At time 1000, User 1 completes data transmission, and departs from the cell leaving User 2 and 3. Figure 3.4 shows that the DPC/ALP algorithm results in a total power expenditure of more than 150 percent at the two network operating points at time 250 and 1000 as compared to DPC, whereas the RDPC algorithm uses an additional extra total power of 15 percent. In the case of DPC, the received SIR's of User

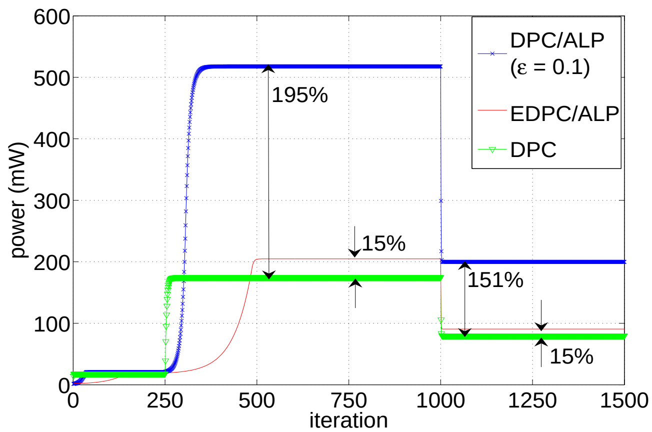


Fig. 3.4 Evolution of the total power with the DPC/ALP, RDPC, and DPC algorithms. The percentage increases in extra power between (i) DPC/ALP and DPC, and (ii) RDPC and DPC at two different operating points (i.e., time slots 250-1000 and 1000-1500) are shown.

1 and 2 are observed to suffer a dip of more than 40 and 60 percent respectively at time 250 when User 3 enters the channel. In contrast, this does not happen with the RDPC and DPC/ALP algorithms.

## 3.5 Open Problems

Transient behaviors of distributed power control remain under-explored compared to equilibrium properties. In terms of analysis, a complete characterization of invariant sets remains open in general. In terms of design, in the RDPC algorithm, even though there are predictive models for parameter choice, the control of tradeoff during transience and the tradeoff at equilibrium is still coupled through a single parameter $\epsilon$.

With network dynamics such as mobility, handoff, and fading, robustness of power control solutions is important yet challenging to ensure. This chapter primarily focused on robustness with respect to new users entering a cell, while other definitions of robustness are still yet to be fully explored. In particular, opportunities arising from channel variations will be discussed in Chapter 5.

Finally, as traffic in wireless cellular networks becomes increasingly multimedia-based, admission control in a power-controlled network presents increasingly difficult issues. A related issue is assignment of SIR target, a degree of freedom that has been fixed as constants in the last and present chapters and will be exploited in the next chapter.

# 4

# Power Control with Variable SIR

## 4.1 Introduction

The fixed SIR approach to power control problem discussed in Chapter 2 is suitable for lightly loaded voice networks. When the network gets more heavily loaded, setting the target $\gamma$ to be feasible becomes challenging. More importantly, in a wireless data network can optimize the SIR assignment according to traffic requirements and channel conditions. Higher SIRs imply better data rates and possibly greater reliability, while smaller SIRs can still provide lower data rates. In addition, a cellular operator of a wireless data network might want to treat higher tariff paying users preferentially by allocating them to higher QoS classes, and the SIR target need to be set differently for users in different QoS classes. Most of the literature that deals with this problem define either the rate or another QoS metric as a bijective mapping to SIR, and optimize their allocation according to a utility function, subject to the constraint that SIR assignment must be feasible, i.e., there is a power vector that can realize the SIR vector. Therefore, the problem becomes a joint SIR assignment and power control.

One approach to vary SIR targets is for each MS to selfishly attempt to maximize its utility without regard to network-wide criteria. This results in a distributed implementation that can be modeled as an $N$-person non-cooperative game. The resulting Nash equilibrium can then be analyzed for properties such as existence, uniqueness, and efficiency loss. This game-theoretic approach will be discussed in Chapter 6.

A second approach is to consider the SIR allocation based on global maximization of the utilities as proposed in [83, 38, 127] and depicted in Figure 4.1. The utility maximization problems considered in [38] and [127] assume an approximation to the rate function and propose centralized algorithms. The work in [83] proposes utilities of data rates approximated as linear functions of SIRs, and proposes a distributed algorithm on a subset of the SIR feasibility set that is easier to decouple and leads to a heuristic solution.

In summary, the range of results in 1992-2005 can provide (1) a distributed and optimal solution in the special case of fixed SIR, or (2) an optimal but centralized solution that requires global coordination across the cells, or (3) a distributed but suboptimal solution based on selfish local power update at MSs. A key difficulty in this problem of jointly optimizing SIR and transmit powers across multiple cells is that the constraint set of SIR feasibility is coupled in a complicated way beyond standard decoupling techniques.

In the case of convex SIR feasibility set, the work in [65] presents a distributed algorithm that does not require coordination across cells and converges to the jointly optimal SIR and power. The main idea of this solution comes from a re-parametrization of the constraint set from power-interference representation to the so-called load-spillage representation, essentially a sophisticated change of coordinates, which then lead to an ascent search-direction for this optimization problem that is locally computable by each mobile user. Convergence and optimality proofs then followed. This Load-Spillage Power Control (LSPC) algorithm has also been recently adopted in the industry, as will be explained in Chapter 10.

This chapter starts with characterizations of the SIR feasibility regions, especially their convexity property, then present the LSPC algorithm, its main theoretical properties, and a large-scale example using the 3GPP2 simulator.

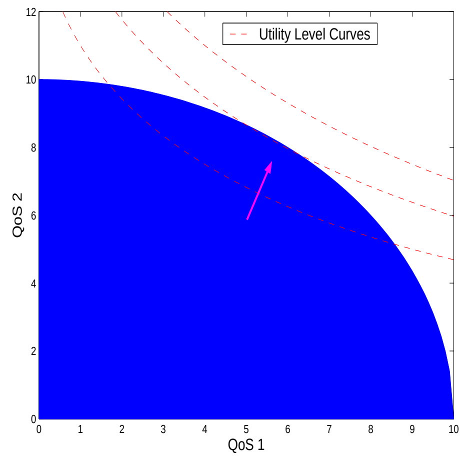


Fig. 4.1 The feasible SIR region has a Pareto-optimal boundary. Points outside the boundary cannot be realized by any power allocation. Utility function's curves intersect at the boundary and define an optimal SIR assignment. The central question in this chapter is how to distributedly move towards this optimal SIR point and the associated power allocation.

## 4.2 SIR Feasibility Region

Consider the system setup in Section 1.3.1 and the SIR feasibility equations (1.7) and (1.6). Due to the interference among links, not all SIR vectors $\boldsymbol{\gamma}$ are achievable. The basic feasibility condition was discussed in Theorem 2.1.

Let the region $\mathbf{B} = \{\boldsymbol{\gamma} \succeq 0 : \rho(\mathbf{FD}(\boldsymbol{\gamma})) < 1\}$ be the set of all feasible SIR vectors $\boldsymbol{\gamma}$. As $\boldsymbol{\gamma}$ approaches the boundary of $\mathbf{B}$, $\rho(\mathbf{FD}(\boldsymbol{\gamma})) \to 1$, $\mathbf{p}(\boldsymbol{\gamma}) \to \infty$, and $\mathbf{q}(\boldsymbol{\gamma}) \to \infty$. To avoid mathematical technicalities right on the boundary of feasibility region and to consider practical limits on power and interference, the following SIR feasibility regions are defined in [65]. Let $\mathbf{q}^m \succ 0$ and $\mathbf{p}^m \succ 0$ be maximum interference and power vectors, and define the corresponding subsets of feasible SIR vectors,

$$\begin{aligned}\mathbf{B}(\mathbf{p}^m) &= \{\gamma \in \mathbf{B} \mid \mathbf{p}(\gamma) \preceq \mathbf{p}^m\},\\ \mathbf{B}(\mathbf{q}^m) &= \{\gamma \in \mathbf{B} \mid \mathbf{q}(\gamma) \preceq \mathbf{q}^m\}.\end{aligned}$$

The set $\mathbf{B}(\mathbf{p}^m)$ limits the transmit power, $p_i$ of each mobile $i$, and is most useful in coverage-limited networks where the transmit power capabilities of the mobiles are the limiting factor in network capacity.

The set $\mathbf{B}(\mathbf{q}^m)$ limits the interference $q_i$ at the BS serving MS $i$, and is most useful in interference-limited networks.

### 4.2.1 Convexity

A well-known result is that the SIR feasibility region $\mathbf{B}$ is convex in log(SIR) as shown in [163]. The result is summarized in the following Lemma.

---

**Lemma 4.1.** [163] If $\boldsymbol{\gamma} \in \mathbf{B}$ and $\boldsymbol{\gamma}' \in \mathbf{B}$, then the vector $\boldsymbol{\gamma}^\alpha$ defined by

$$\boldsymbol{\gamma}^\alpha = \{\gamma_i^\alpha \gamma_i'^{(1-\alpha)}\}$$

where $0 \leq \alpha \leq 1$, is also feasible.

---

A second result on the convexity in [30] shows that $\mathbf{B}$ is convex in 1/SIR.

---

**Lemma 4.2.** [30] The SIR region $\mathbf{B}$ is convex in $1/\boldsymbol{\gamma}$.

---

This result is further extended in [81] where it is shown that, in addition to the general feasible SIR region, the power constrained SIR region $\mathbf{B}(\mathbf{p}^m)$ is also convex. The corresponding lemma applies to the interference constrained region $\mathbf{B}(\mathbf{q}^m)$ as well.

---

**Lemma 4.3.** [81] The SIR regions $\mathbf{B}(\mathbf{p}^m)$ and $\mathbf{B}(\mathbf{q}^m)$ are convex in $\log(\boldsymbol{\gamma})$ and $1/\boldsymbol{\gamma}$.

---

An equivalent result with a different approach is shown in [25, 26].

---

**Lemma 4.4.** [25, 26] The functions $\mathbf{q}(\boldsymbol{\gamma})$, $\mathbf{p}(\boldsymbol{\gamma})$ and $\rho(\mathbf{FD}(\boldsymbol{\gamma}))$ are convex in $\log \boldsymbol{\gamma}$ in the region $\log \mathbf{B}$. In particular, the sets, $\log \mathbf{B}(\mathbf{q}^m)$, $\log \mathbf{B}(\mathbf{q}^m)$ and $\log \mathbf{B}_\rho$ are convex.

---

### 4.2.2 Pareto-Optimality

Let $\mathbf{\Gamma} \subseteq \mathbf{B}$ be a set of feasible SIR vectors. The selection of a feasible $\boldsymbol{\gamma} \in \mathbf{\Gamma}$ is, in general, a multi-objective optimization problem. Increasing the SIR, $\gamma_i$, for one MS will require that the SIR, $\gamma_j$, for another MS be reduced. The Pareto-optimal points of a set $\mathbf{\Gamma}$ form the Pareto-optimal boundary denoted by $\partial\mathbf{\Gamma}$. A characterization of Pareto-optimality for the feasible sets $\mathbf{B}(\mathbf{p}^m)$ and $\mathbf{B}(\mathbf{q}^m)$ is given in [65].

---

**Lemma 4.5.** [65] For $\mathbf{\Gamma} = \mathbf{B}(\mathbf{q}^m)$, $\boldsymbol{\gamma} \in \partial\mathbf{B}(\mathbf{q}^m)$ if and only if $\mathbf{q}(\boldsymbol{\gamma}) \preceq \mathbf{q}^m$ with at least one $i$ such that $q_i(\boldsymbol{\gamma}) = q_i^m$. For $\mathbf{\Gamma} = \mathbf{B}(\mathbf{p}^m)$, $\boldsymbol{\gamma} \in \partial\mathbf{B}(\mathbf{p}^m)$ if and only $\mathbf{p}(\boldsymbol{\gamma}) \preceq \mathbf{p}^m$ with at least one $i$ such that $p_i(\boldsymbol{\gamma}) = p_i^m$

---

## 4.3 Joint SIR Assignment and Power Control

### 4.3.1 Problem formulation

A cellular network has to pick a particular operating point on the Pareto-optimal boundary of the feasibility region, and achieve the point preferably in a distributed manner with minimal message passing. There is an infinite number of Pareto-optimal points on the boundary of feasibility region, and an objective function, like the range of concave utility functions discussed in Chapter 1, define a particular point as the optimum. Given a set of feasible SIR vectors, $\boldsymbol{\gamma} \in \mathbf{\Gamma} \subseteq \mathbf{B}$, the optimal SIR over this set is defined by $\boldsymbol{\gamma}^{opt} = \arg\max_{\boldsymbol{\gamma}\in\mathbf{\Gamma}} \sum_i U_i(\gamma_i)$. For $\mathbf{\Gamma} = \mathbf{B}(\mathbf{p}^m)$, the problem of optimal SIR assignment is given by:

$$\begin{array}{ll} \text{maximize} & \sum_i U_i(\gamma_i) \\ \text{subject to} & \mathbf{p}(\boldsymbol{\gamma}) \preceq \mathbf{p}^m \\ \text{variables} & \boldsymbol{\gamma} \succ 0,\ \mathbf{p} \succ 0. \end{array} \tag{4.1}$$

For $\mathbf{\Gamma} = \mathbf{B}(\mathbf{q}^m)$, the problem of optimal SIR assignment is:

$$\begin{array}{ll} \text{maximize} & \sum_i U_i(\gamma_i) \\ \text{subject to} & \mathbf{q}(\boldsymbol{\gamma}) \preceq \mathbf{q}^m \\ \text{variables} & \boldsymbol{\gamma} \succ 0,\ \mathbf{q} \succ 0. \end{array} \tag{4.2}$$

The problem posed in [38, 127] is a variant of (4.1) and stated in terms of data rates considered as a bijective mapping of SIR.

This chapter focuses on the case where the above problem is convex optimization. This imposes restrictions on both the objective function and constraint set. For example, since SIR feasibility regions are convex in $\log(\boldsymbol{\gamma})$, assuming utility functions $U_i(\gamma_i)$ to be concave in $\log(\gamma_i)$ renders the problem convex. Non-convex formulations will be briefly discussed in Chapter 9.

Sufficient conditions for convexity of feasibility region have just been presented. Concavity of utility function in $\boldsymbol{\gamma}$ or $\mathbf{p}$ can also be readily checked. For example, concavity of $U_i$ in $\log(\gamma_i)$ can be expressed in an alternative form: $U_i(\gamma_i)$ is concave in $\log \gamma_i$ if and only if the negative of the curvature is sufficiently large:

$$U_i''(\gamma_i) \leq -\frac{U_i'(\gamma_i)}{\gamma_i}.$$

In particular, the above condition is satisfied for $\alpha$-fair utilities when $\alpha \geq 1$. Note that the function $U_i(\gamma_i) = \log(\gamma_i)$ satisfies this condition. It is the psuedo-linear utility discussed in Chapter 1 for a QoS $\beta_i = \log(1 + \gamma_i)$ and satisfies the above condition. But $U_i(\gamma_i) = \log(1 + \gamma_i)$ does not satisfy the above condition.

We also assume that $U_i(\gamma_i) \to -\infty$ as $\gamma_i \to 0$, thus prohibiting zero power and SIR allocation. This implies that every link gets a non-zero SIR at equilibrium. Such problem formulations represent a system design where the links are not scheduled in time but can compete with each other for higher SIR in every time slot as is the case in 1xEVD0, a commercial wireless broadband system discussed further in Chapter 10. However, sometimes it is better to allocate zero SIR to some links, i.e., deactivate them, so as to maximize the network's total utility. This situation will be discussed in Chapter 9 for joint power control and scheduling.

Even when problems (4.2) and (4.2) are convex, the structure of the coupled constraint set, where the transmit power of any one MS affects the SIR of every other MS in the network, renders the problem difficult to solve distributively. It turns out that an alternative representation of the Pareto-optimal boundary in terms of the left, rather than right, Perron-Frobenius eigenvectors enables a distributed solution.

### 4.3.2 Load Spillage Power Control

The key to decouple the SIR feasibility constraint set is a set of parameters termed the "load" factors as defined in [65]. The load-factors $\{\ell_i\}$ are positive numbers associated with links. From the load-factors, arise the spillage factors $\{s_i\}$ defined as follows:

(1) For $\mathbf{\Gamma} = \mathbf{B}(\mathbf{p}^m)$:

$$\mathbf{s}(\ell, \boldsymbol{\nu}) = \mathbf{F}^T \ell + \boldsymbol{\nu} \tag{4.3}$$

(2) For $\mathbf{\Gamma} = \mathbf{B}(\mathbf{q}^m)$:

$$\mathbf{s}(\ell, \boldsymbol{\nu}) = \mathbf{F}^T (\ell + \boldsymbol{\nu}) \tag{4.4}$$

The load-factor $\ell_i$ on link $i$ represents the amount of intolerance of that link to interference from neighboring links, and the spillage-factor $s_i$ is a measure of the potential interference that can be caused by link $i$ when it transmits.

The factor $\boldsymbol{\nu}$ is a price that is updated depending upon the local power and interference constraint through a simple subgradient-based update:

$$\text{For } \mathbf{\Gamma} = \mathbf{B}(\mathbf{p}^m): \quad \nu_i[\tau + 1] = [\nu_i[\tau] + \delta[\tau](p_i[\tau] - p_i^m)]^+ \tag{4.5}$$

$$\text{For } \mathbf{\Gamma} = \mathbf{B}(\mathbf{p}^m): \quad \nu_i[\tau + 1] = [\nu_i[\tau] + \delta[\tau](q_i[\tau] - q_i^m)]^+ \tag{4.6}$$

where $\delta[\tau] = \delta_0/\tau, \delta_0 > 0$, is a suitable choice for the step size.

Much more importantly, an ascent-direction update of load factors along the Pareto-optimal boundary can be conducted in a distributed way [65]:

$$\Delta\ell_i = \frac{U_i'(\gamma_i)\gamma_i}{q_i} - \ell_i, \quad \forall i. \tag{4.7}$$

This key step leads to the the LSPC algorithm described as follows:

---

**Algorithm 4.1 (Joint SIR and power optimization).** [65]

- Parameters: Step sizes $\delta_1 > 0$ for load update, $\delta > 0$ for price update, utility functions $U_i(\gamma_i)$, and interference or power constraints, $\mathbf{p}^m$ or $\mathbf{q}^m$.
- Initialize: Arbitrary $\{\ell_i[0] > 0\}$ and $\{\nu_i[0] \geq 0\}$

(1) (a) For $\mathbf{\Gamma} = \mathbf{B}(\mathbf{p}^m)$: Compute $s_i[\tau]$ according to (4.3)

(b) For $\mathbf{\Gamma} = \mathbf{B}(\mathbf{p}^m)$: Compute $s_i[\tau]$ according to (4.4)

(2) Assign SIR target $\gamma_i[\tau] = \ell_i[\tau]/s_i[\tau]$

(3) Measure resulting interference $q_i[\tau]$

(4) Update load $s_i[\tau]$ in the ascent direction given by (4.7)

$$s_i[\tau+1] = s_i[\tau] + \delta_1 \Delta s_i[\tau].$$

(5) (a) For $\mathbf{\Gamma} = \mathbf{B}(\mathbf{p}^m)$: Update price $\nu_i[\tau]$ according to (4.5)

(b) For $\mathbf{\Gamma} = \mathbf{B}(\mathbf{p}^m)$: Update price $\nu_i[\tau]$ according to (4.6)

Continue: $\tau := \tau + 1$

---

The price update is based only on the link power or interference constraint, and the spillage calculation requires only local measurement at the MS of the channel gains to all the neighboring BSs (weighted by the sum of loads supported by links terminating at those BSs). There is no coordination across BSs, provided the BS transmits the sum of the loads from the links it is serving on the downlink. Finally, the load-update can be calculated locally at each MS.

Convergence and optimality of the algorithm have been shown:

---

**Theorem 4.1.** [65] For sufficiently small step size $\delta_1 > 0$ and $\delta > 0$, Algorithm 4.1 converges to the globally optimal solutions of problems (4.1) and (4.2) for $\mathbf{\Gamma} = \mathbf{B}(\mathbf{p}^m)$ and $\mathbf{\Gamma} = \mathbf{B}(\mathbf{q}^m)$ respectively.

---

The key steps of the proof are as follows. Since problems (4.1) and (4.2) are convex optimization problems, one can consider the maximization of Lagrangians of the problems and then consider minimization of the Lagrange dual problem. It is shown in [65] that the load update (4.7) is an ascent update to the Lagrangians, reparameterized in terms of the load factors. The boundedness of the first and second derivative of the utility functions and other technical condition is shown to be sufficient to guarantee the Lipschitz continuity property, thus ensuring the convergence to the Lagrangian maximum.

The update to the price vectors $\boldsymbol{\nu}$ corresponds to the gradient for the Lagrange multipliers if we allow the convergence to the Lagrangian maxima over $\mathbf{s}$ at every price $\boldsymbol{\nu}[t]$. However, the load factor $\mathbf{s}$ and price $\boldsymbol{\nu}$ can be updated simultaneously. Such a joint update can be proven to converge to the optimum of the original constrained optimization problem if the Lagrangian is concave and the maximized Lagrangian for a given price is convex [137]. This is indeed true and therefore the algorithm converges to the optimal.

Finally, it is shown in [65] that upon convergence, the KKT conditions [27] are satisfied and so the convergence point is indeed the optimal solution to the original problems.

### 4.3.3 Large Network Simulation

SIR optimization in a large network is demonstrated through the 3GPP2 simulator. The model consists of 19 cells arranged in a three ring hexagonal structure. Each cell is divided into three identical 120 degree sectors for a total of 57 BSs as depicted in Figure 4.2. Each realization of the network consists of 10 randomly selected MSs in each BS, for a total of 570 MSs.

The convergence of the LSPC algorithm 4.1 is illustrated in Fig. 4.3. The QoS metric $\beta_i$ used is $\beta_i = d\log(1 + c\gamma_i)$, with equal allocation of time-frequency resources across users within a sector. The algorithm is initialized with a random positive load vector $\ell$, and the step size is taken as $\delta_1 = 0.1$. The interference limit in terms of the ROT factor, the ratio of the total interference to noise, is set to 5, 10, and 15 dB, in different experiments. Shown as a horizontal line is the global optimum numerically attained by centralized computation. Each iteration consists of one power control update and is typically of the order of milliseconds as discussed in Chapter 10. It can be seen that the QoS from the distributed algorithm is almost identical to the optimal QoS within about 25, 35, and 50 iterations for ROT=5, 10, and 15dB, respectively. To compare timescale of convergence, the DPC algorithm with SIRs fixed at the optimal values (which is almost impossible to do in practice) is also plotted for each ROT and with random initialization of the powers. Convergence time of the DPC algorithm is about 15, 25,

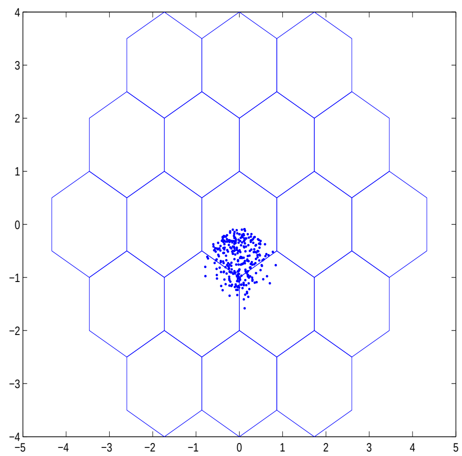


Fig. 4.2 Hexagonal cellular network for the uplink simulation consisting of 19 cells with wrap around. Cells are three-way sectorized for a total of 57 BSs. Cell radii are normalized to unity. Path loss accounts for log-normal shadowing, and angular antenna pattern. Plotted are the locations of 300 random MSs connected to the lower sector of the center cell. Other MSs are not shown explicitly.

and 50 iterations for ROT=5, 10, and 15dB, respectively, similar to the convergence time for the distributed optimal SIR algorithm. This shows that the speed of convergence of the LSPC algorithm is almost as fast as the standard power control for fixed SIR. As expected, the convergence time increases with the ROT limit. However, the convergence times remain reasonable with the practical ROT limits of 6 to 10 dB typically used in commercial networks.

Figure 4.4 shows the cumulative distribution of the user capacities at the final iteration of Algorithm 4.1. As discussed in Chapter 1, one of the desirable features of utility maximization is that this QoS distribution, and the efficiency-fairness tradeoff, can be varied by appropriately adjusting the utility. Figure 4.4 shows the resulting QoS distribution for the pseudo-linear utility, log utility, and the $\alpha$-fair utilities with $\alpha = 2$ and $\alpha = 3$ all with the same realization of MS distribution in the network. It can be seen that the variance in the MS's QoS with the $\{2,3\}$-fair distributions is significantly smaller than with the logarithmic and pseudo-linear utility functions. Consequently, fewer MSs are

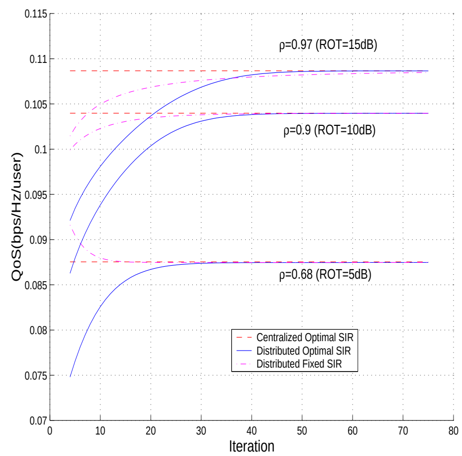


Fig. 4.3 Convergence of Algorithm 4.1 with the logarithmic utility at ROT=5,10,15dB. The logarithmic utility is plotted as the geometric mean user capacity. For comparison of rate of convergence, also shown is DPC algorithm's convergence if its fixed SIR targets so happens to be set at the optimum.

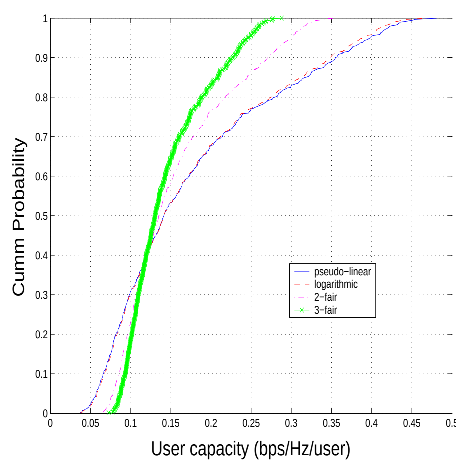


Fig. 4.4 User capacity distribution after 50 iterations of the distributed algorithm under different utility functions: $\alpha$-fair distribution with $\alpha = 1, 2, 3$, and the pseudo-linear utility.

seen with either very high or very low achievable capacities. In general, larger $\alpha$ enhances the fairness of SIR assignment while reducing the spectral efficiency in terms of b/s/Hz.

## 4.4 Open Problems

Two major open problems have already been discussed in the last section. One is problem (4.1) when the feasibility set is non-convex or the utility function non-concave. Two is the problem of joint power control and scheduling, where the equilibrium is not a fixed SIR assignment but a limit cycle of link activation schedule. These will be discussed further in Chapter 9.

Unlike the DPC algorithm where transient behaviors have been studied, SIR evolution before equilibrium in the LSPC algorithm has not been explored.

In all of the remaining chapters of this monograph, there is a dichotomy of problem formulations: those with fixed SIR and total power minimization as the objective function, and those where SIR is part of the optimization variables and total utility function is the objective function. We will see that in most cases, the general formulations with variable SIR remain open.

# 5

# Opportunistic Power Control

## 5.1 Introduction

Power control algorithms can exploit channel variations to improve the performance and fairness. This is achieved by opportunistically leveraging the instantaneous or past information of channel quality obtained through measurement and feedback. Work on opportunistic power control in both uplink and downlink include [109, 140, 171, 98, 200, 74, 99, 6, 152, 153, 171, 98, 200, 99, 6, 61].

The key idea of opportunistic power control is to spend more power and increase rate as channel quality improves, and to avoid using the channel below an optimized cutoff. For example, in uplink transmission in a frequency-flat fading channel, in order to maximize the total throughput, only a set of user with the overall best channel gain should be allowed to transmit its data at each time slot [91].

Opportunistic power control can also bring benefits to a network where the users typically belong to two priority groups, e.g., voice (higher priority) and data (lower priority) transmission in cellular network, or in cognitive radio network. Users in the higher priority group always get to maintain their SIR requirement, but due to the varying channel conditions and user mobility, users in the lower priority group get to share the channel and transmit opportunistically without violating the SIR requirement of the users with higher priority [157, 18].

## 5.2 Opportunistic Throughput Maximization in Uplink

In this section, two opportunistic power control schemes to maximize the total throughput in the network are presented based on [91, 101]. First, the authors in [91] consider a model for a fading channel with full channel state information and no interference among users [91]. The problem of maximizing the average throughput for all users is given as [91]:

$$\begin{array}{ll} \text{maximize} & \mathbb{E}\left[\sum_i \log\left(1+\frac{p_i G_i}{n_i}\right)\right] \\ \text{subject to} & \mathbb{E}\left[\sum_i p_i\right] \le p_{avg} \\ \text{variables} & \mathbf{p}, \end{array} \tag{5.1}$$

where the expectation in (5.1) is taken with respect to the channel fading statistics, $G_i$ is the direct channel gain, $n_i$ is Gaussian noise, nd $p_{avg}$ is the average power budget for all users.

The optimal strategy to (5.1) is such that the user with the largest channel gain is first selected, i.e., select User $k = \arg\max_i G_i$. The resulting optimal power allocation for User $k$ is given by

$$p^* = \left[\frac{1}{\lambda} - \frac{n_i}{\max_i G_i}\right]^+ \tag{5.2}$$

where $\lambda$ (the Lagrange multiplier corresponding to the constraint in (5.1)) is chosen to satisfy the average power constraint. As noted in [91], (5.2) can be geometrically interpreted as water-filling over time. More information-theoretic discussions on related topics can be found in [63].

Using a different channel model, the authors in [101] consider an opportunistic power control scheme for throughput maximization in an uplink channel that is interference-limited. The power control algorithm instructs a transmitter to increase its power when the channel is good and to decrease its power when the channel is bad, using a proposed metric called the *signal-interference product* and defined as follows:

$$\zeta_i = p_i \frac{\sum_{j \neq i} G_{ij} p_j + n_i}{G_{ii}}. \tag{5.3}$$

The transmit power is then adjusted according to the following algorithm [101].

---

**Algorithm 5.1 (Opportunisitc Power Control [101]).**

$$p_i[t+1] = \zeta_i \frac{\mathsf{SIR}_i[t]}{p_i[t]}, \quad \forall i. \tag{5.4}$$

---

The key advantage of the power control scheme in [101] is that all users update their power distributively. Furthermore, their scheme is shown to co-exist with users that use the DPC algorithm in Chapter 2.2. Other extensions include cases where maximum power constraint is imposed and soft handoff is executed distributively in [101], and opportunistic throughput maximization with fairness constraints in [102].

## 5.3 Opportunistic Utility Maximization in Downlink

In this section, opportunistic power control that maximizes the total utilities on the downlink of a cell is considered [171, 98]. In each time-slot, users are selected for transmission and the transmit power for each selected user is determined. The base-station has a maximum transmit power limit $P_T$.

### 5.3.1 Proportional fair scheduling

Consider the following case first. At each time-slot, BS transmits to at most one user, and each user sends a Data Rate Control (DRC) message to BS that indicates the rate at which BS can transmit to that user if it is selected. We also denote the amount of data that can be transmitted to the $i$th user in time-slot $t$ by $DRC_i[t]$. The Proportional Fair Scheduling (PFS) algorithm is an algorithm that schedules the channel for the user that maximizes [19, 171]:

$$\frac{DRC_i[t]}{r_i[t]} \tag{5.5}$$

where $r_i[t]$ is the exponentially smoothed average of the service rate received by the $i$th user, and is updated according to

$$r_i[t+1] = \begin{cases} (1-\theta)r_i[t] + \theta DRC_i[t], & \text{if } i = \arg\max_j \frac{DRC_j[t]}{r_j[t]}, \\ (1-\theta)r_i[t], & \text{otherwise.} \end{cases} \tag{5.6}$$

The PFS algorithm favors users that have a larger DRC value, which helps to keep the system throughput high. However, if the $i$th user is not receiving any service, the value of $1/r_i[t]$ increases, making PFS more likely to serve the $i$th user in the next time-slot. It is shown in [110, 171] that for users with infinite backlogs, the PFS algorithm maximizes the sum of the logarithms of the long-run average data rates provided to the users, i.e., $\sum_i \log r_i$, over all feasible scheduling rules. This objective is known as the proportional fair metric [110, 171].

### 5.3.2 General utility-based scheduling

In [98], the channel is allowed to vary across time-slots and is modeled as a stationary stochastic process. In a time-slot, the system is in one of the possible network states. Each state takes a value from a finite set $\{1, 2, \cdots, S\}$. Denote the probability that the system is in state $s$ by $\pi_s$. In [98], the SIR for the $i$th user when the system is in state $s$ is defined as

$$\gamma_{s,i}(\mathbf{p}_s) = \frac{G_{s,i}p_{s,i}}{\vartheta G_{s,i}(\sum_j p_{s,j} - p_{s,i}) + n_{s,i}}, \tag{5.7}$$

where $\mathbf{p}_s$ is the power allocation vector for all users, $p_{s,i}$ is the power allocation for the $i$th user, $G_{s,i}$ is the path gain from the base-station to the $i$th user, $\vartheta \in [0, 1]$ is a constant to model the non-orthogonality factor in the CDMA code, and $n_{s,i}$ is the background noise and inter-cell interference at the $i$th user, all defined when the system is in state $s$.

Similar to Chapter 4, a utility function $U_{s,i}$ is associated with the $i$th user at state $s$. Following [98], the problem with general constraints is first presented and then some special cases are highlighted in details. The opportunistic power scheduling problem is formulated as a stochastic optimization problem:

$$\begin{array}{ll} \text{maximize} & \sum_{s=1}^{S} \pi_s \sum_{i}^{N} U_{s,i}(\gamma_{s,i}(p_{s,i})) \\ \text{subject to} & \sum_{s=1}^{S} \pi_s g_{s,i}(\mathbf{p}_s) \geq c_i, \ \ \forall i \\ & \sum_i p_{s,i} \leq P_T \\ \text{variables} & \mathbf{p}_s, \ \ \forall s \end{array} \tag{5.8}$$

where $c_i$ is a given constant for all $i$, $\mathbf{p}_s = (p_{s,1}, p_{s,2}, \cdots, p_{s,N})$, $U_{s,i}(p_{s,i}) \stackrel{\triangle}{=} U_i(\gamma_{s,i}(p_{s,i}))$, and $\pi_s$ is the probability that the system is in state $s$. In this problem, $\sum_{s=1}^{S} \pi_s g_{s,i}(\mathbf{p}_s) \geq c_i$ could either be a performance or fairness constraint for the $i$th user, e.g., the generic function $g_{s,i}$ is a performance measure such as the total rate achieved by the $i$th user. Following [98], we assume that $U_{s,i}(p_{s,i})$ is a strictly concave function and $g_{s,i}(\mathbf{p}_s)$ is concave, continuous, and bounded.

Since BS should always transmit at its maximum transmission power, i.e., $\sum_i p_{s,i} = P_T$, we rewrite $\gamma_{s,i}(\mathbf{p}_s)$ in (5.7) as

$$\gamma_{s,i}(p_{s,i}) \stackrel{\triangle}{=} \frac{G_{s,i} p_{s,i}}{\vartheta G_{s,i}(P_T - p_{s,i}) + n_{s,i}}.$$

In (5.8), if the underlying probability distribution for the state of the system (i.e., $\pi_s$, $\forall s$) is known, the problem is equivalent to a deterministic convex optimization problem. However, in practice, no such a priori knowledge can be obtained. An opportunistic power control algorithm without the knowledge of the underlying probability distribution is given in the following. For a given state $s$, define the set of power vector that satisfies the total power constraint in (5.8) as $X_s = \{(p_{s,1}, p_{s,2}, \cdots, p_{s,N}) \mid, \ 0 \leq p_{s,i} \leq P_T, \ \forall\, i\}$.

---

**Algorithm 5.2 (Opportunistic Power Control [98]).** (1)

$$\mathbf{p}_s(\boldsymbol{\mu}) = \arg \max_{\mathbf{p}_s \in X_s} \{\sum_i U_{s,i}(p_{s,i}) + \mu_i g_{s,i}(\mathbf{p}_s)\}, \ s = 1, 2, \cdots, S. \tag{5.9}$$

(2)

$$\varrho_i[t] = g_{s[t],i}(\mathbf{p}_{s[t]}(\boldsymbol{\mu}[t])) - c_i, \ \forall\, i, \tag{5.10}$$

(3)

$$\mu_i[t+1] \ = \ [\mu_i[t] - \delta[t]\varrho_i[t]]^+, \ \forall\, i. \tag{5.11}$$

---

The development of Algorithm 5.2, through Lagrange duality and stochastic subgradient algorithm, is summarized based on [98]. First, consider the Lagrangian associated with (5.8):

$$\mathcal{L}(\boldsymbol{\mu}, \mathbf{p}) = \sum_{s=1}^{S} \pi_s \sum_i U_{s,i}(p_{s,i}) + \sum_i \mu_i (\sum_{s=1}^{S} \pi_s g_{s,i}(\mathbf{p}_s) - c_i), \quad (5.12)$$

where $\boldsymbol{\mu} = (\mu_1, \mu_2, \cdots, \mu_N)$. Then, the dual problem of (5.8) is defined as:

$$\min_{\boldsymbol{\mu} \geq \mathbf{0}} F(\boldsymbol{\mu})$$

where

$$F(\boldsymbol{\mu}) \;=\; \max_{\mathbf{p} \in X} \mathcal{L}(\boldsymbol{\mu}, \mathbf{p}) \quad (5.13)$$

and $X = \{(\mathbf{p}_1, \mathbf{p}_2, \cdots \mathbf{p}_S) \mid \mathbf{p}_s \in X_s,\; s = 1, 2, \cdots, S\}$.

For a given $\boldsymbol{\mu}$, the problem is separable in $s$ and, thus, $\mathbf{p}(\boldsymbol{\mu})$ maximizes $\mathcal{L}(\boldsymbol{\mu}, \mathbf{p})$ if and only if $\mathbf{p}(\boldsymbol{\mu}) = (\mathbf{p}_1(\boldsymbol{\mu}), \mathbf{p}_2(\boldsymbol{\mu}), \cdots, \mathbf{p}_S(\boldsymbol{\mu}))$, where

$$\mathbf{p}_s(\boldsymbol{\mu}) = \arg \max_{\mathbf{p}_s \in X_s} \{\sum_i U_{s,i}(p_{s,i}) + \mu_i g_{s,i}(\mathbf{p}_s)\},\; s = 1, 2, \cdots, S. \quad (5.14)$$

For a given $\boldsymbol{\mu}$ and system state $s$, the problem in (5.14) is a deterministic convex optimization problem.

Next, the dual problem (5.13) is solved in [98]. Note that $F(\boldsymbol{\mu})$ is a convex function of $\boldsymbol{\mu}$ and, thus, (5.13) is a stochastic convex optimization problem. A stochastic subgradient method is used in [98], which is defined by the following iterative process:

$$\mu_i[t+1] \;=\; [\mu_i[t] - \delta[t]\varrho_i[t]]^+,\; \forall\, i, \quad (5.15)$$

where $\varrho_i[t]$ is a random variable that represents the stochastic information of the first order gradient of $F(\boldsymbol{\mu})$. Let the sequence of solutions, $\boldsymbol{\mu}[0], \boldsymbol{\mu}[1], \cdots, \boldsymbol{\mu}[t]$, be generated by (5.15) and $\boldsymbol{\varrho}[t] = (\varrho_1[t], \varrho_2[t], \cdots, \varrho_N[t])$ be chosen such that

$$\mathbb{E}\{\boldsymbol{\varrho}[t] \mid \boldsymbol{\mu}[0], \boldsymbol{\mu}[1], \cdots, \boldsymbol{\mu}[\mathbf{t}]\} = \partial_{\boldsymbol{\mu}} F(\boldsymbol{\mu}[t]),$$

where $\partial_{\boldsymbol{\mu}} F(\boldsymbol{\mu}[t])$ is a subgradient of $F(\boldsymbol{\mu})$ with respect to $\boldsymbol{\mu}$ at $\boldsymbol{\mu} = \boldsymbol{\mu}[t]$. Then, the vector $\boldsymbol{\varrho}[t]$ is called a stochastic subgradient of $F(\boldsymbol{\mu})$ with respect to $\boldsymbol{\mu}$ at $\boldsymbol{\mu} = \boldsymbol{\mu}[t]$. In this case, by solving (5.15), $\boldsymbol{\mu}[t]$ converges to $\boldsymbol{\mu}^*$, the optimal solution of (5.13), with probability 1, if the following conditions are satisfied:

$$\mathbb{E}\{||\boldsymbol{\varrho}[t]||^2 \mid \boldsymbol{\mu}[0], \boldsymbol{\mu}[1], \cdots, \boldsymbol{\mu}[t]\} \leq c \tag{5.16}$$

for a constant $c$, and time-varying stepsizes satisfy the following standard conditions:

$$\delta[t] \geq 0, \ \sum_{t=0}^{\infty} \delta[t] = \infty, \ \text{and} \ \sum_{t=0}^{\infty} (\delta[t])^2 < \infty. \tag{5.17}$$

By Danskin's Theorem [23], $\partial_{\boldsymbol{\mu}} F(\boldsymbol{\mu})$ is obtained by

$$\partial_{\boldsymbol{\mu}} F(\boldsymbol{\mu}) = (d_1, d_2, \cdots, d_N), \tag{5.18}$$

where

$$d_i = \sum_{s=1}^{S} \pi_s g_{s,i}(\mathbf{p}_s(\boldsymbol{\mu})) - c_i, \ \forall i,$$

and $\mathbf{p}_s(\boldsymbol{\mu}) = (p_{s,1}(\boldsymbol{\mu}), p_{s,2}(\boldsymbol{\mu}), \cdots, p_{s,N}(\boldsymbol{\mu}))$ is a solution of the problem in (5.14). Hence, it can be shown that

$$\varrho_i[t] = g_{s[t],i}(\mathbf{p}_{s[t]}(\boldsymbol{\mu}[t])) - c_i, \ \forall i, \tag{5.19}$$

where $s[t]$ is an index of the system state at iteration $t$.

Finally, by the assumption that $g_{s[t],i}$ is bounded, the condition in (5.16) is satisfied, and the algorithm in (5.15) converges to the optimal solution that solves (5.13). Since the primal problem (5.8) has no duality gap, the algorithm also converges to the optimal power scheduling.

### 5.3.3 Special cases

Finally, some applications of the above opportunistic utility maximization framework [98] are illustrated for problem with separable constraints. When the performance or fairness constraint $g_{s,i}(\mathbf{p}_s)$ for each user $i$ can be separable, i.e., the constraint can be represented as

$$g_{s,i}(\mathbf{p}_s) = \sum_j a_{i,j} g_{s,i}^j(p_{s,j}), \ \forall i, \tag{5.20}$$

where $a_{i,j}$ is a given weight on each $g_{s,i}^j(p_{s,j})$ to reflect priority.

Problem (5.14) can be rewritten by

$$\mathbf{p}_s(\boldsymbol{\mu}) = \arg\max_{\mathbf{p}_s \in X_s} \{\sum_i \tilde{U}_{s,i}(\boldsymbol{\mu}, p_{s,i})\}, \tag{5.21}$$

where $\tilde{U}_{s,i}(\boldsymbol{\mu}, p_{s,i})$ is an adjusted utility function of the $i$th user.

$$\tilde{U}_{s,i}(\boldsymbol{\mu}, p_{s,i}) = U_{s,i}(p_{s,i}) + \sum_j \mu_j a_{j,i} g^i_{s,j}(p_{s,i}). \tag{5.22}$$

For a given $\boldsymbol{\mu}$ and system state $s$, $\tilde{U}_{s,i}(\boldsymbol{\mu}, p_{s,i})$ for user $i$ can be represented as a function of its own power allocation, as in the original utility function. Hence, by solving (5.21), the power allocation maximizes the sum of the adjusted utilities, $\tilde{U}_{s,i}(\boldsymbol{\mu}, p_{s,i})$'s, of all users with a constraint only on the total transmission power limit of BS.

**Utility-based fairness constraint.** Now consider an opportunistic power scheduling problem in which the $i$th user is guaranteed to achieve at least a fraction $\tilde{v}_i$ of the expected total system utility. This constraint is formulated as

$$\sum_{s=1}^{S} \pi_s U_{s,i}(p_{s,i}) - \tilde{v}_i \sum_{s=1}^{S} \pi_s \sum_j U_{s,j}(p_{s,i}) \geq 0,$$

where $\tilde{v}_i \geq 0$, and $\sum_i \tilde{v}_i \leq 1$. Hence, $c_i = 0$ and $g_{s,i}(\mathbf{p}_s)$ is separable and represented by (5.20) with

$$a_{i,j} = \begin{cases} 1 - \tilde{v}_i, & \text{if } i = j \\ -\tilde{v}_i, & \text{otherwise} \end{cases}$$

and

$$g^j_{s,i}(p_{s,j}) = U_{s,j}(p_{s,j}).$$

Again, from (5.22), the adjusted utility function

$$\tilde{U}_{s,i}(\boldsymbol{\mu}, p_{s,i}) = (1 + \mu_i - \sum_j \mu_j w_j) U_{s,i}(p_{s,i}),$$

is obtained by multiplying a weight factor $1 + \mu_i - \sum_j \mu_j w_j$ to the original utility function. Further, from (5.19) the stochastic subgradient is obtained as

$$\varrho_i[t] = U_{s[t],i}(p_{s[t],i}(\boldsymbol{\mu}[t])) - \tilde{v}_i \sum_j U_{s[t],j}(p_{s[t],i}(\boldsymbol{\mu}[t])),$$

which is the difference between the achieved utility of the user and its constraint based on power allocation in the current time-slot.

**Resource Based Fairness Constraint** Suppose the $i$th user is guaranteed to consume power by an amount that is at least $\upsilon_i$ fraction of the total transmission power:

$$\sum_{s=1}^{S} \pi_s p_{s,i} - \upsilon_i \sum_{s=1}^{S} \pi_s \sum_j p_{s,j} = \sum_{s=1}^{S} \pi_s p_{s,i} - \upsilon_i P_T \geq 0, \forall i, \tag{5.23}$$

where $\upsilon_i \geq 0$ and $\sum_i \upsilon_i \leq 1$. Hence, $c_i = 0$ and $g_{s,i}(\mathbf{p}_s)$ is separable and represented by (5.20) with

$$a_{i,j} = \begin{cases} 1 - \upsilon_i, & \text{if } i = j \\ -\upsilon_i, & \text{otherwise} \end{cases}$$

and

$$g_{s,i}^{j}(p_{s,j}) = p_{s,j}.$$

From (5.19) and (5.22), the adjusted utility function is obtained as

$$\tilde{U}_{s,i}(\boldsymbol{\mu}, p_{s,i}) = U_{s,i}(p_{s,i}) + \mu_i p_{s,i},$$

which is achieved by adding an offset value $\mu_i p_{s,i}$ to the original utility function and the stochastic subgradient is obtained as

$$\varrho_i[t] = p_{s[t],i}(\boldsymbol{\mu}[t]) - \upsilon_i P_T,$$

i.e., the difference between the amount of power allocated to the user in the current time-slot and its constraint value.

## 5.4 Open Problems

In opportunistic power control, feedback of both channel state and resource allocation is crucial in selecting a set of users to transmit. For example, the opportunistic power control algorithm in [91] is that it requires the prior knowledge of a Lagrange multiplier $\lambda$ that is associated with the average power constraint. Obtaining $\lambda$ requires some form of long-term estimation for the channel state information. An open problem is to characterize the impact of limited, delayed feedback, or inaccurate, out-of-date estimation, on opportunistic power control, such as the suboptimality gap thus caused. Suboptimality gap can also arise due to nonconvex utility functions of users, e.g., in opportunistic power control in [98]. The problem formulation then becomes nonconvex, which is in general difficult to solve as we will see throughout the monograph.

# 6

# Non-cooperative Power Control

## 6.1 Introduction

The interests of MSs are not aligned: they compete for limited radio resources. We have assumed that they will update their powers for social welfare maximization thus far in the monograph, but they may not have to. The interests of the wireless network operator could also be in conflict with those of end users. In both cases, non-cooperative power control problems need to be formulated, solved, and analyzed as games. In these formulations, summarized in this chapter, each game consists of three tuples: a set of players indexed by $i$, a selfish utility function $U_i$ for each player, and a set of feasible strategy space $\mathcal{A}_i$ for each player.

When a problem is formulated and solved as a non-cooperative game [112], game theory provides standard procedures to study its equilibriums, such as existence, uniqueness, stability under various strategies, and optimality gap. The most frequently used concept of equilibrium in game theory is *Nash equilibrium*, which is defined as a set of individual policies at which no player may gain by unilaterally deviating [50]. A Nash equilibrium power allocation $\mathbf{p}^*$ is one where no MS has incentive

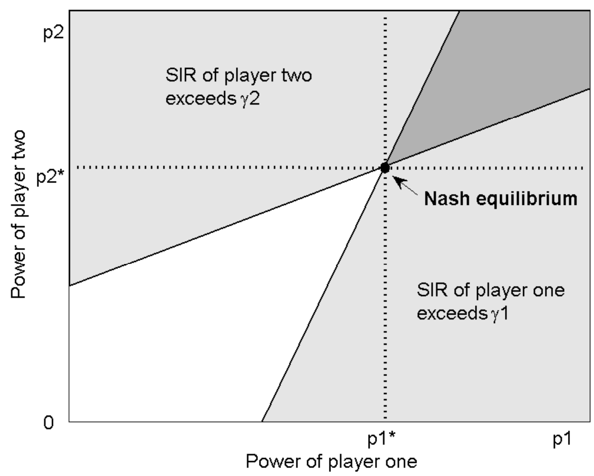


Fig. 6.1 Illustration of a Nash equilibrium for a two-player power control game.

to unilaterally change its power:

$$U_i(p_i^*, \mathbf{p}_{-i}^*) \geq U_i(p_i, \mathbf{p}_{-i}^*), \quad \forall p_i \in \mathcal{A}_i \tag{6.1}$$

where $\mathbf{p}_{-i}$ denote the vector of powers of all MSs other than MS $i$.

The power control problems discussed in Chapter 2 and Chapter 4 can also be reformulated and analyzed in the game-theoretic framework. With fixed SIR targets, the authors in [9, 170] show that the classical power control problems studied by [57, 197, 17] can be modeled as noncooperative games with submodularity structure [162, 9, 170]. Let $\mathcal{A}_i(\mathbf{p}_{-i})$ be the set of feasible power policies for MS $i$ that depends on power allocations of all other MSs. A game is *submodular* if all sets $\mathcal{A}_i(\cdot)$ are compact and descending in all values of their argument

$$\mathbf{p}_{-i} < \tilde{\mathbf{p}}_{-i} \implies \mathcal{A}_i(\mathbf{p}_{-i}) \supset \mathcal{A}_i(\tilde{\mathbf{p}}_{-i}). \tag{6.2}$$

It has been shown that the best-response strategy of this game is equivalent to the DPC algorithm discussed in Chapter 2 [9, 170]. On the other hand, when variable SIRs are considered, individual utility functions can be assigned to MSs measuring transmission power they consume and the SIR that they attain. Each MS is then assumed to decide on his own transmission power level so as to maximize his utility. Possible utility functions and their properties for both voice and data sources have been investigated in detail in [49, 117].

Continuing our discussion on utility function in Chapter 1, we will see that a variety of selfish utility functions have been used in noncooperative power control formulations. For example, in [162], utility is defined for single carrier systems such that each MS seeks to minimize the distance between its achieved SIR and its specified target. In [84], linear and exponential utility functions based on carrier SIR are proposed for multi-carrier systems. In both work, the existence of a Nash equilibrium is proven under certain assumptions on the utility functions, and an algorithm for solving the noncooperative power control game suggested. To take transmit power consumption also into account, in [145], the authors introduce a utility function defined as the ratio of throughput to transmit power. This result has since been generalized in [114] to multi-carrier CDMA networks, in [120, 115, 28] to study the cross-layer problem of joint power control and modulation-receiver design, and in [118, 119] to allow for QoS constraints (e.g. delay and average rate) and to quantify the tradeoffs between energy efficiency and QoS metrics. These utility functions have also been applied to wireless ad-hoc networks [77, 76] and ultrawideband networks in frequency-selective multi-path environments [15, 14].

Nash equilibrium are often suboptimal in total utility attained [10]. This optimality gap due to non-cooperation among MSs motivates pricing mechanisms to align selfish interests [173] to social welfare maximization. This approach is complementary to the one where a global optimization is first formulated and decomposition techniques are then used to derive a distributed algorithm. Both approaches eventually hope to arrive at an optimal and distributed solution.

A pricing scheme is first studied in [143] using submodular games. It quantifies the intuition that a noncooperative power control game with a pricing scheme is superior to one without pricing, in terms of fairness and algorithm convergence. Other works studying pricing include [187, 165, 8, 166, 41, 182, 181, 97, 96] for different utility functions and network models. In particular, in [8, 166], a cost function is introduced as the difference between the pricing of transmission power and user-centric utility functions, and the existence of a unique Nash equilibrium is established. Later, these results are extended to a more general scenario, where a network-centric pricing scheme is considered and each MS has the freedom to choose its own BS [96, 97]. This joint power control, network pricing and BS assignment problem has also been considered in [55] as a hybrid non-cooperative game.

This chapter provides an overview of the above results. In each section, when a design problem is formulated as a game, the following common set of questions will be considered: Does the game have a steady state (existence of Nash equilibrium)? What are those steady states (characterization of Nash equilibrium)? Is the steady state(s) desirable (optimality of Nash equilibrium)? When will the game dynamics reach the steady state (convergence of Nash equilibrium), especially under the best response strategy where each MS adjusts its variable by maximizing selfish utility under the assumption that no other MSs would change?

## 6.2 Fixed-SIR Power Control as Game

The power control problem with fixed SIRs discussed in Chapter 2 can be reformulated and analyzed within the game-theoretic framework, where each MS decide dynamically on his own transmission power level so as to minimize it.

The power control problem in Chapter 2 is repeated here:

$$\begin{array}{ll} \text{minimize} & \sum_i p_i \\ \text{subject to} & \mathsf{SIR}_i(\mathbf{p}) \geq \gamma_i, \ \ \forall i \\ \text{variables} & \mathbf{p}. \end{array} \tag{6.3}$$

First observed that although power control decisions are coupled due to the SIR constraints, total power can be computed so as to minimize the power of each MS separately while satisfying the SIR constraints. Therefore, problem (6.3) can be viewed as a noncooperative game: the utilities (i.e., transmit powers) are each assigned to one MS, and maximization subject to SIR constraints is performed by each MS.

In this game, each MS solves the following selfish optimization:

$$\begin{array}{ll} \text{minimize} & p_i \\ \text{subject to} & p_i \in \mathcal{A}_i(\mathbf{p}_{-i}) \\ \text{variable} & p_i \end{array} \tag{6.4}$$

where $\mathcal{A}_i(\mathbf{p}_{-i})$ is the set of feasible power policies for MS $i$ that depends on the power allocations $\mathbf{p}_{-i}$ of all other MSs, i.e.

$$\mathcal{A}_i(\mathbf{p}_{-i}) = \{p_i \geq 0 : \mathsf{SIR}_i(p_i, \mathbf{p}_{-i}) \geq \gamma_i\}. \tag{6.5}$$

It can be verified that

$$\mathbf{p}_{-i} < \tilde{\mathbf{p}}_{-i} \implies \mathcal{A}_i(\mathbf{p}_{-i}) \supset \mathcal{A}_i(\tilde{\mathbf{p}}_{-i}), \tag{6.6}$$

i.e., the policy sets $\mathcal{A}_i(\cdot)$ are submodular [9]. The power control algorithms described in Chapter 2 can be viewed as submodular games defined by (6.4) and (6.5) with coupled policy sets, where the set of feasible transmit powers for each MS depends on the powers of all other MSs. The best response strategy of MS $i$ gives

$$p_i^* = \gamma_i \left( \sum_{j \neq i} G_{ij} p_j + n \right) \tag{6.7}$$

recovering the DPC algorithm in Chapter 2. The next result naturally follows:

---

**Theorem 6.1.** [9] For the power-control submodular game defined by (6.4) and (6.5), a unique Nash equilibrium exists. Further, starting with any feasible power allocation, a sequence of best-response power updates defined by (6.7) monotonically converges to the equilibrium.

---

This game-theoretic approach provides an alternative angle to the approach of fixed-point iteration for standard interference functions in Chapter 2. The result has also been generalized to the case where perfect channel state information is not available through a model of min-max game [68]. When variable SIR and maximum transmission power constraints are considered, other power control games could be formulated by assigning more complicated utility functions to individual MSs. For example, one possible way to handle the variable-SIR case is to formulate a game with no power constraints, but in which the objective of each MS is to minimize a specific cost function incorporating both SIR and transmit power. This approach will be discussed in the next section.

## 6.3 Linear Pricing Game

For power control with variable SIRs, a cost function can be introduced as the difference between the price of transmission power and data rates. For example, authors in [8] define a utility function as the difference between a linear pricing function proportional to transmitted power and a logarithmic function of SIR:

$$U_i(p_i, \mathbf{p}_{-i}) = \mu_i \log(1+\gamma_i) - \lambda_i p_i, \tag{6.8}$$

with pricing parameters $\lambda_i$ and $\mu_i$.

Consider a single-cell with $N$ MSs, where the cost function is defined by (6.8) and the SIR for MS $i$ is given by

$$\gamma_i(p_i, \mathbf{p}_{-i}) = D \frac{G_{ii} p_i}{\sum_{j \neq i} G_{ij} p_j + n}. \tag{6.9}$$

where $D > 1$ is the spreading gain of a CDMA system [8] [1]. The MS problem for this game is then formulated as

$$\begin{array}{ll} \text{minimize} & U_i(p_i, \mathbf{p}_{-i}) \\ \text{subject to} & p_i \in \mathcal{A}_i \\ \text{variable} & p_i \end{array} \tag{6.10}$$

where $\mathcal{A}_i = \{p_i \geq 0\}$ is the set of non-nonnegative power allocations. Taking the derivative of the cost function (6.8) with respect to $p_i$ , the first-order necessary condition can be obtained as follows:

$$\frac{\partial U_i(p_i, \mathbf{p}_{-i})}{\partial p_i} = \lambda_i - \frac{\mu_i D G_{ii}}{\sum_{j \neq i} G_{ij} p_j + D G_{ii} p_i + n} = 0 \tag{6.11}$$

At a Nash equilibrium, equation (6.11) holds for $i = 1, \ldots, N$. It is easy to see that the second derivative is positive, and hence the Nash equilibrium, if it exists, is the unique point minimizing the cost function.

[1] We have suppressed spreading gain by absorbing it into the $G_{ii}$ term when talking about CDMA systems in other chapters, but in this chapter certain results are best illustrated by making spreading gains explicit in the formula of SIR.

Therefore, based on (6.11), the best response of MS $i$ is derived as

$$p_i^* = \frac{1}{G_{ii}} \left[ \frac{\mu_i G_{ii}}{\lambda_i} - \frac{n}{D} - \frac{1}{D} \sum_{j \neq i} G_{ij} p_j \right]^+ . \tag{6.12}$$

The best response in (6.12) depends on both user-specific parameters, like $\mu_i$ and $\lambda_i$, and network parameters, such as $D$ and the total interference received at the BS. A parallel update algorithm for computing the Nash equilibrium is proposed in [8].

---

**Algorithm 6.1 (Best Response for Linear Pricing Game [8]).**

(1) BS measures interference $q_i[t] = \sum_{j \neq i} G_{ij} p_i[t] + n$, and feedbacks it to MSs.
(2) Each MS update power according to (6.12):

$$p_i[t+1] = \frac{1}{G_{ii}} \left[ \frac{\mu_i G_{ii}}{\lambda_i} - \frac{1}{D} q_i[t] \right]^+$$

---

The convergence of Algorithm 6.1 and the uniqueness of its equilibrium solution is characterized by the following theorem.

---

**Theorem 6.2.** [8] The power game by (6.10) admits a unique Nash equilibrium. Algorithm 6.1 is globally stable and converges to the unique equilibrium solution from any feasible starting point $\mathbf{p}[0]$ if the spreading gain is sufficiently large: $\frac{N-1}{D} < 1$.

---

## 6.4 Energy-efficiency Utility Game: Single-carrier

The tradeoff between higher throughput and higher energy expenditure can also be quantified by defining a utility function that depends on the ratio, rather than the difference, between throughput and energy [64, 117], i.e.,

$$U_i(p_i, \mathbf{p}_{-i}) = \frac{T_i(\mathbf{p})}{p_i}. \tag{6.13}$$

This utility has units of *bits/Joule*. It measures the total number of reliable bits transmitted per Joule of energy consumed and is particularly suitable for applications where saving transmit power is critical. Throughput $T_i(\mathbf{p})$ in equation (6.13) represents the net number of information bits that are transmitted without error per unit time, instead of the capacity-formula based expression. For a single-carrier CDMA uplink, it can be expressed as [145]

$$T_i(\mathbf{p}) = \frac{D_t}{D_f} r_i f(\gamma_i) \quad \text{and} \quad \gamma_i = D \frac{G_{ii} p_i}{\sum_{j \neq i} G_{ij} p_j + n} \tag{6.14}$$

where $D$ is the spreading gain of the CDMA system; $D_t$ and $D_f$ are the number of information bits and the total number of bits in a packet, respectively; $r_i$ and $\gamma_i$ are the transmission rate and the SIR for MS $i$, respectively; and $f(\gamma_k)$ is the Packet Success Rate (PSR) function, i.e., the probability that a packet is received without an error. The PSR function is assumed to be increasing, continuous, and S-shaped [2] with $f(\infty) = 1$ and $f(0) = 0$. It has be shown that for a PSR function satisfying these assumptions, the utility function in (6.13) is a quasiconcave function [3] of the MS transmit power [144]. This is also true if the throughput in (6.14) is replaced with an increasing and concave function of $\gamma_i$.

The problem of maximizing the sum of energy-efficient utilities (6.13) can be viewed as a noncooperative game. In the best response strategy, each MS $i$ optimizes its own utility $U_i(p_i, \mathbf{p}_{-i})$, given the transmission powers $\mathbf{p}_{-i}$ of other MSs fixed. This MS problem is formulated as follows

$$\begin{array}{ll} \text{maximize} & U_i(p_i, \mathbf{p}_{-i}) \\ \text{subject to} & p_i \in \mathcal{A}_i \\ \text{variable} & p_i \end{array} \tag{6.15}$$

where $\mathcal{A}_i = \{0 \leq p_i \leq p_i^m\}$ is the set of feasible power allocations for MS $i$. It is shown in [145] that the best response solution can be

[2] An increasing function is S-shaped if there is a point above which the function is concave, and below which the function is convex

[3] The function $f$ defined on a convex set $\mathcal{S}$ is quasiconcave if every superlevel set of $f$ is convex, i.e., $\{x \in \mathcal{S} | f(x) \geq a\}$ is convex for every value of $a$.

obtained by truncating the solution of an unconstrained optimization, i.e.

$$p_i^* = \min\{\tilde{p}_i, p_i^m\} \tag{6.16}$$

where $\tilde{p}_i$ $=\text{argmax}_{p_i \geq 0} U_i(p_i, \mathbf{p}_{-i})$ is the unconstrained maximizer of the utility in (6.13). The property of Nash equilibrium is summarized in following theorem.

---

**Theorem 6.3.** [145] The power game by (6.15) has a unique Nash equilibrium. At the equilibrium, a MS either attains the utility-maximizing power allocation or it fails to do so and transmits at maximum power $p_i^m$.

---

This result simplifies the computation of the best response solution and leads to the an efficient update algorithm below for computing the Nash equilibrium. It is shown [145] that the algorithm converges to the unique equilibrium solution from any feasible starting point.

---

**Algorithm 6.2 (Single-carrier energy-efficient power control [145]).**

(1) Each MS computes the unconstrained maximizer $\tilde{p}_i[t]$ for his individual utility $U_i$ in (6.13).
(2) Each MS updates power according to (6.17), i.e.,

$$p_i[t+1] = \min\{\tilde{p}_i[t], p_i^m\}$$

.

---

This game-theoretic approach with energy-efficient utility functions has also been extended in [116] to multiuser receivers, in [114, 201] to multi-carrier systems, in [202] to CDMA systems with multiple antennas, and in [15, 14] to ultrawideband systems.

## 6.5 Energy-efficiency Utility Game: Multi-carrier

Consider the uplink of a synchronous multi-carrier CDMA data network with $N$ MSs, $L$ carriers, and processing gain $D$ (for each carrier). The carriers are assumed to be sufficiently far apart so that inter-carrier interference is negligible. [44]. At the transmitter, the incoming bits for MS $i$ are divided into $L$ parallel streams and each stream is spread using the spreading code of MS $i$. The $L$ parallel streams are then sent over the $L$ (orthogonal) carriers. If random spreading sequences are used, the output SIR for the $\ell$th carrier of the $i$th MS with a matched filter receiver is given by

$$\gamma_i^\ell(p_i^\ell, \mathbf{p}_{-i}^\ell) = D\frac{p_i^\ell G_{ii}^\ell}{\sum_{j\neq k} p_j^\ell G_{ij}^\ell + n^\ell} \tag{6.17}$$

where $G_{ij}^\ell$ is the path gain for the $\ell$th carrier of MS $i$.

Then, similar to the single carrier case discussed in Section 6.4, a non-cooperative game in which each MS chooses its transmit powers over the $L$ carriers to maximize its overall energy-efficient utility can be formulated. Let $\mathbf{p}_i = [p_i^1, \ldots, p_i^L]$ be the power allocation vector of MS $i$ on the $L$ carriers. The utility function for MS $i$ is defined as the ratio of the total throughput to the total transmit power for the $L$ carriers, i.e.,

$$U_i(\mathbf{p}_i, \mathbf{p}_{-i}) = \frac{\sum_{\ell=1}^L T_i^\ell}{\sum_{\ell=1}^L p_i^\ell}, \tag{6.18}$$

where $T_i^\ell$ is the throughput achieved by MS $i$ over the $\ell$th carrier, and is given by $T_i^\ell = \frac{D_t}{D_f} r_i f(\gamma_i^\ell)$. Let $\mathcal{A}_i = \{p_i^\ell, \forall \ell : 0 \le p_i^\ell \le p^m\}$ be the set of feasible power allocations for MS $i$. The resulting non-cooperative game can be expressed as the following maximization problem:

$$\begin{array}{ll} \text{maximize} & U_i(\mathbf{p}_i, \mathbf{p}_{-i}) \\ \text{subject to} & \mathbf{p}_i \in \mathcal{A}_i \\ \text{variables} & \mathbf{p}_i. \end{array} \tag{6.19}$$

If equal transmission rates for all MSs are assumed, (6.19) can be simplified to

$$\begin{array}{ll} \text{maximize} & \frac{\sum_\ell f(\gamma_i^\ell)}{\sum_\ell p_i^\ell} \\ \text{subject to} & \mathbf{p}_i \in \mathcal{A}_i \\ \text{variables} & \mathbf{p}_i. \end{array} \tag{6.20}$$

Compared to the non-cooperative power control game in the single carrier case, there are two difficulties to the problem (6.20). One is that power allocation strategies of MSs in the multi-carrier case are vectors (rather than scalars) and this leads to an exponentially larger strategy set for each MS. Secondly, the energy efficiency utility function is now non-quasiconcave. This means that many of the standard theorems from game theory cannot be used here, even for the existence of Nash equilibrium.

To understand the structure of the best response of MS $i$ in this game, it has been shown in [114] that, when power allocation of other MSs are fixed, the utility maximization of a single MS (6.20) can be solved by the following optimal solution. Let $\gamma^*$ denote the unique (positive) solution of $f(\gamma) = \gamma f'(\gamma)$.

---

**Theorem 6.4.** [114] For all linear receivers and with transmit powers of all other MSs fixed, the utility function of MS $i$, given by (6.18), is maximized when

$$p_i^\ell = \begin{cases} p_i^{L_i,*} & \text{for} \quad \ell = L_i \\ 0 & \text{for} \quad \ell \neq L_i \end{cases}, \tag{6.21}$$

where $L_i = \arg\min_\ell p_i^{\ell,*}$ with $p_i^{\ell,*}$ being the transmit power required by MS $i$ to achieve an output SIR equal to $\gamma^*$ on the $\ell$th carrier, or $p^m$ if $\gamma^*$ cannot be achieved.

---

This theorem states that the utility for MS $i$ is maximized when the MS transmits only over its best carrier such that the achieved SIR at the output of the uplink receiver is equal to $\gamma^*$. The best carrier is defined as the one that requires the least amount of transmit power to achieve $\gamma^*$ at the output of the uplink receiver. A set of power vectors, $\mathbf{p}_1^*, \cdots, \mathbf{p}_N^*$, is a Nash equilibrium if and only if they simultaneously satisfy (6.21).

For the existence and uniqueness of Nash equilibriums, it has been shown in [114] that, depending on the set of channel gains, the proposed power control game may have no equilibrium, a unique equilibrium, or more than one equilibrium. The following theorem helps identify the Nash equilibrium (when it exists) for a set of given channel gains and matched filter receiver.

---

**Theorem 6.5.** [114] A necessary condition for MS $i$ to transmit on the carrier $\ell$ at equilibrium is that

$$\frac{G_{ii}^{\ell}}{G_{ii}^{(\tilde{\ell})}} > \frac{\Theta_{n(\ell)}}{\Theta_{n(\tilde{\ell})}}\,\Theta_0, \quad \text{for all } \tilde{\ell} \neq \ell\ , \tag{6.22}$$

where $n(\ell)$ is the number of MSs transmitting on the $\ell$th carrier and

$$\Theta_n = \frac{1}{1-(n-1)\frac{\gamma^*}{D}}, \quad n = 0, 1, \cdots, N. \tag{6.23}$$

When this condition is satisfied, the optimal transmit power for MS $i$ is given by $p_i^{\ell,*} = \frac{\gamma^*}{G_{ii}^{\ell}} n\Theta_{n(\ell)}$.

---

Based on (6.23), when the gain is sufficiently large: $D > (N-1)\gamma^*$, it follows that $0 < \Theta_0 < \Theta_1 < \Theta_2 < \cdots < \Theta_N$ with $\Theta_1 = 1$. For each of the $L^N$ possible equilibria, the channel gains for each MS must satisfy $L-1$ inequalities similar to (6.22). Furthermore, satisfying a set of $N(L-1)$ of such inequalities by the $N$ MSs is sufficient for existence of Nash equilibrium but the uniqueness is not guaranteed. For example, for the case of $N = L = 2$, the four possible equilibria can be characterized as follows.

- For both MSs to transmit on the first carrier at equilibrium, a necessary condition is $\frac{G_{11}^{(1)}}{G_{11}^{(2)}} > \Theta_2$ and $\frac{G_{22}^{(1)}}{G_{22}^{(2)}} > \Theta_2$.
- For both MSs to transmit on the second carrier at equilibrium, a necessary condition is $\frac{G_{11}^{(1)}}{G_{11}^{(2)}} < \frac{1}{\Theta_2}$ and $\frac{G_{22}^{(1)}}{G_{22}^{(2)}} < \frac{1}{\Theta_2}$.
- For MS 1 and MS 2 to transmit on the first and second carriers, respectively, at equilibrium, a necessary condition is $\frac{G_{11}^{(1)}}{G_{11}^{(2)}} > \Theta_0$ and $\frac{G_{22}^{(1)}}{G_{22}^{(2)}} < \frac{1}{\Theta_0}$.

- For MS 1 and MS 2 to transmit on the second and first carriers, respectively, at equilibrium, a necessary condition is $\frac{G_{11}^{(1)}}{G_{11}^{(2)}} < \frac{1}{\Theta_0}$ and $\frac{G_{22}^{(1)}}{G_{22}^{(2)}} > \Theta_0$.

A sequential, distributed algorithm is proposed in [114] to compute a Nash equilibrium of this game. The algorithm is applicable to all linear receivers including the matched filter, decorrelating and MMSE detectors.

---

**Algorithm 6.3 (Multi-carrier Energy-efficient Power Control [114]).**

(1) Start with MS $i = 1$.
(2) Given the transmit powers of other MSs, MS $i$ picks its best carrier which requires the least amount of transmit power for achieving $\gamma^*$.
(3) MS $i$ transmits only on this carrier at a power level $p_i^\ell[t]$ such that it achieves an output SIR equal to $\gamma^*$.
(4) Let $i = i + 1$ and consider the next MS.
(5) If $i \leq N$ then go back to step (2).
(6) Stop if the powers have converged; otherwise go to step (1).

---

This is a sequential best response algorithm. In particular, it is sufficient for the MS to only know its own received SIRs on each carrier. This information can for example be fed back to MS from BS.

It is clear that if the above algorithm converges, it will converge to a Nash equilibrium. The question that remains to be answered is whether or not the above algorithm converges whenever a Nash equilibrium exists. In [114], it has been shown that for the two-MS two-carrier case, Algorithm 6.3 converges to a Nash equilibrium when it exists. Tracing the possible combinations of best response dynamics, convergence is also proved for the case of two MSs and $L$ carriers as well as for the three-MS two-carrier case. In the case of multiple Nash equilibria, the algorithm converges to one of the equilibria depending on the starting point. Properties of Nash equilibrium, such as the number of MSs on each carrier, are also characterized in [114].

## 6.6 Game with Network Pricing and BS Assignment

Game models for power control can be further extended by adding the network as an active player to the game. In this section, we survey a joint game formulation for power control, network pricing and BS assignment.

The following network pricing mechanism is proposed by [54] to mediate between conflicting MS and network objectives: Each MS's objective is to maximize its net utility, while the network operator's objective is to maximize its revenue. Suppose the network charges MS $i$ proportional to its throughput $T_i$ with a unit price $\lambda_i$. Let $U_i$ be the utility function for MS $i$ as introduced in Section 6.4. Then the net utility for MS $i$ is defined by

$$U_i^{net} = U_i - \lambda_i T_i \tag{6.24}$$

where $T_i$ is the throughput that depends on the PSR function introduced in the last section. On the network side, the objective is to choose the optimal unit price vector $\boldsymbol{\lambda}$ that maximizes the total revenue, i.e.,

$$U^{rev}(\boldsymbol{\lambda}) = \sum_i \lambda_i T_i. \tag{6.25}$$

Consider the system model and utility function $U_i$ introduced in Section 6.4. Let $\sigma_i$ denotes the index of the BS serving MS $i$. Taking BS assignment into account, we have

$$U_i(\sigma_i, p_i, \mathbf{p}_{-i}) = \frac{T_i(\sigma_i, p_i, \mathbf{p}_{-i})}{p_i} = \left(\frac{D_t}{D_f} r_i\right) \frac{f(\gamma_i)}{p_i}. \tag{6.26}$$

Now $|h_{\sigma_i j}|^2$ denotes the channel from MS $j$ to BS $\sigma_i$. The SIR $\gamma_i$ in equation (6.26) depends on the BS-assignment and is given by

$$\gamma_i = \mathsf{SIR}_i(\sigma_i, p_i, \mathbf{p}_{-i}) = D \frac{|h_{\sigma_i i}|^2 p_i}{\sum_{j \in C_i(\boldsymbol{\sigma})} |h_{\sigma_i j}|^2 p_j + n}. \tag{6.27}$$

where $C_i(\boldsymbol{\sigma})$ is the set of MSs interfering with MS $i$ under current BS assignment $\boldsymbol{\sigma}$.

The joint power control, BS assignment, and network pricing problem can be modeled as game among MSs and the network. Let $\mathcal{S}_i$ be the set of allowable BSs that MS $i$ can connect to. With the network broadcasts unit price vector $\boldsymbol{\lambda}$, each MS individually maximizes its net utility, over two degrees of freedom: transmit power and BS assignment:

$$\begin{array}{ll} \text{maximize} & U_i(\sigma_i, p_i, \mathbf{p}_{-i}) - \lambda_i T_i(\sigma_i, p_i, \mathbf{p}_{-i}) \\ \text{subject to} & \sigma_i \in \mathcal{S}_i \\ \text{variables} & p_i, \sigma_i \end{array} \tag{6.28}$$

On the other side, network operator tries to find its highest revenue by searching over all feasible price vector $\boldsymbol{\lambda}$ in some constraint set $\Lambda$:

$$\begin{array}{ll} \text{maximize} & \sum_i \lambda_i T_i(\sigma_i, \mathbf{p}) \\ \text{subject to} & \boldsymbol{\lambda} \in \Lambda \\ \text{variables} & \boldsymbol{\lambda} \end{array} \tag{6.29}$$

Solving the joint user-network game described by (6.28) and (6.29) is difficult. So far, it is not even clear whether there exists a Nash equilibrium for this game, although some heuristic algorithms seem to solve the problem according to numerical experiments [55]. As a result, previous work usually makes the assumption that the price vector $\boldsymbol{\lambda}$ is known or given by a separate algorithm, and then focuses on Nash equilibrium of the user game (6.28) only.

Solving Nash equilibrium for the joint BS assignment and power control problem (6.28) is not trivial either. It is easy to see that an exhaustive searching over all possible combination of BS assignments and transmitter powers would be computationally intensive. The search can be simplified by noting that the objective function in (6.28) is monotonically increasing in $\lambda_i$, leading to the following result:

---

**Theorem 6.6.** [55] Given an interference vector $\mathbf{p}_{-k}$, the BS assignment based on the net utility maximization (6.28) is equivalent to the one based on maximizing SIR, i.e.,

$$\begin{aligned} \sigma_i^* &= \arg\max_{\sigma_i} U_i(\sigma_i, \mathbf{p}) - \lambda_i T_i(\sigma_i, \mathbf{p}) \\ &= \arg\max_{\sigma_i} \gamma_i(\sigma_i, \mathbf{p}). \end{aligned} \tag{6.30}$$

---

Furthermore, the SIR maximization for MS $i$ over the BS assignment can be carried out independently of its power optimization. Therefore, the user problem can be optimally solved by assigning the BS first, followed by power control. The algorithm proposed in [55] is summarized as follows.

---

**Algorithm 6.4 (Joint Power Control and BS assignment [55]).**

(1) MSs find the optimal BS assignment

$$\sigma_i[t+1] = \arg\max_{\sigma_i} \gamma_i(\sigma_i[t], \mathbf{p}[t])$$

.

(2) Given the transmit powers of other MSs, each MS updates its transmit power by

$$p_i[t+1] = \arg\max_{p_i} U_i(\sigma_i[t+1], p_i, \mathbf{p}_{-i}[t]) - \lambda_i T_i(\sigma_i[t+1], p_i, \mathbf{p}_{-i}[t])$$

.

---

If Algorithm 6.4 converges, it achieves a Nash equilibrium of the joint BS assignment and power control game, with equilibrium power vector $\mathbf{p}^*$ and BS assignment vector $\sigma^*$. The condition for the existence of the Nash equilibrium is stated in the following theorem.

---

**Theorem 6.7.** [55] A unique Nash equilibrium vector exists for the power-control game (6.28) if bit error rate $\mathsf{BER}(\gamma)$ decays exponentially in SIR $\gamma$ and the PSR function $f(\gamma_i)$ is given by

$$f(\gamma_i) = [1 - 2\mathsf{BER}(\gamma_i)]^{D_f} . \tag{6.31}$$

---

Given any fixed unit price vector $\boldsymbol{\lambda}$, starting from any initial point, Algorithm 6.4 always converges to a unique Nash equilibrium power vector $\mathbf{p}^*$ and BS assignment vector $\sigma^*$. The user-centric optimization can be carried out by autonomous BS assignment and power control.

## 6.7 Open Problems

Non-cooperative behaviors in cellular networks have not been exhaustively formulated yet. Indeed, for almost all of the formulations in other chapters of this monograph, game-theory and mechanism-design questions can be raised. For example, when the network is considered as an active player who interacts with individual MSs and tries to maximize its total revenue, a general class of joint user-network games can be formulated. In the last section, the special case of joint power control, BS assignment, and networking pricing is formulated. Now let $T_i$ be a resource allocation for MS $i$, including power and other spatial-temporal-spectral resources, and function $\phi(T_i)$ be a pricing policy adopted by the network. The general user-network game can be formulated over any set of feasible resource allocations and network pricing policies,

$$\left\{ \text{MSs}: \ \max_{T_i} U_i(T_i) - \phi(T_i), \quad \text{Network}: \ \max_{\phi(\cdot)} \sum_i \phi(T_i) \right\}$$

This general set of games, taking financial incentives of operator and multiple degrees of freedom of MSs into account, is yet to be studied. Even for existing formulations, the issues related to mixed strategy, rather than pure strategy, and to mechanism design often remain open.

# 7

# Joint PC and Beamforming

Starting with this chapter, we will incorporate additional degrees of freedom that work together with power control (PC) in cellular networks. These include multi-antenna beamforming in this chapter, BS assignment in the next chapter, and bandwidth allocation and scheduling in Chapter 9. With non-convexity and more coupling in their formulations, these joint optimization problems present new challenges to the design of optimal and distributed algorithms.

## 7.1 Introduction

The use of multiple antennas provides an extra degree of freedom in addition to power, spatial diversity can be leveraged by deploying multiple antennas at both transmitter and receiver. Due to hardware and cost limitations at MS, linear beamforming with multi-antenna BS and single-antenna MS has been considered as a compromise between performance and complexity [29, 179, 71, 87, 149]. Such a system is also referred to as a multiple-input-multiple-output (MIMO) system with partial antenna cooperation, where cooperation is only allowed between the BS antennas but not between the decentralized MSs. Fig.8.1 illustrates a typical wireless cellular environment. Discussions in this chapter focuses on joint power control and beamforming within a single cell, although some of the results can be extended to multiple cells.

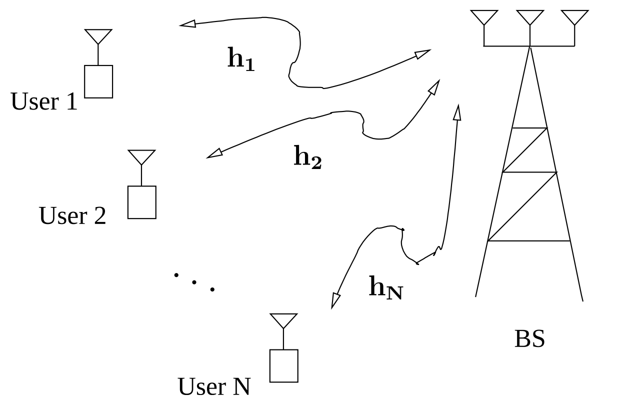


Fig. 7.1 A single cell with multiple antenna at BS.

In the uplink, spatial diversity of multiple antennas is exploited by independently adjusting beamforming vectors at the receiver. In the downlink, the beamforming vectors act as linear pre-equalizers, spreading the signals over the antenna array prior to transmission. Depending on the availability of full channel information, beamforming problems can be formulated in several different ways: In case the transmitter has no knowledge of the channel information, [148, 178] show that, by constructing random beam vectors and transmitting to the MSs with the highest SIR, the achievable sum rate has the same scaling law as the sum capacity for downlink broadcast channels when the number of MSs is large. This approach is referred to as random (or opportunistic) beamforming. It has since been generalized to beamforming with partial channel information [192, 122, 159, 203, 78, 86, 191]. On the other hand, when full channel information is available at the transmitter, the beamforming vectors can be adjusted adaptively to minimize interference and enhance SIR. One of the approaches is to invert the channel through the beamforming vector to eliminate interference completely, and it is referred to as the zero-forcing (ZF) beamforming approach

[179, 180, 158, 190, 151]. The main drawback of the ZF beamforming is its degraded performance in low SIR regime, since inverting the channel increases the need for more transmit power [22]. This motivates the design of optimal beamforming vectors for a known MIMO channel, which is the main subject of this chapter.

In uplink transmission, for a fixed power allocation, the SIR of all MSs can be independently maximized by minimizing the respective Minimum Mean Square Error (MMSE) between the received and the transmitted signal. Thus uplink beamforming can be decoupled, such that each MS performs an independent optimization of its own beamforming vector and the optimal solution is referred to as an MMSE filter. However, the usage of beamforming impacts SIR, and therefore on the optimal power allocation.

On the other hand, for fixed beamforming vectors, an overview of power control techniques is given in Chapter 2 and 4. It was assumed that the beamforming vectors are given by a separate algorithm that either fixes the beamforming vectors for each MS, or alters the beamforming vectors according to a fixed pattern, or even adaptively changes the beamforming vectors in response to some suitable feedback. For example, the opportunistic beamforming mechanism in [178] changes the beamforming vector in a fixed pattern so as to let every MS achieve the optimal beamforming configuration at which its SIR is maximized.

This chapter considers the interaction between power control and beamforming, and addresses their joint optimization [123, 52, 136, 24, 146, 45, 93]. For joint power control and beamforming, a distributed algorithms is first proposed in [136]. The algorithm computes the transmission powers and the beamforming vectors iteratively, such that a target SIR is achieved for each link (if it is achievable) with minimal transmission power. This work has been extended in several directions, e.g., in [93], the nonconvex and globally coupled problem of joint beamforming and power control is considered to maximize the network-wide utility as a function of attained SIR.

Downlink joint power control and beamforming, on the other hand, is more complicated than uplink because transmit beamforming vectors are coupled and must be optimized jointly. When nonorthogonal transmission is allowed, the choice of one MS's beamforming vector may affect the crosstalk experienced by other MSs. For fixed SIR targets, a downlink joint power control and beamforming problem has been solved in [135, 176, 141, 21, 22, 183]. Another result in [146] deals with optimal joint power control and beamforming for max-min SIR fairness. A key technique in the solutions of both the minimum-power beamforming problem and the maximum-utility beamforming problem is the idea of an uplink-downlink duality, which leverages the better-understood structures in uplink beamforming for the downlink problem. This duality result states that, under the same power constraint, the best achievable SIR region with joint transmitter beamforming and power control is the same as that of an uplink channel with joint receiver beamforming and power control [24, 193, 177, 175, 176, 183]. The optimal beamforming vectors in the downlink is also the optimal beamforming vectors in the uplink.

This chapter will first focus on joint power control and beamforming in the uplink case, starting with fixed SIR then moving to variable SIR. We will then present the uplink-downlink duality and discuss the downlink case.

## 7.2 Uplink with Fixed SIR

Consider the uplink of a wireless cellular network with $N$ MSs, each equipped with 1 transmit antenna sending independent information to a BS equipped with $M$ receive antennas. Denote $\mathbf{h}_{\sigma_i i}$ as the $M \times 1$ channel amplitude vector from MS $i$ to its serving BS, indexed by $\sigma_i$. Since this chapter focuses wireless networks with a single cell , all $\sigma_i$'s are equal. The received signal at the BS given by

$$\mathbf{x} = \sum_{i=1}^{N} \sqrt{p_i}\mathbf{h}_{\sigma_i i} u_i + \mathbf{z}, \tag{7.1}$$

where $u_i$ is an information symbol with unit power $\mathbb{E}\,|u_i|^2 = 1$, and $\mathbf{z}$ is the resulting $M \times 1$ Gaussian noise vector with zero mean and covariance matrix $n\mathbf{I}$. The vectors $\mathbf{h}_{\sigma_i i}$ are collected in an $M \times N$ matrix $\mathbf{H} = [\mathbf{h}_{\sigma_1 1}, \ldots, \mathbf{h}_{\sigma_N N}]$, such that $\mathbf{H}_{mi}$ denotes effective channel amplitude from MS $i$ to the $m$th BS antenna. So $\mathbf{H}$ represents the effective channel amplitude matrix of the MIMO system.

For uplink linear beamforming, the BS implements a set of beamforming vectors to map the received vector signal into independent scalar decoders for recovering information $u_i$'s. Let $\mathbf{w} \in \mathbb{R}^M$ denote the beamforming vector designed for MS $i$ and $p_i$ be its transmit power. The output signal at the BS for MS $i$ is given by

$$y_i = \left(\mathbf{w}_i^T \mathbf{h}_{\sigma_i i}\right) \sqrt{p_i} u_i + \sum_{j \neq i} \left(\mathbf{w}_i^T \mathbf{h}_{\sigma_i j}\right) \sqrt{p_j} u_j + \mathbf{w}_i^T \mathbf{z}. \tag{7.2}$$

For notational convenience, the beamforming vectors are collected in a matrix $\mathbf{W} = \{\mathbf{w}_i\}$. The three terms on the right hand side of (7.2) correspond to signal, interference, and noise, respectively. The data rate of uplink joint beamforming and power control then depends on the SIRs achieved by MSs.

Now the absolute path gain from MS $i$ to the BS is $|\mathbf{w}_i \mathbf{h}_{\sigma_i i}|^2$. An $N \times N$ coupling matrix which now depends on the beamforming vectors can be defined:

$$G_{ij}(\mathbf{W}) = \begin{cases} \frac{\left|\mathbf{w}_i^T \mathbf{h}_{\sigma_i j}\right|^2}{\left|\mathbf{w}_i^T \mathbf{h}_{\sigma_i i}\right|^2} & \text{if } \ j \in C_i, \\ 0 & \text{if } j \notin C_i. \end{cases} \tag{7.3}$$

Since $C_i = \{j : j \neq i\}$ for the single-cell case considered in this chapter, the total interference (including noise) for MS $i$ is given by,

$$q_i(\mathbf{W}, \mathbf{p}) = \sum_{j \neq i} G_{ij}(\mathbf{W}) p_j + \eta_i(\mathbf{W}), \tag{7.4}$$

where $p_i$ is the transmit power of MS $i$ and $\eta_i$ is an equivalent noise given by

$$\eta_i(\mathbf{W}) = \frac{||\mathbf{w}_i||_2^2}{\left|\mathbf{w}_i^T \mathbf{h}_{\sigma_i i}\right|^2} \cdot n. \tag{7.5}$$

In vector form, equation (7.4) can be written as

$$\mathbf{q}(\mathbf{W}, \mathbf{p}) = \mathbf{G}(\mathbf{W})\mathbf{p} + \boldsymbol{\eta}(\mathbf{W}). \tag{7.6}$$

The SIR achieved by MS $i$ becomes:

$$\begin{aligned} \mathsf{SIR}_i(\mathbf{W}, \mathbf{p}) &= \frac{|\mathbf{w}_i \mathbf{h}_{\sigma_i i}|^2 p_i}{\sum_{j \neq i} |\mathbf{w}_i \mathbf{h}_{\sigma_i j}|^2 p_j + n||\mathbf{w}_i||_2^2} \\ &= \frac{p_i}{\sum_{j \neq i} G_{ij}(\mathbf{W}) p_j + \eta_i(\mathbf{W})}. \end{aligned} \tag{7.7}$$

In this section, consider a joint power control and beamforming problem, where the objective is to find the optimal beamforming vector and power allocations such that a set of given SIR threshold $\gamma_i$ is achieved by all MSs, and total power minimized. This fixed SIR problem formulation for joint uplink beamforming and power control is given by

$$\begin{array}{ll} \text{minimize} & \sum_{i=1}^{N} p_i \\ \text{subject to} & \mathsf{SIR}_i(\mathbf{W}, \mathbf{p}) \geq \gamma_i, \ \forall i \\ \text{variables} & \mathbf{W}, \mathbf{p}. \end{array} \tag{7.8}$$

Note that for fixed beamforming vectors $\mathbf{W}$, problem (7.8) reduces to a power control problem that has been discussed in Chapters 2 and 4. The optimal power vector can be computed as the limit of the following iteration of the distributed power control algorithm:

$$p_i[t+1] = \gamma_i \sum_{j \neq i} G_{ij}(\mathbf{W}) p_j[t] + \gamma_i \eta_i(\mathbf{W}), \ \forall i. \tag{7.9}$$

Since the transmit power in (7.9) only depends on beamforming vector $\mathbf{w}_i$, beamforming optimization with respect to fixed power allocation is solved by

$$\mathbf{w}_i^* = \arg\min_{\mathbf{w}_i} \ \gamma_i \sum_{j \neq i} G_{ij}(\mathbf{W}) p_j + \gamma_i \eta_i(\mathbf{W}). \tag{7.10}$$

It is easy to see that the solution to (7.10) is MMSE filter[1] given by

$$\mathbf{w}_i^* = \left( \sum_{j \neq i} p_j \mathbf{h}_{\sigma_i j} \mathbf{h}_{\sigma_i j}^H + nI \right)^{\dagger} \mathbf{h}_{\sigma_i i}, \tag{7.11}$$

where $(.)^{\dagger}$ denotes the matrix pseudoinverse. When this MMSE filter is used, the SIR constraints in (7.8) are always met with equality.

In [136], the authors proposed an algorithm for the joint beamforming and power control problem (7.8), based on the above two updates. The algorithm operates by alternating between two optimization steps.

[1] The $\mathbf{w_i^*}$ as expressed in (7.10) is optimal up to an arbitrary scaling factor.

For a fixed power allocation, BS updates the beamfroming vectors using the MMSE filter. Next, MS powers are updated to minimize total transmit power under given SIR constraints. The algorithm is summarized as follows:

---

**Algorithm 7.1 (Joint Power Control and Beamforming [136]).**

(1) BS updates beamforming vectors $\mathbf{w}_i[t]$, according to (7.11).
(2) BS estimates the resulting channel coupling matrix $\mathbf{G}(W[t])$ and equivalent noise $\boldsymbol{\eta}(W[t])$.
(3) MSs perform power update for $\mathbf{p}[t]$, according to (7.9).

---

Algorithm 7.1 can be implemented distributively at BS and MSs. In [136], it has been proved that the joint power and beamfroming vector update in each round is a contraction mapping, hence Algorithm 7.1 always converge to a fixed point.

---

**Theorem 7.1.** [136] The sequence $(\mathbf{p}[t], \mathbf{W}[t])$ produced by the iterations in Algorithm 7.1, starting from an arbitrary power vector $\mathbf{p}[0]$, converges to the optimal pair $(\mathbf{p}^*, \mathbf{W}^*)$ of the joint power control and beamforming problem (7.8).

---

In [183], the authors re-examine the power and beamforming updates in Algorithm 7.1 by introducing a joint update method. Plugging (7.11) into (7.9), they obtain

$$p_i[t+1] = \frac{\gamma_i}{1+\gamma_i} \cdot \frac{1}{\mathbf{h}_{\sigma_i i}^H \left(\sum_{j \neq i} p_j[t] \mathbf{h}_{\sigma_i j} \mathbf{h}_{\sigma_i j}^H + nI\right)^{\dagger} \mathbf{h}_{\sigma_i i}}. \quad (7.12)$$

It can be shown that the above update rule, incorporating both power and beamforming updates in Algorithm 7.1, is a standard interference function (see Chapter 2 for a definition) of the power vector [183]. Therefore the optimal solution is the unique fixed-point of (7.12) and its convergence and optimality follow.

## 7.3 Uplink with Variable SIR

In this section, rather than fixing SIR, we consider a joint beamforming and power control problem in order to maximize total utility as a function of attained SIRs. This can be viewed as a simultaneous generalization of the formulation in the last section and that in Chapter 4.

In [146, 147], a max-min utility optimization has been studied, under a sum power constraint [2] across all MSs :

$$\begin{array}{ll} \text{maximize} & \min_i \gamma_i \\ \text{subject to} & \mathsf{SIR}_i(\mathbf{W},\mathbf{p}) \geq \gamma_i, \ \forall i \\ & \mathbf{1}^T\mathbf{p} \leq p^m \\ \text{variables} & \boldsymbol{\gamma}, \mathbf{W}, \mathbf{p}. \end{array} \tag{7.13}$$

This optimization problem is difficult to solve because the SIR constraints in (7.13) are not convex, and all three variables $\boldsymbol{\gamma}$, $\mathbf{W}$ and $\mathbf{p}$ are coupled. By introducing a notion of *extended coupling matrix* $\mathbf{G}_{\text{ex}}(\mathbf{W})$:

$$\mathbf{G}_{\text{ex}}(\mathbf{W}) = \begin{bmatrix} \mathbf{D}(\boldsymbol{\gamma})\mathbf{G}(\mathbf{W}) & \mathbf{D}(\boldsymbol{\gamma})\boldsymbol{\eta}(\mathbf{W}) \\ \frac{1}{p^m}\mathbf{1}^T\mathbf{D}(\boldsymbol{\gamma})\mathbf{G}(\mathbf{W}) & \frac{1}{p^m}\mathbf{1}^T\mathbf{D}(\boldsymbol{\gamma})\boldsymbol{\eta}(\mathbf{W}) \end{bmatrix}, \tag{7.14}$$

it has been observed that, if beamforming vector $\mathbf{W}$ is fixed in problem (7.13), power control for maximizing the smallest SIR can readily be solved. If $(\boldsymbol{\gamma}^*, \mathbf{p}^*)$ is the optimal solution for (7.13) with fixed beamforming vector $\mathbf{W}$, then with some matrix manipulations, it is easy to see that all SIRs are equal ($\gamma_i = \gamma^*$, $\forall i$) and

$$\mathbf{G}_{\text{ex}}(\mathbf{W})[\mathbf{p}^*;1]^T = \frac{1}{\gamma^*}[\mathbf{p}^*;1]^T. \tag{7.15}$$

The result has been strengthened in [188] to show that the maximal eigenvalue and its associated eigenvector of $\mathbf{G}_{\text{ex}}(\mathbf{W})$ are strictly positive. No other eigenvalue fulfills the positivity requirement. Hence, the solution of the power control problem with fixed beamforming vectors is given by [146]

$$\gamma^* = \frac{1}{\lambda_{\max}[\mathbf{G}_{\text{ex}}(\mathbf{W})]}, \tag{7.16}$$

[2] A sum power constraint normally applies to downlink channels. However, as it will be shown later in Section 7.4, this uplink beamforming formulation with a sum power constraint serves as an equivalent dual problem for downlink beamforming, which is difficult to tackle directly [146].

where $\lambda_{\max}[.]$ is a maximum eigenvalue function.

On the other hand, if power allocation $\mathbf{p}$ is fixed in problem (7.13), optimization over beamforming variables is solved by maximizing individual SIR:

$$\mathbf{w}_i^* = \arg\max_{\mathbf{w}_i} \frac{|\mathbf{w}_i \mathbf{h}_{\sigma_i i}|^2 p_i}{\sum_{j \neq i} |\mathbf{w}_i \mathbf{h}_{\sigma_i j}|^2 p_j + n||\mathbf{w}_i||_2^2}. \tag{7.17}$$

Its solution is again the MMSE filter, given by

$$\mathbf{w}_i{}^* = \left( \sum_{j \neq i} p_j \mathbf{h}_{\sigma_i j} \mathbf{h}_{\sigma_i j}^H + nI \right)^{\dagger} \mathbf{h}_{\sigma_i i}. \tag{7.18}$$

Based on the above derivation, [146, 147] propose an iterative algorithm for the joint power control and beamforming problem (7.13).

---

**Algorithm 7.2 (Joint Power Control and Beamforming [146]).**

(1) BS updates beamforming vectors $\mathbf{w}_i[t]$, according to (7.18).
(2) BS estimates the extended coupling matrix $\mathbf{G}_{\text{ex}}(W[t])$.
(3) Maximal eigenvalue $\lambda_{\max}$ of $\mathbf{G}_{\text{ex}}(\mathbf{W}[t])$ is computed at BS.
(4) BS computes power $\mathbf{p}[t]$ as the eigenvector for $\lambda_{\max}$, i.e.,

$$\mathbf{G}_{\text{ex}}(\mathbf{W}[t])\,[\mathbf{p}[t];1] = \lambda_{\max} \cdot [\mathbf{p}[t];1]$$

(5) MSs update power allocations to achieve $\gamma_i[t] = 1/\lambda_{\max}$, $\forall i$.

---

The updates in Algorithm 7.2 are done iteratively until both the transmit powers and the beamforming vectors converge. Convergence and optimality are characterized by the following theorem.

---

**Theorem 7.2.** [146] For a given sum power constraint $p^m$, the sequence $(\boldsymbol{\gamma}[t], \mathbf{p}[t], \mathbf{W}[t])$ obtained by Algorithm 7.2 converges to the globally optimal solution for the joint power control and beamforming problem (7.13).

---

Max-min objective function in problem (7.13) is a special case of the problem formulation in this section. Joint beamforming and power control for maximizing a general concave utility function is much more difficult, since the optimal beamforming and power vectors are non-linearly coupled in a way that cannot be treated using the extended coupling matrix. Assume that utility function $U_i(\gamma_i)$ satisfies all properties discussed in Section 4.3. The problem of joint beamforming and power control can be formulated as

$$\begin{array}{ll} \text{maximize} & \sum_{i=1}^{N} U_i(\gamma_i) \\ \text{subject to} & \mathsf{SIR}_i(\mathbf{W}, \mathbf{p}) \geq \gamma_i, \ \forall i \\ & p_i \leq p_i^m, \ \forall i \\ \text{variables} & \boldsymbol{\gamma}, \mathbf{W}, \mathbf{p}. \end{array} \tag{7.19}$$

To overcome this difficulties in solving (7.19), the authors in [65] took the load-spillage approach introduced in Chapter 4. The basic idea is still to iteratively solve the two power control and beamforming subproblems, but using alternative optimization variables: load $\boldsymbol{\ell}$ and spillage $\mathbf{s}$. For given beamforming vectors $\mathbf{W}$, Problem (7.19) can be solved using the load-spillage algorithm in Chapter 4, where the optimization over power $\mathbf{p}$ is transformed into an optimization over spillage vector $\mathbf{s}$ and the SIR constraint is replaced by

$$\boldsymbol{\gamma} = \boldsymbol{\ell}/\mathbf{s}, \ \mathbf{s} = \mathbf{G}(\mathbf{W})^T \boldsymbol{\ell} + \boldsymbol{\nu}, \tag{7.20}$$

where the division of the vectors is component-wise. The power price vector $\boldsymbol{\nu}$ is determined through an iterative subgradient update

$$\boldsymbol{\nu}[t+1] = [\boldsymbol{\nu}[t] + \delta_\nu(\mathbf{p}[t] - \mathbf{P}^m)]^+ \tag{7.21}$$

where $\delta_\nu > 0$ is a sufficiently small constant. (See Chapter 4 for details on the LSPC algorithm.)

A solution to problem (7.19) requires the determination of the optimal power vector and the beamforming vectors subject to the imposed transmit power constraint. Alternatively, using a load-spillage characterization, one can determine the optimal load vector and the beamforming vectors, with the power prices updated to achieve the required power constraint. Consider the following load and beamforming vector update:

$$\boldsymbol{\ell}[t+1] = \left[\boldsymbol{\ell}[t] + \delta_\ell \Delta\boldsymbol{\ell}\right]^+, \quad \Delta\ell_i = \frac{U_i'(\gamma_i)\gamma_i}{q_i} - \ell_i, \tag{7.22}$$

$$\mathbf{w}_i[t+1] = \left[nI + \sum_{j\neq i} p_j[t] \cdot \mathbf{h}_{\sigma_i j}\mathbf{h}_{\sigma_i j}^H\right]^\dagger \mathbf{h}_{\sigma_i i}. \tag{7.23}$$

The authors [65] propose the following algorithm for joint beamforming and power control problem (7.19) for a general concave utility function.

---

**Algorithm 7.3 (Joint Power Control and Beamforming [65]).**

- Parameters: step size $\delta_\ell > 0, \delta_\nu > 0$.

(1) Load-spillage factors are updated assuming fixed beamforming vectors until convergence:
   (a) BS computes the spillage-factor $s_i[t]$.
   (b) BS assigns SIR $\gamma_i[t] = \ell_i[t]/s_i[t]$ to MS $i$.
   (c) MSs adjust transmission power $\mathbf{p}[t]$ until their actual SIR converges to the target SIR, i.e.

$$\mathsf{SIR}_i(\mathbf{p}[t], \mathbf{W}[t]) = \gamma_i[t], \ \forall i$$

   (d) MS update its load factor $\ell_i[t]$ in the ascent direction given by (7.22) and broadcast it to BS.

(2) BS updates power price according to (7.21).
(3) Beamforming vector $\mathbf{w}_i[t]$ is updated at the BS serving MS $i$, using (7.23).

---

This algorithm's convergence property is known:

**Theorem 7.3.** [65] For sufficiently small step sizes $\delta_\ell > 0$ and $\delta_\nu > 0$, Algorithm 7.2 converges to a stationary point of Problem (7.19).

It is also proved to be globally optimal in the 1-BS, 2-MS case. Empirical evidence suggests optimality of equilibrium of Algorithm 7.3 in general [65].

## 7.4 Uplink-downlink Duality

For downlink joint power control and beamforming, the BS constructs one data stream to each MS and spreads the data stream over $M$ antenna elements, with beamforming vectors to exploit spatial diversity. Consider a cellular network with one BS equipped with $M$ transmit antennas and $N$ MSs each equipped with one receive antenna. The transmitted signal is of the form $\mathbf{X} = \sum_{i=1}^{N} \hat{\mathbf{w}}_i u_i$, where $\hat{\mathbf{w}}_i$ is a $M \times 1$ beamforming vector for information signal $u_i$ of MS $i$. Let $\mathbb{E}|u_i|^2 = 1$. The received signal for MS $i$ is

$$y_i = \left(\mathbf{h}_{\sigma_i i}^H \hat{\mathbf{w}}_i\right) u_i + \sum_{j \neq i} \left(\mathbf{h}_{\sigma_i i}^H \hat{\mathbf{w}}_j\right) u_j + \mathbf{z}_i, \tag{7.24}$$

where $\mathbf{h}_{\sigma_i j}$ denotes the $M \times 1$ equivalent channel vector for MS $j$ and $\mathbf{z}_i$ is an addictive white Gaussian noise with variance $n$. Consider a fixed-SIR approach for the downlink joint power control and beamforming problem, whose objective is to find optimal beamforming vectors that minimize the total transmit power and satisfy the given SIR targets for each MS. Since $\mathbb{E}[\mathbf{X}^H \mathbf{X}] = \sum_{i=1}^{N} \hat{\mathbf{w}}_i^H \hat{\mathbf{w}}_i$, the downlink joint power control and beamforming problem can be formulated as follows. Note that downlink transmit power is absorbed into the beamforming vectors, i.e. $\hat{p}_i = \hat{\mathbf{w}}_i^H \hat{\mathbf{w}}_i$, $\forall i$.

$$\begin{array}{ll} \text{minimize} & \displaystyle\sum_{i=1}^{N} \hat{\mathbf{w}}_i^H \hat{\mathbf{w}}_i \\ \text{subject to} & \dfrac{|\mathbf{h}_{\sigma_i i}^H \hat{\mathbf{w}}_i|^2}{\sum_{j \neq i} |\mathbf{h}_{\sigma_i i}^H \hat{\mathbf{w}}_j|^2 + n} \geq \gamma_i, \ \forall i \\ \text{variables} & \hat{\mathbf{W}} \end{array} \tag{7.25}$$

Problem (7.25) is complicated in that the beamforming vectors must be optimized jointly since the interference suffered by MS $i$ depends on the beamforming vectors of all other MSs.

To overcome this difficulty, a duality between uplink and downlink has been developed in [24, 193, 177, 175, 176, 88, 183]. The duality property states that the achievable SIR region for a downlink channel with joint transmitter beamforming and power control is the same as that of an uplink channel with joint receiver beamforming and power control, under the same sum power constraint: $\sum_i p_i = \sum_i ||\hat{\mathbf{w}}_i||_2^2$. Further, the optimal beamforming vectors for the uplink is also the optimal beamforming vectors for the downlink. Since uplink joint power control and beamforming discussed in previous sections are easier to solve, any downlink problem can be transformed and more efficiently solved in its dual uplink domain.

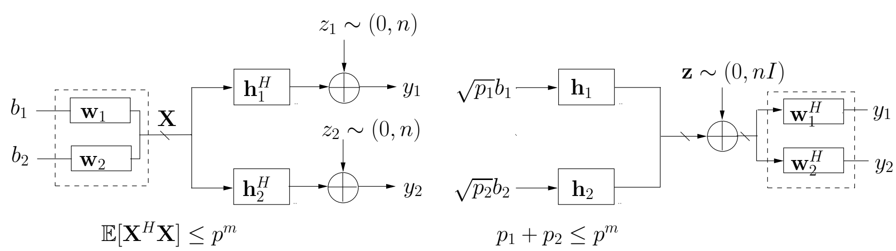


Fig. 7.2 Beamforming uplink-downlink duality with sum power constraints [193].

This uplink-downlink duality is illustrated in Fig.7.2, and has been proven in many different ways. In [135] and [176]. The authors first show that the same SIR targets can be achieved in both the uplink and the downlink channels with the same beamforming and sum transmit power. Therefore, downlink joint power control and beamforming problems with fixed SINR targets can be solved efficiently by an iterative uplink joint beamforming and power update algorithm. In particular, [176] offered an optimality proof for uplink-downlink duality based on an examination of the KKT conditions for the optimization problems. It is shown that the uplink problem and downlink problem have the same KKT conditions and the same set of stationary points. Later, in

[183], a convex optimization framework for downlink joint power control and beamforming was introduced to show that problem can be formulated as a semi-definite programming (SDP) problem. Therefore, one can numerically verify the feasibility of the SDP problem and find its globally optimal solution. Based on this observation, the authors [193] propose a unified interpretation to the uplink-downlink duality, which is shown to be equivalent to Lagrangian duality in optimization theory. This viewpoint illustrates the previously known duality result in a new perspective, and allows the downlink joint power control and beamforming problem with per-antenna power constraint to be solved.

Here the proof for the convexity of problem (7.25), which leads to strong Lagrange duality for the problem, is summarized [193]. Since the objective function in (7.25) is convex in beamforming vectors $\hat{\mathbf{w}}_i$, it remains to show that the SIR constraints are convex. The key observation is that the SIR constraints in (7.8) can be cast into a standard convex form [3]:

$$\begin{aligned}
&\frac{|\mathbf{h}_{\sigma_i i}^H \hat{\mathbf{w}}_i|^2}{\sum_{j\neq i} |\mathbf{h}_{\sigma_i i}^H \hat{\mathbf{w}}_j|^2 + n} \geq \gamma_i \\
&\Leftrightarrow \frac{1}{\gamma_i}|\hat{\mathbf{w}}_i^H \mathbf{h}_{\sigma_i i}|^2 \geq \sum_{j\neq i} |\hat{\mathbf{w}}_j^H \mathbf{h}_{\sigma_i i}|^2 + n \\
&\Leftrightarrow (1+\frac{1}{\gamma_i})|\hat{\mathbf{w}}_i^H \mathbf{h}_{\sigma_i i}|^2 \geq \sum_{j} |\hat{\mathbf{w}}_j^H \mathbf{h}_{\sigma_i i}|^2 + n \\
&\Leftrightarrow \sqrt{1+\frac{1}{\gamma_i}}\hat{\mathbf{w}}_i^H \mathbf{h}_{\sigma_i i} \geq \left\| \begin{matrix} \hat{\mathbf{W}}^H \mathbf{h}_{\sigma_i i} \\ \sqrt{n} \end{matrix} \right\|.
\end{aligned} \tag{7.26}$$

It is easy to see that the new SIR constraint (7.26) is convex in beamforming vectors $\hat{\mathbf{w}}_i$. Thus downlink joiint power control and beamforming problem (7.25) can be transformed into a convex optimization problem, which can be solved by any standard convex optimization program. As a convex optimization satisfying constraint qualifications [193], problem (7.25) has strong Lagrange duality. This allows us to

[3] The last step is obtained by taking a squire-root on both side. It is valid because an arbitrary phase rotation can be added to the beamforming vectors without affecting the SIR. Thus, if $\{\hat{\mathbf{w}}_i\}$ is optimal, then so is $\{\hat{\mathbf{w}}_i e^{j\phi_i}\}$. Without loss of generality, $\{\phi_i\}$ can be chosen such that $\hat{\mathbf{w}}_i \mathbf{h}_{\sigma_i i}$ is real and positive [193].

derive a dual uplink joint power control and beamforming problem for (7.25).

---

**Theorem 7.4.** [193] The SIR region achieved by joint power control and beamforming for a downlink channel is identical to that of a dual uplink channel in which the transmitter and the receivers are reversed and the channel matrices are transposed. The downlink joint power control and beamforming problem (7.25) has the following dual uplink problem:

$$
\begin{array}{ll}
\text{minimize} & \displaystyle\sum_{i=1}^{N}(n\lambda_i) \\
\text{subject to} & \dfrac{|\mathbf{w}_i^H \mathbf{h}_{\sigma_i i}|^2 \cdot (n\lambda_i)}{\sum_{j\neq i}|\mathbf{w}_i^H \mathbf{h}_{\sigma_i j}|^2 \cdot (n\lambda_j) + n||\mathbf{w}_i||_2^2} \geq \gamma_i, \ \forall i \\
\text{variables} & \mathbf{W}, \boldsymbol{\lambda}
\end{array}
\tag{7.27}
$$

where $\boldsymbol{\lambda}$ is Lagrangian multiplier for the downlink SIR constraints. Optimization problem (7.27) is equivalent to the Lagrange dual problem of (7.25).

---

The dual uplink problem (7.27) is exactly the uplink joint power control and beamforming problem with fixed-SIR, by changing the optimization variables $p_i = n\lambda_i$. The dual uplink channel is constructed from the downlink channel by interchanging the input and the output vectors and by transposing the channel matrices. The optimal beamfroming vectors for uplink and downlink are also the same. According to [194], the duality relation is summarized in Table 7.1.

| Downlink | | Uplink |
|---|---|---|
| $\mathbf{h}_{\sigma_i i}^H$ | $\Longleftrightarrow$ | $\mathbf{h}_{\sigma_i i}$ |
| $\hat{\mathbf{w}}_i$ | $\Longleftrightarrow$ | $\mathbf{w}_i$ |
| $n\lambda_i$ | $\Longleftrightarrow$ | $p_i$ |

Table 7.1 This table summarizes the correspondence between the downlink problem (7.25) and the uplink problem (7.27). It shows that the Lagrange multipliers $\lambda_i$ corresponding to the SINR constraints in the downlink problem play the role of the transmit power in the uplink problem, while the channel matrices and the beamforming vectors are equal [194].

## 7.5 Open Problems

In this chapter, we review results for joint beamforming and power control in a cellular network with multiple antennas, assuming full channel information is known to the BS. The joint beamforming and power control problem of minimizing total transmit power with fixed SIRs has been solved by adding a beamforming vector update to previous power control algorithms. The more complicated problem of maximizing a concave utility under a sum power constraint has only been solved in special cases. Several algorithms for the uplink channels are summarized and discussed. Due to an interesting uplink-downlink duality introduced in the last section, all the algorithms also apply to the downlink channels.

Besides the joint beamforming and power control problem for general utility functions in Section 7.3, there are several other open problems. First, most results so far focus on a single cell where interference from neighboring cells are regarded as Gaussian noise. Distributed beamforming for a multi-cellular network need to be considered. Second, beamforming problems joint with network resource allocation, such as bandwidth, time, or BS-assignment have not been fully explored. Third, beamforming problems with mobility, fading, and inaccurate channel information are yet to be fully studied.

# 8

# Joint PC and BS Assignment

## 8.1 Introduction

The assumption of static connectivity patterns between MSs and BSs, adopted in most of the results surveyed thus far, is not realistic due to two reasons. First, channels and BSs can be reassigned to MSs at any time, even in the middle of a call. As MSs move around the network and change positions, SIR changes and reassignment of both BS and transmit power may be required. When a new call request arises, a reassignment of the existing calls might be required to accommodate it. Second, connectivity can also be viewed as an extra system resource in addition to power, time, bandwidth, and multiple antennas. When such a joint resource allocation is considered, performance of a cellular network and experience of the end-users could be further improved.

As a numerical example, Figure 8.2 considers a network with 2 BSs and 10 MSs and compares the minimum required transmit power of the DPC algorithm and a joint BS assignment and power control algorithm, for achieving an equal SIR target $\gamma$ at all MSs. It is shown that the minimum required transmit power can be reduced by as much as 20dB under a joint optimization.

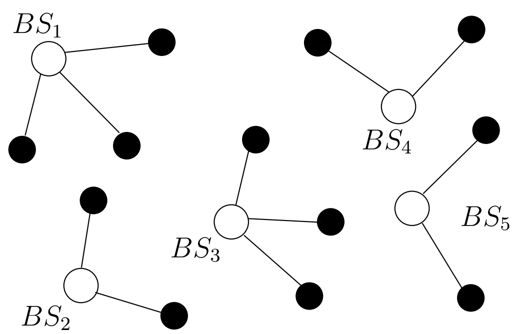


Fig. 8.1 A BS is selected by each MS to establish a link. This figure shows the connectivity between 5 BSs and 12 MSs.

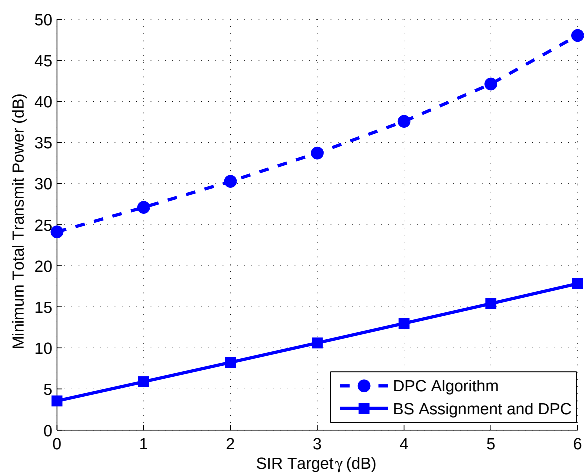


Fig. 8.2 The minimum required transmit power (normalized to noise, i.e., $\frac{\sum_i p_i}{n}$) to achieve a given SIR target $\gamma$ in a network with 2 BSs and 10 MSs. Channels are randomly generated from Normal distribution with variance 1.

This chapter studies the joint problem of BS assignment and power control. As in Chapter 7, we consider two types of problem formulations: minimize the total transmit power for fixed SIR, or maximize total utility for variable SIR. The discussion will focus on the uplink channel of cellular networks, and then extended to downlink using the uplink-downlink duality in Chapter 7.

The joint power allocation and BS assignment problem in uplink has been studied, e.g., in [113, 66, 189, 136, 125]. The main objective is to determine the BS assignment that minimizes the required transmit power for fixed SIRs on each link. Let $\mathsf{SIR}_i(\mathbf{p}, \boldsymbol{\sigma})$ be the SIR function for MS $i$ that now depends on both power allocation $\mathbf{p}$ and BS assignment $\boldsymbol{\sigma}$. The joint optimization problem for uplink is formulated:

$$\begin{array}{ll} \text{minimize} & \sum_{i=1}^{N} p_i \\ \text{subject to} & \mathsf{SIR}_i(\mathbf{p}, \boldsymbol{\sigma}) \geq \gamma_i, \ \forall i \\ & \sigma_i \in \mathcal{S}_i, \ \forall i \\ \text{variables} & \boldsymbol{\sigma}, \mathbf{p} \end{array} \tag{8.1}$$

where $\mathcal{S}_i$ is a set of feasible BS assignment for MS $i$. In particular, [66] characterizes the optimal solution of problem (8.1), and showed that at the optimum, all SIR constraints are met with equality, and there exists an optimal BS assignment for which the optimal transmit power is minimized for each MS. Then an algorithm based on selecting the BS to achieve the minimum transmit power is proposed. Similar algorithms are also presented in [189, 136, 125], where the joint power and BS update is shown to be a contraction mapping that is guaranteed to converges to a unique fixed-point. In addition, [136] proposes an algorithm for the joint power control, beamforming, and BS assignment problem. All these results are based on previous power control and beamforming algorithms discussed in Chapter 2 and 7, together with choosing a BS that requires the minimum transmit power.

Later, these results are generalized in [134, 133, 20] to downlink channels, using the uplink-downlink duality in Section 7.4. In [128], for a network with two BSs, an algorithm that achieves the optimal power and BS assignment for both the uplink and the downlink simultaneously is provided. It turns out that the SIR simultaneously achieved by the uplink and downlink channels are equal.

Utility optimization for joint power control and BS assignment has also been studied in several special cases [129, 96, 144, 55, 60, 97]. By extending the basic power control problem in Chapter 4, the problem can be formulated as follows:

$$\begin{array}{ll} \text{maximize} & \sum_{i=1}^{N} U_i(\gamma_i) \\ \text{subject to} & \gamma_i \leq \mathsf{SIR}_i(\mathbf{p}, \boldsymbol{\sigma}),\ \forall i \\ & \mathbf{p} \leq \mathbf{p}^m \\ & \sigma_i \in \mathcal{S}_i,\ \forall i \\ \text{variables} & \boldsymbol{\gamma}, \boldsymbol{\sigma}, \mathbf{p} \end{array} \tag{8.2}$$

Problem (8.2) has a difficult-to-handle structure due to the interaction between the integer connectivity constraints on individual MSs and the joint utility maximization over all SIRs. This problem remains under-explored. In Chapter 6, a game-theoretic approach for problem (8.2) has been discussed [96, 144, 55, 97] for certain utility functions. It is shown in [60] that the joint power control and BS assignment problem for maximal throughput is NP complete. A simple algorithm has been proposed in [60] under the assumption that all MSs use orthogonal codes and the resulting inter-cell interference is zero.

## 8.2 Joint PC and BS Assignment

Consider the uplink of a wireless cellular network with $N$ MSs and $K$ BSs. At any given time, MS $i$ is transmitting to one of these BSs, denoted by $\sigma_i$. The vector $\boldsymbol{\sigma} = [\sigma_1, \ldots, \sigma_N]^T$ represents the allocation of MSs to cells. For each MS $i$, there is a set $\mathcal{S}_i$ consisting of precisely those BSs that the MS $i$ is allowed to connect to, i.e. $\sigma_i \in \mathcal{S}_i$. Note that the sets of allowable cells $\mathcal{S}_i$'s are regarded as fixed in the chapter, but with mobility $\mathcal{S}_i$'s should be allowed to adapt on a slow time scale to the changes in the network geometry. Let $\mathbf{G}(\boldsymbol{\sigma})$ be the channel coupling matrix, now defined as a function of the BS assignment $\boldsymbol{\sigma}$. We have

$$\left[\mathbf{G}(\boldsymbol{\sigma})\right]_{ij} = \begin{cases} \frac{|h_{\sigma_i j}|^2}{|h_{\sigma_i i}|^2}, & \text{if } \ j \in C_i(\boldsymbol{\sigma}), \\ 0, & \text{if } j \notin C_i(\boldsymbol{\sigma}). \end{cases} \tag{8.3}$$

where $C_i(\boldsymbol{\sigma})$ is the set of MSs interfering with MS $i$ under current BS assignment $\boldsymbol{\sigma}$, and $\mathbf{h}_{\sigma_i j}$ is the channel amplitude form MS $j$ to BS $\sigma_i$.

Again, the joint power control and BS assignment problem, for fixed

SIR targets, is formulated as follows:

$$\begin{array}{ll} \text{minimize} & \sum_{i=1}^{N} p_i \\ \text{subject to} & \dfrac{p_i}{\sum_{j \in C_i(\boldsymbol{\sigma})} \mathbf{G}_{ij}(\boldsymbol{\sigma}) p_j + \eta_i} \geq \gamma_i, \ \forall i \\ & \sigma_i \in \mathcal{S}_i, \ \forall i \\ \text{variables} & \boldsymbol{\sigma}, \mathbf{p} \end{array} \tag{8.4}$$

When BS assignment is fixed and no switching between cells are allowed in the cellular network, the problem reduces to the power control problem that has been discussed in Chapter 2. For the joint power control and BS assignment problem, previous power control algorithms can be extended to optimize the transmit power $\mathbf{p}$ and the BS assignment $\boldsymbol{\sigma}$ jointly. It has been shown [66] that there exists an optimal solution for problem (8.4) such that the resulting transmit power is minimal and unique, as characterized by the following theorem.

---

**Theorem 8.1.** [66] If there exists one feasible BS assignment, such that SIR targets $\boldsymbol{\gamma}$ are achievable, then there exists an optimal solution $(\mathbf{p}^*, \boldsymbol{\sigma}^*)$ to problem (8.4). The optimal power allocation satisfies $\mathbf{p}^* \leq \mathbf{p}$ where $\mathbf{p}$ is any feasible power vector.

---

Based on this observation, the authors in [66] propose an algorithm to solve problem (8.4). The algorithm is similar to the Algorithm 2.3 for distributed power control, but now with each MS $i$ measuring the interference levels at each BS in $\mathcal{S}_i$ and connecting to the BS with the minimum power level required.

---

**Algorithm 8.1 (Joint PC and BS-assignment [66]).**

(1) Given transmit powers $\mathbf{p}[t]$, MS $i$ computes the required transmit power at the next step for connecting to each BS

in $\mathcal{S}_i$:

$$\tilde{p}_{i,k} = \gamma_i \left( \sum_{j \in C_i(\boldsymbol{\sigma})} \frac{|h_{kj}|^2}{|h_{ki}|^2} p_j[t] + \eta_i \right), \text{ for } k \in \mathcal{S}_i.$$

(2) MS $i$ connects to BS $\sigma_i[t+1]$, satisfying

$$\sigma_i[t+1] = \arg\min_{k \in \mathcal{S}_i} \tilde{p}_{i,k}.$$

(3) MS $i$ updates its transmit power by $p_i[t+1] = \tilde{p}_{i,\sigma_i[t+1]}$.

(4) Consider the next MS and go back to step (1)

---

The algorithm can be implemented distributively at BSs and MSs: Each BS measures the total interference it receives from all MSs in the network and broadcast this value via control channels. MS $i$, receiving the broadcasted values, compute the required transmit power levels and decide which BS to connect to. In particular, a MS does not need to know the individual transmit powers of the other MSs. Only the channel gains and interference of the BSs in $\mathcal{S}_i$ are reqiured. In [66], it has been proved that Algorithm 8.1 converges to the optimal solution of problem (8.4).

---

**Theorem 8.2.** [66] Algorithm 8.1 converges to the optimal power allocation and BS assignment $(\mathbf{p}^*, \boldsymbol{\sigma}^*)$ of problem (8.4), i.e. $\lim_{t\to\infty} (\mathbf{p}[t], \boldsymbol{\sigma}[t]) = (\mathbf{p}^*, \boldsymbol{\sigma}^*)$.

---

For joint power control and BS assignment in downlink, the joint optimization cannot be solved by Algorithm 8.1 due to the following limitation of the standard interference function approach. In the uplink, whenever a MS can reduce its transmitted power, all other MSs will benefit from that power reduction. This property does not hold for joint power control and BS assignment in downlink. The power reduction associated with changing the BS assignment for MS $i$ from BS $k_1$ to $k_2$ may create greater interference for those MSs near BS $k_2$. To overcome this difficulty, the uplink-downlink duality discussed in previous chapters is applied. An algorithm is proposed in [134], where the downlink problem is solved by constructing a equivalent virtual uplink problem and generating sequence of BS assignment and power vector for the uplink. If the thermal noise power at all receivers are equal, Algorithm (8.1) generates a feasible solution that minimizes the sum of downlink powers.

## 8.3 Joint PC, Beamforming, and BS Assignment

Consider a joint optimization problem over power, BS assignment, and beamforming:

$$\begin{array}{ll} \text{minimize} & \sum_{i=1}^{N} p_i \\ \text{subject to} & \frac{|\mathbf{w}_i^H \mathbf{h}_{\sigma_i i}|^2 p_i}{\sum_{j \in C_i(\boldsymbol{\sigma})} |\mathbf{w}_i^H \mathbf{h}_{\sigma_i j}|^2 p_j + n||\mathbf{w}_i||_2^2} \geq \gamma_i, \forall i \\ & \sigma_i \in \mathcal{S}_i, \ \forall i \\ \text{variables} & \mathbf{W}, \mathbf{p}, \boldsymbol{\sigma} \end{array} \tag{8.5}$$

Algorithm 8.1 can be modified to support beamforming as well [136]:

---

**Algorithm 8.2 (Joint PC, BF and BS-assignment [136]).**

(1) Each BS in the allowable set ($i.e.$ $k \in \mathcal{S}_i$) of MS $i$ finds the optimal beamforming vector for MS $i$:

$$\begin{aligned} \tilde{\mathbf{w}}_{i,k} &= \arg\max_{\mathbf{w}_i} \frac{|\mathbf{w}_i^H \mathbf{h}_{ki}|^2 p_i[t]}{\sum_{j \in C_i(\boldsymbol{\sigma})} |\mathbf{w}_i^H \mathbf{h}_{kj}|^2 p_j[t] + n||\mathbf{w}_i||_2^2}, \\ &= \left( \sum_{j \in C_i(\boldsymbol{\sigma})} p_j[t] \mathbf{h}_{kj} \mathbf{h}_{kj}^H + nI \right)^{\dagger} \mathbf{h}_{ki}. \end{aligned} \tag{8.6}$$

(2) Given these beamforming vectors, MS $i$ computes the required transmit power for connecting to each BS in $\mathcal{S}_i$:

$$\tilde{p}_{i,k} = \gamma_i \left( \sum_{j \in C_i(\boldsymbol{\sigma})} \frac{|\tilde{\mathbf{w}}_{i,k} \mathbf{h}_{kj}|^2}{|\tilde{\mathbf{w}}_{i,k} \mathbf{h}_{ki}|^2} p_j[t] + \frac{n}{|\tilde{\mathbf{w}}_{i,k} \mathbf{h}_{ki}|^2} \right).$$

(3) MS $i$ connects to BS $\sigma_i[t+1]$, satisfying

$$\sigma_i[t+1] = \arg\min_{k\in\mathcal{S}_i} \tilde{p}_{i,k}.$$

(4) MS $i$ updates its transmit power by $p_i[t+1] = \tilde{p}_{i,\sigma_i[t+1]}$.
(5) The BS $\sigma_i[t+1]$updates the beamforming vector for MS $i$ by

$$\mathbf{w}_i[t+1] = \tilde{\mathbf{w}}_{i,\sigma_i[t+1]}$$

---

In Algorithm 8.2, at each iteration all of the BSs in the allowable set $\mathcal{S}_i$ perform beamforming and the required MS transmit power for the next iteration is calculated. This step introduces both communication and computation overhead. The BS assignment is performed by comparing the power requirements of different BSs. The BS with the least required transmit power will be selected for the MS. The beamforming vector updated in step 2 above is the same as the MMSE filter derived in Chapter 7. In summary, algorithm 8.2 can be viewed as a combination of Algorithm 8.1 and Algorithm 7.1.

For the joint power control and BS assignment problem in Section 8.2, it is shown that the optimal power allocation is unique. In the joint problem with beamforming, using the same approach as in Theorem 8.2 [66], it can be shown [136] that the optimal power allocation is also unique. However, the optimal BS and beamforming vectors may not be unique. Optimality of Algorithm 8.2 is summarized in the next theorem.

---

**Theorem 8.3.** [136] Algorithm 8.2 converges to the optimal power allocation, beamforming, and BS assignment $(\mathbf{p}^*, \boldsymbol{\sigma}^*, \mathbf{W}^*)$, which solves the joint optimization problem (8.5).

---

## 8.4 Open Problems

In this chapter, we review results for joint power control and BS assignment for cellular network with single or multiple antennas. The problem of minimizing total transmit power with fixed SIR targets has been solved by adding BS selections to previous distributed power control algorithms, while the more complicated problem of achieving the optimal SIRs through a utility maximization is largely open, except for a few special cases [96, 144, 55, 60, 97].

Unlike the power minimization problem where BS assignment for minimum transmit power always reduces interference suffered by other MSs, the utility maximization problem requires optimal SIRs to be achieved by possibly increasing the transmit power. Thus, improving the utility of a particular MS by joint BS assignment and power control may cause more interference for all MSs in $C_i(\boldsymbol{\sigma})$ due to the coupling in the SIR function:

$$\mathsf{SIR}_i(\mathbf{p}, \boldsymbol{\sigma}) = \frac{p_i}{\sum_{j \in C_i(\boldsymbol{\sigma})} \mathbf{G}_{ij}(\boldsymbol{\sigma}) p_j + \eta_i} \tag{8.7}$$

This coupling, combined with the integer constraints on the connectivity variables, leads to a problem structure that is hard to handle. We conclude this chapter by presenting the open problem of joint power control and BS assignment for utility optimization:

$$\begin{array}{ll} \text{maximize} & \sum_{i=1}^{N} U_i(\gamma_i) \\ \text{subject to} & \gamma_i \leq \mathsf{SIR}_i(\mathbf{p}, \boldsymbol{\sigma}), \ \forall i \\ & \mathbf{p} \leq \mathbf{p}^m \\ & \sigma_i \in \mathcal{S}_i, \ \forall i \\ \text{variables} & \boldsymbol{\gamma}, \boldsymbol{\sigma}, \mathbf{p} \end{array} \tag{8.8}$$

# 9

# Joint PC and Spectral-Temporal Scheduling

## 9.1 Introduction

In addition to power, the achieved QoS of an MS obviously depends on the allocated frequency bandwidth and time slots. The discussion in Chapter 4 implicitly assumed equal and static allocation of spectral-temporal resources among MSs. The discussion in Chapter 5 focused on optimizing the power allocation to the MSs over time as the channel varies. The interference was either assumed fixed or the variation in interference was not explicitly considered. This chapter will instead discuss joint optimization of allocation of power along with the time-frequency resources for fixed channels. The joint optimizer will be referred to as the scheduler in the rest of this chapter. It turns out that joint power control and frequency allocation is not easy to formulate in the general case, and joint power control and scheduling difficult to solve optimally and distributedly. Many problems in this topic remain open.

## 9.2 Joint PC and Bandwidth Allocation

### 9.2.1 General formulation

Consider a bandwidth $B^m$ available for scheduling among the $N$ MSs, divided into $L$ orthogonal resources of width $b_l$ each. The division of bandwidth into orthogonal resources is modulation dependent, an OFDM modulation scheme provides tone-level granularity, and a CDMA modulation scheme provides code-level granularity. Each MS divides it's power $p_i$ among the $L$ orthogonal resources so as to maximize a network wide utility. For each parameter, let super-script $l$ denote the parameter pertaining to the $l$th orthogonal resource. With this, the following equations can be written for the $l$th resource similar to (1.3):

$$q_i^l = \sum_{j \in C_i} G_{jj}^l p_j^l + \eta_i^l. \tag{9.1}$$

The SIR $\gamma_i^l$ is then given by

$$\gamma_i^l = G_{ii}^l p_i^l / q_i^l. \tag{9.2}$$

Let $\mathbf{\Gamma}^l = \mathbf{B}^l(\mathbf{p}^l)$ denote a feasible SIR region for resource $l$ as defined in Chapter 4, with the super-script $l$ indicating that each feasible region is specific to the $l$th block of bandwidth. The $L$ resources are coupled by a sum power constraint $\sum_l p_i^l \leq p_i^m$. The total rate achieved is then the summation of the rates achieved in each of the L resources:

$$r_i = \sum_{l=1}^{L} b_l \log(1 + c\gamma_i^l). \tag{9.3}$$

The bandwidth allocation problem for variable SIR can then be written as

$$\begin{array}{ll} \text{maximize} & \sum_i U_i(r_i) \\ \text{subject to} & r_i = \sum_{l=1}^{L} b_l \log(1 + c\gamma_i^l), \ \ \forall i \\ & \boldsymbol{\gamma}^l \in \mathbf{\Gamma}^l, \ \ \forall l \\ & \sum_l p_i^l \leq p_i^m, \ \ \forall i \\ \text{variables} & \boldsymbol{\gamma}^l, \mathbf{p}^l \ \ \forall l \end{array} \tag{9.4}$$

This problem is non-convex and has no known distributed optimal solution.

The representation (9.4) is in-fact very similar to the spectrum balancing problems [32] in DSL systems. There are several distributed solutions ([32, 195, 196, 31]) with different complexities and optimality gap. For example, a key idea in Autonomous Spectrum Balancing [31], is to decouple the joint power constraint across the $L$ resources by dual decomposition and to decouple the competing users by reference line, which does not directly apply to wireless networks. Even in DSL case, optimality of practical algorithms can only be proved in special cases since the general problem is non-convex.

### 9.2.2 Interference spread formulation

The problem definition in (9.4) assumes frequency dependent channels, $G_{ij}^l$, thus frequency specific SIR feasible regions $\mathbf{\Gamma}^l$. In some cases, wireless channels tend to be frequency independent since the bandwidth of interest, even for some wideband wireless system, is small compared to the carrier frequency. Channel variation across the band may be small. Furthermore, some systems incorporate interference averaging mechanism along the frequency domain. The frequency hopping mechanism in an OFDM system and the cover sequences in a CDMA system are interference averaging mechanisms motivated by the intention to spread the interference due to an MS across all of the $L$ resources. In these systems, inter-cell interference is averaged across the available bandwidth, while intra-cell interference is negligible since MSs within a cell are allocated orthogonal resources.

Therefore, a special case of joint power control and bandwidth allocation problem can be formulated as follows. Each MS $j$ transmits with power $p_j$ on resource $b_j$ of the total available bandwidth of $B^m$. The interference averaging mechanism ensures that a neighboring MS $i$ sees an interference of $G_{ij}p_j$ spread equally across the available bandwidth $W$. The average interference seen by MS $i$ becomes $q_i = \sum_{j \in C_i} G_{ij}p_j + n_i$ and the rate $r_i$ achieved by MS $i$ is given by

$$r_i = b_i \log(1 + cB^m\gamma_i/b_i) \tag{9.5}$$

where $\gamma_i = p_i/q_i$ is the SIR across the total bandwidth $B^m$, and $B^m\gamma_i/b_i$ is the boosted SIR for MS $i$ on resource $b_i$. Orthogonalization of MSs within the same cell requires an additional constraint that $\sum_{i \in S_k} b_i \leq B^m$. The following optimization problem is thus formulated:

$$\begin{array}{ll} \text{maximize} & \sum_i U_i(r_i) \\ \text{subject to} & r_i = b_i \log(1 + cB^m \gamma_i(\mathbf{p})/b_i) \\ & \sum_{i \in S_k} b_i \leq B^m \\ \text{variables} & \mathbf{r}, \boldsymbol{\gamma}, \mathbf{p}, \mathbf{b}. \end{array} \tag{9.6}$$

It can be verified that $r_i$ is a concave function of $b_i$. Under assumptions that $U_i(r_i)$ is concave in $r_i$, and, in addition, concave in $\log(\gamma_i)$, problem (9.6) is a convex optimization problem whose Lagrangian is

$$\mathcal{L}(\{\gamma_i\}, \{b_i\}, \{\nu_i\}, \{\lambda_k\}) = \sum_i U_i(r_i) + \sum_i \nu_i(p_i^m - p_i(\boldsymbol{\gamma})) + \sum_k \lambda_k(B^m - \sum_{i \in S_k} b_i). \tag{9.7}$$

In terms of the load-spillage factors discussed in Chapter 4 and [65], the KKT conditions can be written as

$$\begin{aligned} U_i'(r_i)\frac{\partial r_i}{\partial \gamma_i} &= \boldsymbol{\nu}^T \frac{\partial \mathbf{p}}{\partial \boldsymbol{\gamma}} \mathbf{e}_i = s_i q_i, \quad \forall i, \\ U_i'(r_i)\frac{\partial r_i}{\partial b_i} &= \lambda_k, \quad \forall i \in S_k. \end{aligned} \tag{9.8}$$

For example, consider the case where $U_i(r_i) = \log(r_i)$ and $r_i = b_i \log(1 + cB^m \gamma_i / b_i)$. The KKT conditions have the following structure.

$$\begin{aligned} \frac{cB^m}{b_i(1 + cB^m\theta_i)\log(1 + cB^m\theta_i)} &= s_i q_i, \quad \forall i, \\ 1/b_i &= s_i q_i \theta_i + \lambda_k, \quad \forall i \in S_k \end{aligned} \tag{9.9}$$

where $\theta_i = \gamma_i / b_i$ has the interpretation of SIR per resource. The optimality of equation (9.9) is established by the following Lemma.

---

**Lemma 9.1.** For $U_i(r_i) = \log(r_i)$, problem (9.6) is a convex optimization problem and satisfies equation (9.9) at optimality.

---

Figure 9.1 plots the trend of power and bandwidth allocation against spillage and interference at optimality. The points are obtained by solving the KKT equations above. Note that both power and bandwidth

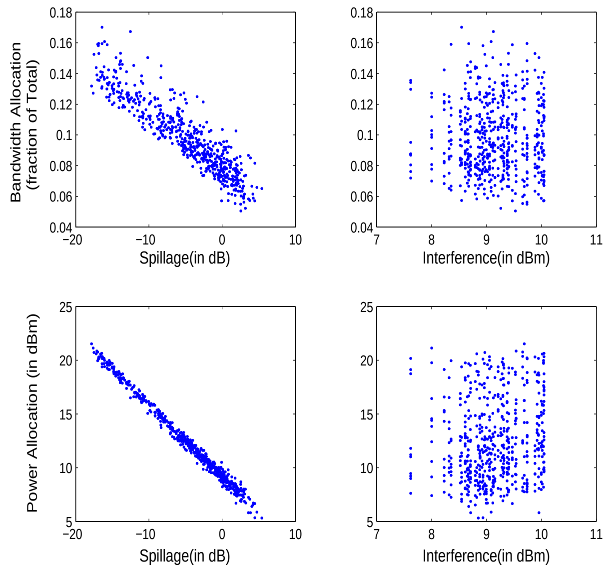


Fig. 9.1 Bandwidth and power allocation against spillage and interference at optimality.

allocation decreases with increasing spillage in the optimal allocation. This confirms the intuition that spillage acts as a measure of potential interference to the network, as discussed in Chapter 4. Distributed algorithm for this problem has not appeared yet.

## 9.3 Joint PC and Scheduling

One of the key functionalities of power control, and indeed the one that most of this monograph has been focusing on, is interference management. Since both schedules and powers are degrees of freedom that help manage interference, we need to investigate their joint control.

A simple view is to extend the basic power control models, both power minimization (for fixed SIR) and utility maximization (for variable SIR), by incorporating a new boolean variable $\xi_i \in \{0,1\}$, indicating whether MS $i$ is scheduled to transmit or not. This would be similar to the model of joint power control and BS assignment, leading to a mixed integer nonlinear optimization problem.

Assuming that the timescale of scheduling is shorter than the coherent time, another possible formulation would be similar to joint power control and bandwidth allocation with interference spread, as discussed in the last section, except now bandwidth chunk would be replaced by the fraction of time allocated to each MS.

However, neither of the above formulations completely captures the essence of joint power control and scheduling. All power control formulations surveyed so far assume that the objective is defined for the equilibrium state, therefore must activate all users in its power control solutions, for otherwise those users allocated with zero transmit power will be disconnected from the network. To properly study joint power control and scheduling, a generalization of such formulations to allow limit cycles, rather than a single point, at the equilibrium, is necessary.

On the other hand, on the topic of scheduling, existing research literature often assumes the $M$-hop collision model, which does not take into account that received SIR determines the amount of interference, nor the opportunity of varying transmit powers jointly with scheduling to increase stability region and the attained utility.

Both scheduling problem formulations (without power control) and power control problem formulations (without scheduling) are incomplete. They represent two sides of one common issue, one by deciding when can a subset of MSs transmit and the other by changing the power with which MSs can transmit. Their unification remains an open problem. Starting with the scheduling part of the problem, SIR based interference model often leads to NP-hard problems. Starting with the power control part of the problem, neither convexity of power-controlled rate region nor distributed convexification are well-understood. This overdue union between power control and scheduling presents fundamental research challenges, and is briefly discussed in this section from the point of view of power control.

Separation of scheduling and power control is proposed in [42, 46, 107]. The work in [42] proposes a centralized link scheduling algorithm that minimizes the power required to achieve a set of data rates that can potentially lie outside the instantaneous rate region but within the convex hull of the rate region. The authors make a low SIR approximation and assume that the data rate is linearly related to the SIR. In the resulting schedule, links either switch off or transmit with maximum power. An extension in [107] removes the low SIR approximation, resulting in additional complexity in the centralized solution. The work in [46] proposes a heuristic for link scheduling in each time slot, followed by the DPC algorithm for explicit rate requirements.

There are two major challenges in fully understanding the joint control of power and scheduling:

(1) When is power control adequate without time-sharing?
(2) If power control alone is inadequate, how should MSs be scheduled?

Here, the word "adequate" may be quantified by the optimality gap with respect to an objective function, e.g., cost function of power or utility function of rate. It is also often quantified by the size of stability region attained by an algorithm. Roughly speaking, when there are stochastic arrivals and departures of users, each carrying a finite workload, stability region is the set of arrivals that can be served by the system while keeping the queues finite. As mentioned in Section 1.1, stochastic arrivals will not be discussed in this monograph due to space limitation.

To answer these questions, an analysis of the convexity property of the rate regions attained by power control algorithms is needed, and a scheduling algorithm activating or silencing MSs in the right pattern is required when the rate region is non-convex.

Consider some functional dependence of rate on SIR, e.g.,

$$r_i(\gamma_i) = d \log(1 + c\gamma_i). \tag{9.10}$$

The instantaneous rate region $\mathcal{R}(\Gamma)$ is defined as the set of feasible rates in any time-frequency resource $v$:

$$\mathcal{R}(\Gamma) = \{r_i : r_i = r_i(\gamma_i), \boldsymbol{\gamma} \in \Gamma\} \tag{9.11}$$

where $\Gamma$ is a feasible SIR region introduced in Chapters 1 and 4. In particular, it is possible that $\Gamma = \mathbf{B}(\mathbf{p}^m)$ or $\Gamma = \mathbf{B}(\mathbf{q}^m)$, depending upon the constraints.

Let $x_i$ denote the traffic arrival rate for MS $i$, assumed time independent for simplicity of exposition. If MS $i$ is served rate $r_i[t]$ in slot $t$, then the queue for traffic intended for MS $i$, denoted by $y_i[t]$, evolves as

$$y_i[t+1] \leq [y_i[t] - r_i[t]]^+ + x_i. \tag{9.12}$$

where the time slot is assumed to be of unit length for simplicity.

Let $\mathcal{X}$ be the stability region. It is well known that $\mathcal{X} = Conv(\mathcal{R})$ where $Conv(\mathcal{R})$ is the convex-hull of the instantaneous rate region $\mathcal{R}$. In one of the possible formulations of the problem, the arrival rates are assigned a utility $U_i(x_i)$ and the problem is formulated as a utility maximization problem over $\mathcal{X}$:

$$\begin{array}{ll} \text{maximize} & \sum_i U_i(x_i) \\ \text{subject to} & \mathbf{x} \in \mathcal{X} = Conv(\mathcal{R}(\Gamma)) \\ \text{variables} & \mathbf{x}, \boldsymbol{\gamma}. \end{array} \tag{9.13}$$

This problem is considered in a number of papers both in the cellular setup [109, 7, 92] as well as the adhoc network setup [105, 160, 106, 124, 47, 36]. The problem can be split for each time instant $t$ into a rate control problem

$$x_i[t] = \arg\max U_i(x_i) - y_i[t]x_i, \tag{9.14}$$

a queue update as given in 9.12, and a resource scheduling problem given by

$$\begin{array}{ll} \text{maximize} & \sum_i y_i[t] r_i(\gamma_i) \\ \text{subject to} & \boldsymbol{\gamma} \in \Gamma \\ \text{variables} & \boldsymbol{\gamma}, \mathbf{r}. \end{array} \tag{9.15}$$

The queues $\{y_i[t]\}$ evolve over time and problem (9.15) is to be solved in every time slot $t$ with the resulting $x_i[t]$ converging to the optimal of problem (9.13). The queues have the interpretation of prices for the rate control problem, and the terms prices and queues are used interchangeably in the rest of the chapter.

Most of the work on power-control based interference model either make the "high-SIR" approximation where $\log(1 + c\gamma_i) \approx \log(c\gamma_i)$, which immediately renders $\mathcal{R} = Conv(\mathcal{R})$, or explicitly assume that $\mathcal{R}$ is convex, in which case again $\mathcal{R} = Conv(\mathcal{R})$. If the underlying instantaneous rate region $\mathcal{R}$ given by a power control algorithm is convex, then all MSs are allowed to participate in data transmission in every time-frequency resource and the power control algorithm can find the appropriate power levels to maximize the weighted rates. Distributed solutions with this simplification is proposed in [37, 65, 185]. The work in [39] develops the geometric programming framework of high SIR and successive GP approximation for general SIR regime. The work in [185] tackles problem (9.15) under the high-SIR approximation. The work in [65] can be applied to solve (9.15) if $\mathcal{R}$ is assumed to be convex.

However, if $\mathcal{R}$ is non-convex, there has been no distributed mechanism that determines the set of MSs allowed to participate in data transmission in each time slot and then determine the power levels of transmission among the activated MSs. Intuitively, an appropriate time sharing mechanism silences links whose queues are relatively small and whose activation would contribute adversely to the achievable rates of other links with relatively larger queues.

In the rest of this section, we will discuss a partial answer to the second question posed before, through a heuristic based on Algorithm LSPC in Chapter 4. There has been proof of convergence or optimality yet. The iterations are stated in terms of $\tau$ to distinguish between iteration index and queue update time.

---

**Algorithm 9.1 (Link Selection and Power Control).**

- Parameters: step size $\delta > 0, \delta_\nu > 0$.

(1) At $\tau = -1$, set spillage $s_i[-1] = 0$ at MS and communicate to BS.

(2) At $\tau = 0$, the BS for link $i$ picks $\ell_i[0]$ as the load-factor. The MS on link $i$ picks $\nu_i[0]$ as the power-price.

(3) At time $\tau$, the BSs calculate indicator functions $\xi_i[\tau]$ where

$$\xi_i[\tau] = I(\ell_i[\tau]/s_i[\tau - 1] \geq \beta_i).$$

The factor $\beta_i$ has to be adjusted appropriately so as to achieve a performance close to optimal.

(4) The load-factor $\ell_i[\tau]$ is broadcast if $\xi_i[\tau] \neq 0$.

(5) MS $i$ reads the broadcast load-factors from neighboring BSs with whom it can potentially interfere with, and calculates the spillage-factor $s_i$ as

$$s_i[\tau] = \sum_j G_{ji} b_j[t] \ell_j[\tau] + \nu_i[\tau]$$

(6) BS communicates the interference in the last slot $q_i[\tau - 1]$ on a feedback channel to MS $i$.

(7) MS $i$ uses transmit power level $p_i[\tau] = \gamma_i[\tau] q_i[\tau - 1]$ where SIR $\gamma_i[\tau] = \ell_i[\tau]/s_i[\tau]$.

(8) MS $i$ updates the power-price as

$$\nu_i[\tau + 1] = [\nu_i[\tau] + \delta_\nu (p_i[\tau] - p_i^m)]^+.$$

(9) MS $i$ updates the queue lengths $y_i[\tau]$ according to equation (9.12).

(10) BS measures the interference $q_i[\tau]$, and updates the load-factor: $\ell_i[\tau + 1]$

$$\Delta \ell_i[\tau] = \frac{y_i[\tau] r_i'(\gamma_i[\tau]) \gamma_i[\tau]}{q_i[\tau]} - \ell_i[\tau]$$

$$\ell_i[\tau + 1] = \ell_i[\tau] + \delta \Delta \ell_i[\tau]$$

---

The performance of Algorithm 9.1 is plotted in Figure 9.2 for a simple numerical example with 2 links. The channel parameters between the links are picked to result in a non-convex rate region as shown in the figure. An arrival rate within the convex hull of the rate region is picked. The algorithm is shown to stabilize the queues by alternating the capacity allocation between the links.

The basic idea in the algorithm is to silence links that are expected to contribute adversely to the objective of maximizing the overall network criteria. A link with a high spillage will thus be silenced until the queue builds up large enough to turn the link back on. With the large queue that has built up, a high load-factor is broadcast, resulting in possibly silencing the links that would have adversely affected this link. The factors $\beta_i$ are the silencing threshold. Low values of $\beta_i$ will prevent appropriate silencing and result in a set of data rates closer to the

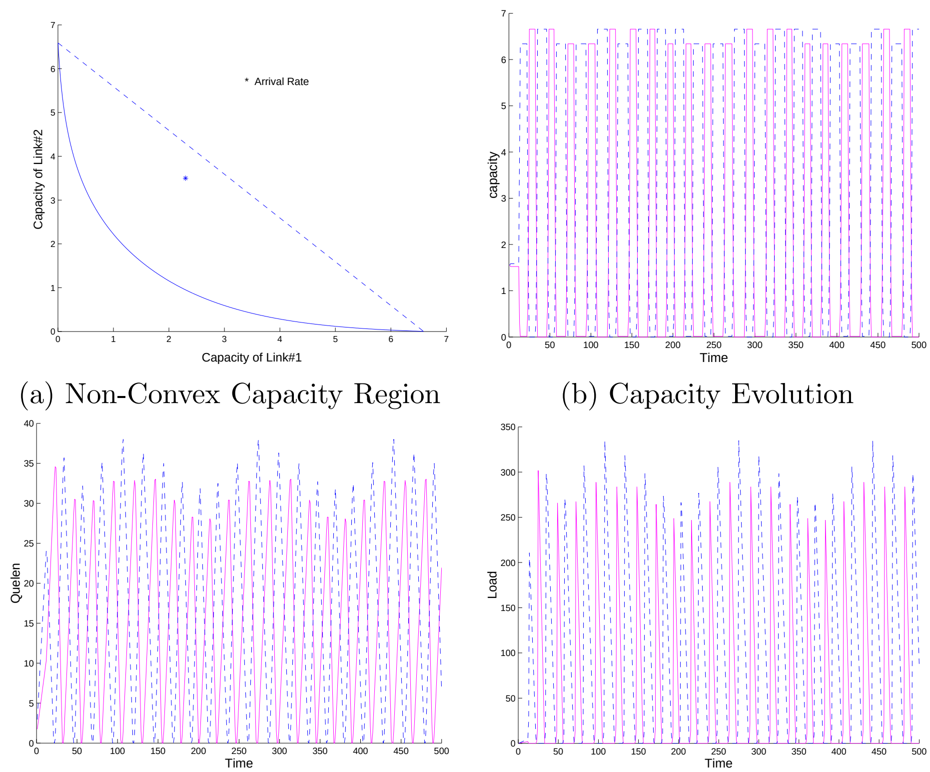


(a) Non-Convex Capacity Region (b) Capacity Evolution

(c) Queue Evolution (d) Load Evolution

Fig. 9.2 Performance of Algorithm 9.1 for two link case: The rate region is non-convex and the arrival rate in this example is within the convex hull but outside of the non-convex region as shown in Fig. 9.2a. The queues, loads and the assigned data rates oscillate between the two links as shown in Fig. 9.2b,c,d.

non-convex instantaneous rate region, and high values of $\beta_i$ will result in too many links being unnecessarily turned off, lowering the overall network utility. Determining the appropriate values of $\beta_i$ remains an open problem.

## 9.4 Joint PC, Beamforming, and Bandwidth Allocation

The joint optimization problems considered so far involved power control along with one other resource. It is apparent that optimizing over all resources jointly results in more efficient utilization of the resources but leads to increased complexity of implementation. Considering joint optimization of several resources together may also give the system designer insight into the trade-off involved among the resources to achieve a target value for the objective function. One such joint optimization is formulated in this section.

Consider the case where each BS is equipped with $M$ transmit antennas as in Chapter 7 and the total available bandwidth $B^m$ is split up into $L$ orthogonal resources $\{b_l\}$. The $N$ users build up queues $\{y_i[t]\}$ according to (9.12). As discussed in Section 9.3, the problem of maximizing the sum of the price-weighted rates becomes:

$$\begin{array}{ll} \text{maximize} & \sum_i y_i[t] r_i \\ \text{subject to} & r_i = \sum_{l=1}^{L} b_l \log(1 + c\gamma_i^l), \ \ \forall i \\ & \gamma_i^l \leq \mathsf{SIR}_i(\mathbf{W}, \mathbf{p}^l), \ \forall i \text{ and } \forall l \\ & \sum_l p_i^l \leq p_i^m, \ \forall i \\ \text{variables} & \boldsymbol{\gamma}, \mathbf{r}, \mathbf{W}, \mathbf{b}, \mathbf{p}. \end{array} \tag{9.16}$$

This joint optimization over space, time and frequency is a globally coupled, non-convex problem. A solution to this problem will be highly instructive to a system designer trading off resources in time, frequency, space and power. Now consider a simplification of problem (9.16), where queue evolution and time-domain scheduling are removed from consideration, and interference spreading mentioned in Section 9.2.2 is used in frequency-domain. The utility maximization problem becomes:

$$\begin{array}{ll} \text{maximize} & \sum_i U_i(r_i) \\ \text{subject to} & r_i = b_i \log(1 + B^m \gamma_i / b_i), \forall i \\ & \sum_{j:\sigma_j = k} b_j = B^m, \ \forall k \\ & \gamma_i \leq \mathsf{SIR}_i(\mathbf{W}, \mathbf{p}), \ \forall i \\ & \mathbf{p} \leq \mathbf{p}^m \\ \text{variables} & \boldsymbol{\gamma}, \mathbf{r}, \mathbf{W}, \mathbf{b}, \mathbf{p}. \end{array} \tag{9.17}$$

MSs within a cell are allocated orthogonal bandwidth resources so that each MS suffers only inter-cell interference, and beamforming in space is used to reduce the inter-cell interference. This joint optimization is still a globally coupled, non-convex problem, difficult to solve optimally or distributedly. However, the following approach to the solution is intuitively appealing. First, fixing the bandwidth allocation, the problem of jointly optimizing over receiver beamforming and transmit power can be solved by a distributed algorithm as in Section 7.3, which is proved to be convergent. Next, as shown in Section 9.2.2, the joint power-bandwidth optimization with fixed beamforming vectors is a convex optimization problem. Finally, an alternating maximization method is used to combine these two algorithms and shown to be convergent.

---

**Algorithm 9.2 (Joint optimization of three resources).**

(1) BSs and MSs perform joint beamforming and power control in Algorithm 7.3 until it converges:
   (a) MSs updates transmit power control using the load and spillage, for fixed beamforming vectors.
   (b) The BS that serves MS $i$ optimizes the beamforming vector of MS $i$.

(2) Resulting $\mathbf{p}[t]$ and $\mathbf{W}[t+1]$ are inputs for the next step.

(3) BSs and MSs solve for joint bandwidth allocation and power control using any standard convex optimization method.

(4) Resulting $\mathbf{p}[t+1]$ and $\mathbf{b}[t+1]$ are inputs for the next step.

---

The joint optimization framework like the above is more than an intellectual curiosity, it leads to a quantitative understanding of the engineering tradeoff among increasing power, partitioning the spectrum, and installing multiple antennas. Fig. 9.3 illustrate an achievable, equi-utility contour surface, obtained by solving the above optimization problem, as a function of three resource constraint parameters: transmit power $\mathbf{p}^m$, total bandwidth $B^m$ and number of BS antennas $K$. In a network with $N = 10$ users, $\mathbf{p}^m/n = 0$dB, and $B^m = 1$MHz, Algorithm 9.2 and rate control algorithm (9.14) are employed for solving the joint utility optimization problem under these three constraints. Fig. 9.3 illustrates a Pareto-optimal tradeoff surface for the optimized utility contour over 3-D bases, by plotting a set of resource bundles $\{B^m, \mathbf{p}^m, M\}$ providing the same optimal utility. Each axis represents

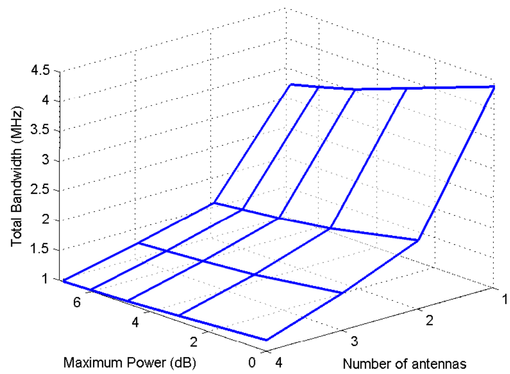


Fig. 9.3 A Pareto-optimal tradeoff surface among different resource allocations that achieve the same utility. Each axis represent a resource constraint parameter. The optimal resource allocation itself is not shown.

the constraint value on one of the resources, and each point on the surface states that for this set of constraint values, the optimized resource allocation (not shown in the graph) attains the same utility value as other points on the surface.

Imposing a cost model on top of this Pareto-optimal surface will further provide a cost-effectiveness analysis to the wireless cellular operator. For example, since bandwidth is a scarce resource in a wireless cellular network, a large cost function should be associated with the total bandwidth usage, whereas smaller costs are assigned to power and number of antennas. This choice of costs would result in a resource bundle of $\{B^m = 1\text{MHz}, p^m = 5, M = 4\}$, in which the total bandwidth usage has been minimized. This is in contrast to a different resource bundle of $\{W = 4.37\text{MHz}, p^m = 1, M = 1\}$ lying on the same tradeoff surface, where number of antennas and transmit power has been minimized.

## 9.5 Open Problems

There is a large number of open problems on topics discussed in this chapter. Many of them are due to the delicate balance between tractability and accuracy of models of resource allocation in wireless networks. In addition, neither algorithm presented in this chapters has a full characterization of convergence or optimality.

For joint power control and bandwidth allocation, the interference spread approach is only an approximation. The original formulation (9.4) in Section 9.2 does not have yet a scalable solution. A good understanding of the solution would provide further insights into the classical question of what frequency reuse factor is best for the efficient performance of a cellular network.

For joint power control and scheduling, the two fundamental difficulties listed in Section 9.3 both remain open problems. In particular, we need to characterize the convexity of various power controlled rate regions without assuming convexity of SIR feasibility region in the first place. Distributed solution to the convex problem of maximizing utility over the convex hull of rate region has not been found. Even a proper model of jointly deciding when and how much power to transmit will require innovative optimization formulations. Further challenges will arise as both channel variations and traffic's stochastic arrivals are incorporated like in Chapter 5.

In general, a complete understanding of how to design cellular networks by jointly considering transmit power and all other degrees of freedom remain a long-term goal, with continuous progress being made as documented in the last three chapters.

# 10

# Industry Adoption

## 10.1 Introduction

Power control mechanisms have played an important role in the success of most digital cellular systems. Power control offers substantial benefits for the efficient and fair operation of the cellular system, supports QoS adaptations like rate control, and yet the basic power control algorithms involve feedback with as few as 1-bit and are simple to implement. These motivate most cellular systems to incorporate power control in the physical layer specification of the standard. In this concluding chapter of the monograph, we survey a selection of the implementations of the algorithms in previous chapters in operational networks, including those listed in Table 10.1.

Power control implementations in cellular systems often consist of Open-loop power control (OLPC) and Closed-loop power control (CLPC). OLPC is a simple scheme that allows the transmitter to optimally select the transmit power by exploiting the similarity of the uplink and downlink channel in properties including distance-dependent attenuation and frequency-independent slow fading. For asymmetric channel properties like fast fading, a CLPC scheme, as discussed in

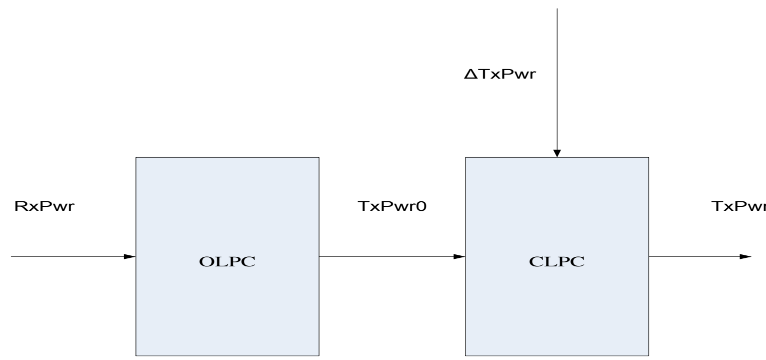


Fig. 10.1 Power-control loops in cellular networks.

Chapter 2, will have to be implemented. CLPC schemes are more expensive to implement and are most beneficial in the uplink communication or for a Frequency Division Duplex (FDD) system where uplink and downlink are on different frequencies and the channel on the two links are uncorrelated with respect to fast fading. Time Division Duplex (TDD) systems, on the other hand, see correlated channel on the uplink and downlink even for fast fading and can adjust the transmit power on either link by directly measuring the the receiver power and channel quality on the other link. As such, CLPC tends to be prevalent in the uplinks of FDD systems and less so in the downlink or the TDD systems. Typically, tolerance levels for OLPC is in the range 9-12dB and tolerance levels for CLPC in the range 1-2dB.

## 10.2 Power Control in 2G Networks

Early digital cellular systems are typically referred to as 2G systems to set them apart from 1G analog cellular systems. The 2G systems were primarily designed for voice which is generated at a fixed bit rate, and the power control mechanisms were geared towards targeting a fixed SIR, determined by the quality of voice that needs to be supported.

Table 10.1 Power control basic parameters in cellular network standards

| Cellular System | Update Frequency | Supported Step-Size |
|---|---|---|
| GSM | 2Hz | 2-3dB |
| IS-95 | 800Hz | 1dB |
| WCDMA | 1500Hz | 0.2dB-1dB |
| 1xEVDO-Rel0 | 600Hz | 0.25-1dB |
| 1xEVDO-RevA | 150Hz | 0.2dB-1dB |
| Flash-OFDM | 800Hz | 0.5-1dB |

Qualcomm proposed an OLPC scheme for a CDMA based cellular system where the transmit power is set inversely proportional to the received power [154]. The OLPC scheme was augmented by a CLPC scheme where the receive powers were equalized through a 1-bit feedback [62]. This power control solution to the near-far problem was instrumental in enabling the success of CDMA networks.

More recent CLPC algorithms implement a discretized version of the DPC algorithm where the feedback from the BS is limited to a finite number of bits, and the transmit power at the MS is altered by a fixed step-size update based on the feedback. The feedback is typically 1-bit or 2-bits, and represents either a increment or decrement of the power level rather than the absolute power level. For example, a 1-bit power control feedback with a step-size of $\delta$dB increases the transmit power by $\delta$dB if the feedback is "0" and decreases the transmit power if the feedback is "1". It is shown in [90] that this CLPC implementation converges to within $2\delta$dB of the SIR target. A two-bit feedback (more precisely, a 3-level or a 1.5-bit feedback) either increases or decreases the transmit power level by $\delta$dB or maintains the transmit power at the same level based on the feedback. The result in [164] shows that the 3-level feedback converges to within $\delta$dB of the SIR target.

The feedback frequency presents a trade-off between power-control overhead and the doppler tolerance. For example, it is shown in [40] that the number of users in an IS-95 sector that can be supported drops by 25% when the doppler changes from 25Hz to 50Hz at a power control update rate of 800 per second. The step-size choice presents a trade-off between doppler tolerance, robustness, and spectral efficiency. Typically, higher doppler requires larger step-size to be able to track the fast fades. An approximate but useful calculation of doppler tolerance levels based on CLPC feedback rate and step-size parameters is as follows. If feedback is at the rate of $F$ updates every second and the step-size is $\delta$dB, then a a Rayleigh fade of upto 30dB requires $30/(F\delta)$ seconds to bring the power level back to the nominal. This implies that the channel coherence time can be no less than $30/(F\delta)$ seconds or equivalently doppler level no more than $F\delta/30$Hz. However, larger step-sizes result in more SIR variation in steady state and larger variations when dopplers exceed what can be supported. Therefore, step-sizes needs to be chosen with care.

CLPC is an important component of the CDMA based IS-95 [169] system where neighboring sectors use the same frequency. It helps in minimizing inter-sector interference and enabling frequency reuse of one. In addition, MSs in the same sector of an IS-95 system are not orthogonal on the uplink since it is prohibitively expensive to maintain CDMA chip-level synchronization among MSs. CLPC ensures that the MSs closer to the BS does not swamp out the MSs further away from the BS. The CLPC scheme on the uplink in IS-95 uses 1-bit feedback at the rate of 800 every second. The power control update is in steps of 1dB with choices of smaller steps allowed in later revisions of the standard. On the downlink, CLPC is less important since the downlink signals emanating from the same BS are orthogonal, and as such the feedback rate is once every 20ms reporting a frame error in 1-bit.

The GSM[5] based 2G standard is an orthogonal scheme where the MSs within a sector are allocated a separate time and frequency slot for both uplink and downlink. Maintaining orthogonality between MSs of the same sector implies that the time-frequency resource for each MS is limited and the SIR requirement for voice communication is higher in comparison to IS-95. This rules out frequency reuse of one in GSM systems. The non-existence of inter-sector interference from the immediate neighbors of a sector and the non-existence of intra-cell interference due to the orthogonality of MSs within a sector imply that the need for CLPC in GSM standard is less in comparison to IS-95. As such, GSM implements a CLPC scheme both on the uplink as well as the downlink with updates every 480ms based on two parameters referred to as “RxLev” and “RxQual”. The “RxLev” is the receive power level and the “RxQual” is the receive signal quality in terms of SIR or BER.

## 10.3 Power Control and Scheduling in 3G/4G Networks

In addition to voice, the 3G and 4G cellular systems support data of varying rates and QoS needs. Rather than formulating power control as a fixed SIR feasibility problem, SIR assignment and power control need to be jointly designed as in Chapter 4. The time and frequency allocation for each MS, unlike the case in a 2G system, is not static but depends on the traffic arrivals, channel conditions, and QoS classes. Scheduling refers to allocation of time and frequency slots to the MSs, as discussed in detail in 9. Power control determines the transmit power allocated to the links. Power control and scheduling are therefore done in conjunction in 3G systems to maximize the efficiency of the system.

The time and frequency resources are split into chunks that form the time-frequency slabs. For each time-frequency slab, the scheduling algorithm decides the set of MSs that are allowed to participate in data transmission in that slab, and the power control part determines the data rate of transmission by allocating appropriate power levels to the participating MSs through a power-control algorithm. The ultimate objective, whether stabilizing queues resulting from a set of arrivals or maximizing network-wide criteria, is realized through both scheduling and rate selection through power control.

The scheduling mechanism requires a control channel over which the allocation of the MSs for a given time-frequency slot is indicated to the MSs. This overhead is an important factor to consider in the design of the scheduler. If the traffic pattern over the links is predictable, then it might be beneficial to pre-allocate the time-frequency resources and reduce the overhead associated with an explicit scheduler implementation. Such a system is then an unscheduled system supporting more uniform data rates in comparison to a scheduled system. For example, the 1xEVDO system is a scheduled system on the downlink but an unscheduled system on the uplink. An unscheduled system is still designed to support different data rates according to the traffic requirements but would be efficient only in supporting uniform data rates.

An important factor that determines the total uplink capacity in commercial networks is the interference limit $\mathbf{q}^m$, often stated in terms of IOT and ROT factors that were discussed in Chapter 1. The IOT limits bound the interference to the cell ensuring stability of rate allocation on the uplink, and in addition limits the power required for new mobiles to access the network. Typical IOT values in commercial networks range from 3 to 10 dB.

### 10.3.1 1xEVD0 Rel0 and RevA

The 1xEVDO Rel0 [2] and RevA [3] are CDMA based 3G systems that implement a scheduled downlink and an unscheduled uplink. On the downlink, the transmit power is fixed and the rate of transmission is adapted according to the interference experienced by the MS. No power control is employed. The long-term data rates depend upon the fraction of time-frequency slabs scheduled to each MS.

The uplink, however, is unscheduled and relies on power control to achieve a required data rate. Two independent control mechanisms together determine the uplink data rate as explained in [33].

First is the basic power control that measures the received SIR on pilot signals transmitted by the MS and feeds back 1-bit power up-downs. Rel0 uses a feedback rate of 600Hz with step-seize of 1dB. The Pilot channel transmit power is determined entirely by this power-control loop. The traffic channel transmit power is expressed in relation to the pilot channel transmit power and is referred to as the T2P (Traffic-to-Pilot Power). The data rate on the traffic channel has a one-to-one relationship, with T2P with higher rates requiring higher T2P.

The second control mechanism determines the data rate of transmission. Each BS measures the interference level and sets a control bit referred to as the "Reverse Activity Bit" (RAB) if the level is beyond a certain threshold. The MS maintains an "active set" of BSs that it can detect with some strength including the serving BS. The RAB-bit from any one of the BSs causes the MS to backoff it's current data rate with a certain probability. If no RAB-bit is detected to be set, then the

MS increases the data rate with a certain probability. The RAB-bits are fed back at the rate of 37.5Hz. The probabilities are set to values dependent on the desired interference level and can be set on the each MS to satisfy QoS requirements. Since the supported data rates are not a continuum of values but take some discrete values based on the chosen code rate and modulation, the T2P is discrete the interference tends to be bursty.

The uplink in RevA is an improvement over that of Rel0. Higher data rates are defined, supporting a larger range of data rates, and hybrid ARQ is introduced, making effective use of any T2P and providing a contiguous set of data rates. The MS decreases and increases the T2P in deterministic amounts based on whether the RAB bit is set or not. The T2P and the hybrid ARQ-induced latency requirement for the traffic determine the rate of transmission. The RAB bit is transmitted more frequently in RevA, at the rate of 600Hz, and hybrid ARQ allows a continuum of T2P, making the interference less bursty with RevA in comparison to Rel0. Indeed, the RevA uplink is two to three fold more efficient in comparison to Rel0 uplink as shown in [51].

### 10.3.2 Flash-OFDM

The Flash-OFDM system [94] is based on OFDM modulation with orthogonality among MSs within the same cell maintained by allocating different tones to different MSs. The orthogonality among MSs removes intra-cellular interference, improving the range of attainable SIRs. Maintaining orthogonality among MSs is easier in OFDM than in CDMA since the MSs have to match their timing alignment with the BS only upto the cyclic prefix inserted in the OFDM symbol. However, this gain in SIR due to removal of intra-cellular interference comes at the expense of the extra resource occupied by the cyclic prefix.

Another advantage of the timing alignment of the MSs within a cell in an OFDM system is that it opens up the possibility of having a scheduled uplink. The true advantages of a scheduler should be evaluated in terms of the overhead carrying information of the assignment of the MSs to the time-slots and the benefits offered by a scheduler in managing various traffic arrival patterns. The Flash-OFDM system is a scheduled downlink and uplink system. Similar to the 1xEVDO systems, the Flash-OFDM system has the MS transmitting pilots that are power-controlled to a given SIR target. The traffic channel transmit power is not determined by the MS directly. Instead, the MSs report to the BS a quantity similar to the "spillage" as explained in Chapter 4. The uplink scheduling algorithm at the BS picks MSs that can transmit in any given time-frequency slab and indicates the maximum T2P that each scheduled MS can use in the time-frequency slab. The MS then picks a data rate that can be supported within the maximum T2P that it gets from the BS.

The Flash-OFDM network is the first network with a scheduled uplink with the power control and rate selection based partly on the optimization framework presented in Section 4.3.2. Time is slotted into units of 1.4ms with a power-control feedback expected every slot. Scheduling decision made every time-slot about the set of MSs that will participate in data transmission in that slot and the rate at which the MSs transmit. This gives the scheduler flexibility in catering to various traffic patterns and QoS requirements. However, power control feedback at the same rate as the scheduling decision and the possible fluctuation in transmit power of MSs due to scheduling decisions can potentially destabilize the system. The Flash-OFDM system implements a simple rule derived from the results in Section 4.3.2 to maintain stability. If $L_k$ is the load-budget allocated to BS $k$, then every time slot the BS schedules a set of users such that $\sum_i s_i \gamma_i < L_k$, where $s_i$ is the spillage reported by MS $i$ and $\gamma_i$ is the SIR corresponding to the intended rate allocation. With this rule and with a suitable averaging of the interference used in rate allocation, it can be shown that the Flash-OFDM system maintains a stable uplink with rate allocation close to optimal.

### 10.3.3 WiMax

Power control in the WiMax broadband wireless system [1] is based on the uplink ranging signal, which is a fixed waveform transmitted by the terminals for the BS to make power and timing corrections. The downlink power corrections, however, are not defined as part of the standard and left to the implementation to be sent down as control data packets. The power control mechanism is expected to support fluctuations of 30dB per second with depths of at least 10dB. WiMax defines a scheduled uplink and the BS picks the MSs that can transmit in any given time-frequency slab. The MS maintains the same transmit power level per tone and the total power transmitted depends upon the number of traffic tones transmitted.

## 10.4 Power Control in WiFi Networks

The IEEE 802.11 standard defines a wireless local area network that is typically not considered "cellular". However, the most prevalent model of deployment for the WiFi standard is in a mode where the WiFi access terminals (ATs) communicate with an access point (AP), similar to the MSs communicating with a BS in cellular topologies. In such a scenario, power control can result in significant improvement to the performance of the network both by reducing the overall power consumption of the ATs and reducing the interference level and thereby increasing the data rates.

The 802.11 standard implements a MAC algorithm that involves carrier sense and exponential backoff and does not dictate any explicit power control scheme. Researchers have attempted to remedy the situation by proposing various MAC layer schemes that can be implemented on top of the PHY layer. One such mechanism is for the receiver to send back the power level of data transmission in a control channel at the maximum power, in response to intention of data transmission indicated by the transmitter [130]. However, transmitting data and control channel at different power levels results in inefficient operation in an unplanned spread of APs. Improvements to this scheme were suggested in [89] to get around the problem by occasionally transmitting data at the maximum power to prevent neighboring APs from taking over the channel.

## 10.5 Open Issues

The 3G cellular data systems mostly designed power control based on principles developed for the 2G networks, often retaining the assumption of a fixed date rate demand, and sometimes leveraging joint SIR assignment and power control. As cellular data and multimedia transmission become more prevalent in mobile applications, the expectation is that the data rate demands will have a high dynamic range both among users and in time. It becomes important for the industry to adopt techniques for admission control as discussed in Chapter 3, for better power allocation under channel variation as discussed in Chapter 5, for joint power control and beamforming design in cells equipped with multiple antennas as discussed in Chapter 7, for joint power control and BS allocation as discussed in Chapter 8, and for joint power control and time-frequency allocation as discussed in Chapter 9.

For example, the Fractional Frequency Reuse (FFR) scheme proposed in the design of Universal Mobile Broadband [4], the next generation mobile broadband system from the 3GPP group, is an effort to revisit the joint power control and frequency allocation design. The available bandwidth is sub-divided into multiple sub-bands, with frequency-hopping restricted to within the sub-band. This allows the power allocation to be varied in different sub-bands. The envisioned use of the sub-bands is static allocation of powers to result in frequency reuse of 1 in some sub-bands and higher frequency reuse in other sub-bands. Dynamic power allocation across sub-bands in response to varying QoS demands remains an open issue that demands an answer to problems in Section 9.4. As the general industry trend continues towards scheduled allocation of time and frequency resources, an efficient way to implement a solution to Problem 9.13 in Chapter 9 is required. Since it is desirable to have network architectures that preclude centralized Base Station Controllers, a distributed solution to Problem 9.13 that only requires BS MS message passing would be even better.

Indeed, most of the open problems in power control discussed in Chapters 2–9 are clearly motivated by the needs of operational wireless cellular networks. Their solutions would require new modeling techniques, theoretical advances, and mathematical machinery, which will in turn help push the cellular technology as in the last 15 years of this research area.

# Acknowledgement

We would like to acknowledge collaborations on cellular network power control papers with J. Huang, D. Julian, M. Fazel, D. Gayme, F. Meshkati, D.O'Neill, D. Palomar, H. V. Poor, S. Rangan, S. Schwartz, X. Wu, and W. Yu.

We are also grateful to helpful discussions on the subject, as well as power control in ad hoc networks, with many other colleagues, including N. Bambos, S. Boyd, A. R. Calderbank, A. Ephremides, A. Goldsmith, Z. Han, P. R. Kumar, J. W. Lee, N. Mandayam, S. Sooroshyari, N. B. Shroff, R. Srikant, R. Yates, Y. Yi, and X. Zhang.

Our own work surveyed in this monograph has been supported in part by NSF Combined Research and Curriculum Development grant CNS-0417607, NSF CAREER grant CCF-0448012, NSF FIND grant CNS-0720570, DARPA Control Based MANET grant, and ONR Young Investigator Program grant N00014-07-1-0864.

# References

[1] Air interface for fixed and mobile broadband wireless access systems. Technical report, IEEE 802.16e Working Group, URL: http://standards.ieee.org/getieee802/download/802.16e-2005.pdf, December 2005.

[2] 3rd Generation Partership Project 2 (3GPP2). CDMA2000 high rate packet data air interface specification. Technical Report C.S20024 v2.0, URL: http://www.3gpp2.org, October 2000.

[3] 3rd Generation Partership Project 2 (3GPP2). CDMA2000 high rate packet data air interface specification revision a. Technical Report C.S20024-A, URL: http://www.3gpp2.org, March 2004.

[4] 3rd Generation Partership Project 2 (3GPP2). Ultra mobile broadband technical specifications. Technical report, URL: http://www.3gpp2.org, March 2007.

[5] 3rd Generation Partership Project (3GPP) TS 45.008. Radio access network; radio subsystem link control. Technical Report version 5.3.0, Release 5, URL: http://www.3gpp.org, 2001.

[6] R. Agarwal, V. Abhishek, R. Vannithamby, and J. Cioffi. Opportunistic feedback protocol for minimizing power in uplink with heterogeneous traffic. *Proceedings of IEEE VTC*, September 2007.

[7] R. Agrawal and V. Subramanian. Optimality of certain channel aware scheduling policies. *Proceedings of Allerton Conference on Communication, Control and Computing*, 2002.

[8] T. Alpcan, T. Basar, and R. Srikant. CDMA uplink power control as a noncooperative game. *IEEE Transactions on Wireless Networkss*, 8(6):659–670, December 2002.

[9] E. Altman and Z. Altman. S-modular games and power control in wireless networks. *IEEE Transactions on Automatic Control*, 48(5):839–842, 2003.

[10] E. Altman, T. Boulogne, R. Azouzi, and T. Jimenez. A survey on networking games in telecommunications. Technical report, URL: citeseer.ist.psu.edu/altman00survey.html, 2000.

[11] S. Anand and A. Chockalingam. Performance analysis of voice/data cellular CDMA with sir-based admission control. *IEEE Journal of Selected Areas in Communications*, 21(10):1674– 1684, December 2003.

[12] M. Andersin, Z. Rosberg, and J. Zander. Soft and safe admission control in cellular networks. *IEEE/ACM Transactions on Networking*, 5(2):255–265, April 1997.

[13] F. Baccelli, B. Blaszczyszyn, and F. Tournois. Downlink amission/congestion control and maximal load in CDMA networks. *Proceedings of IEEE Infocom*, April 2003.

[14] G. Bacci, M. Luise, and H. V. Poor. Game theory and resource allocation in multiuser impulse radio networks. *To appear in Physical Communication*, 1(1), January 2008.

[15] G. Bacci, M. Luise, H. V. Poor, and A. Tulino. Energy-efficient power control in impulse radio uwb wireless networks. *IEEE Journal of Selected Areas in Communications*, 1(3):508–520, October 2007.

[16] N. Bambos. Toward power-sensitive network architectures in wireless communications: concepts, issues, and design aspects. *IEEE Personal Communications*, 5(3):50–59, June 1998.

[17] N. Bambos, C. Chen, and G. Pottie. Channel access algorithms with active link protection for wireless communication networks with power control. *IEEE/ACM Transactions on Networking*, 8(5):583–597, October 2000.

[18] N. Bambos and S. Kandukuri. Power-controlled matiple access schemes for next-generation wireless packet networks. *IEEE Wireless Communications*, 9(3):58–64, June 2002.

[19] P. Bender, P. Black, M. Grob, R. Padovani, N. Sindhushayana, and A. Viterbi. CDMA/HDR: a bandwidth-efficient high-speed wireless data service for nomadic users. *IEEE Communications Magazine*, pages 70–77, July 2000.

[20] M. Bengtsson. Jointly optimal downlink beamforming and base station assignment. *Proceedings of IEEE ICASSP*, May 2001.

[21] M. Bengtsson and B. Ottersten. Optimal downlink beamforming using semidefinite optimization. *Proceedings of Allerton Conference on Communication, Control and Computing*, September 1999.

[22] M. Bengtsson and B. Ottersten. *Handbook of Antennas in Wireless Communications: Chapter 18: Optimal and Suboptimal Transmit Beamforming.* CRC press, 2001.

[23] D. P. Bertsekas. *Nonlinear Programming.* Athena Scientific, 2nd edition, 1999.

[24] H. Boche and M. Schubert. A general duality theory for uplink and downlink beamforming. *Proceedings of IEEE VTC*, September 2000.

[25] H. Boche and S. Stanczak. Convexity of some feasible qos regions and asymptotic behavior of the minimum total power in CDMA systems. *IEEE Transactions on Communications*, 52(12):2190–2197, December 2004.

[26] H. Boche and S. Stanczak. Optimal qos tradeoff and power control in CDMA systems. *Proceedings of IEEE Infocom*, March 2004.

[27] S. Boyd and L. Vandenberghe. *Convex Optimization*. Cambridge University Press, 2004.

[28] S. Buzzi and H. V. Poor. Non-cooperative games for spreading code optimization, power control and receiver design in wireless data networks. *Proceedings of European Wireless Conference*, April 2007.

[29] G. Caire and S. Shamai. On the achievable throughput of a multi-antenna gaussian broadcast channel. *IEEE Transactions on Vehicular Technology*, 49(7):1691–1706, July 2003.

[30] D. Catrein, L. A. Imhof, and R. Mathar. Power control, capacity, and duality of uplink and downlink in cellular CDMA systems. *IEEE Transactions on Communications*, 52(10):1777–1785, October 2004.

[31] R. Cendrillon, J. Huang, M. Chiang, and M. Moonen. Autonomous spectrum balancing for digital subscriber lines. *IEEE Transaction on Signal Processing*, 55(8):4241–4257, August 2007.

[32] R. Cendrillon, W. Yu, M. Moonen, J. Verlinden, and T. Bostoen. Optimal multi-user spectrum management for digital subscriber lines. *IEEE Transactions on Communications*, 54(5):922–933, May 2006.

[33] S. Chakravarty, R. Pankaj, and E. Esteves. An algorithm for reverse traffic channel rate control for CDMA2000 high rate packet data systems. *Proceedings of IEEE Globecom*, November 2001.

[34] J. F. Chamberland and V. V. Veeravalli. Decentralized dynamic power control for cellular CDMA systems. *IEEE Transactions on Wireless Communications*, 2(3):549–559, May 2003.

[35] B.-S. Chen, B.-K. Lee, and S. Chen. Adaptive power control of cellular CDMA systems via the optimal predictive model. *IEEE Transactions on Wireless Communications*, 4(4):1914–1927, July 2005.

[36] L. Chen, S. H. Low, M. Chiang, and J. C. Doyle. Joint optimal congestion control, routing, and scheduling in wireless ad hoc networks. *Proceedings of IEEE Infocom*, 2006.

[37] M. Chiang. Balancing transport and physical layers in wireless multihop networks: Jointly optimal congestion control and power control. *IEEE Journal of Selected Areas in Communications*, 23(1):104–116, January 2005.

[38] M. Chiang and J. Bell. Balancing supply and demand of bandwidth in wireless cellular networks: Utility maximization over power and rates. *Proceedings of IEEE Infocom*, March 2004.

[39] M. Chiang, C. W. Tan, D. P. Palomar, D. O'neill, and D. Julian. Power control by geometric programming. *IEEE Transactions on Wireless Communications*, 6(7):2640–2651, July 2007.

[40] A. Chockalingam, P. Dietrich, L. B. Milstein, and R. R. Rao. Performance of closed-loop power control in DS-CDMA cellular systems. *IEEE Transactions on Vehicular Technology*, 47(3):774–789, August 1998.

[41] J. Crowcroft, R. Gibbens, F. Kelly, and S.Ostring. Modelling incentives for collaboration in mobile ad hoc networks. *Proceedings of IEEE WiOpt*, March 2003.

[42] R. L. Cruz and A. V. Santhanam. Optimal routing, link scheduling and power control in multi-hop wireless networks. *Proceedings of IEEE Infocom*, April 2003.

[43] S. Das and H. Viswanathan. A comparison of reverse link access schemes for next-generation cellular systems. *IEEE Journal of Selected Areas in Communications*, 24(3):684–692, March 2006.

[44] V. M. DaSilva and E. S. Sousa. Performance of orthogonal CDMA codes for quasi-synchronous communication systems. *Proceedings of IEEE International Conference on Universal Personal Communications*, June 1993.

[45] J. Duplicy, J. Louveaux, and L. Vandendorpe. Utility-based MIMO uplink beamforming. *Proceedings of IEEE Workshop on Sensor Array and Multichannel Signal Processing*, July 2006.

[46] T. ElBatt and A. Ephremides. Joint scheduling and power control for wireless ad hoc networks. *IEEE Transactions on Wireless Communications*, 3(1):74C85, January 2004.

[47] A. Eryilmaz and R. Srikant. Fair resource allocation in wireless networks using queue-length-based scheduling and congestion control. *Proceedings of IEEE Infocom*, March 2005.

[48] J. S. Evans and D. Everitt. Effective bandwidth-based admission control for multiservice CDMA cellular networks. *IEEE Transactions on Vehicular Technology*, 48(1):36–46, January 1999.

[49] D. Falomari, N. Mandayam, and D. Goodman. A new framework for power control in wireless data networks: Games utility and pricing. *Proceedings of Allerton Conference on Communication, Control and Computing*, September 1998.

[50] D. Famolari, N. B. Mandayam, D. Goodman, and V. Shah. *A New Framework for Power Control in Wireless Data Networks: Games, Utility and Pricing: Wireless Multimedia Network Technologies*. Kluwer Academic Publishers, editors: ganesh, pahlavan, zvonar edition, 1999.

[51] M. Fan, D. Ghosh, N. Bhushan, R. Attar, C. Lott, and J. Au. On the reverse link performance of CDMA2000 1xev-do revision a system. *Proceedings of IEEE ICC*, May 2005.

[52] F. R. Farrokhi, K. J. R. Liu, and L. Tassiulas. Transmit and receive diversity and equalization in wireless networks with fading channels. *Proceedings of IEEE Globecom*, August 1997.

[53] M. Fazel, D. Gayme, and M. Chiang. Transient analysis of power control. *Proceedings of IEEE Globecom*, November 2006.

[54] N. Feng, S. Mau, and N. Mandayam. Pricing and power control for joint network-centric and user-centric radio resource management. *IEEE Transactions on Communications*, 52(9):1547–1557, September 2004.

[55] N. Feng, S. C. Mau, and N. B. Mandayam. Joint network-centric and user-centric radio resource management in a multicell system. *IEEE Transactions on Communications*, 53(7):1114–1118, July 2005.

[56] C. Fischer. Load in CDMA cellular systems and its relation to the perron root. *IEEE Transactions on Wireless Communications*, 6(7):2660–2668, July 2007.

[57] G. J. Foschini and Z. Miljanic. A simple distributed autonomous power control algorithm and its convergence. *IEEE Transactions on Vehicular Technology*, 42(4):641–646, November 1993.

[58] G. J. Foschini and Z. Miljanic. Distributed autonomous wireless channel assignment algorithm with power control. *IEEE Transactions on Vehicular Technology*, 44(3):420–429, 1995.

[59] S. Friedland and S. Karlin. Some inequalities for the spectral radius of non-negative matrices and applications. *Duke Mathematical Journal*, 42(3):459–490, November 1975.

[60] A. Ganti, T. Klein, and M. Haner. Base station assignment and power control algorithms for data users in a wireless multiaccess framework. *IEEE Transactions on Wireless Communications*, 5(9):2493–2503, September 2006.

[61] A. Giannoulis, K. P. Tsoukatos, and L. Tassiulas. Maximum throughput power control in CDMA wireless networks. *Proceedings of IEEE ICC*, June 2006.

[62] S. K. Gilhousen, R. Padovani, and C. E. Wheatley. Method and apparatus for controlling transmission power in a CDMA cellular mobile telephone system. *United States Patent 5,056,109*, October 1991.

[63] A. Goldsmith and P. Varaiya. Capacity of fading channels with channel side information. *IEEE Transactions on Information Theory*, 43(6):1986–1992, November 1997.

[64] D. Goodman and N. Mandayam. Power control for wireless data. *IEEE Personal Communications*, 7(3):48–54, April 2000.

[65] P. Hande and M. Chiang. Distributed uplink power control for optimal sir assignment in cellular data networks. *Proceedings of IEEE Infocom*, April 2006.

[66] S. Hanly. An algorithm for combined cell-site selection and power control to maximize cellular spread spectrum capacity. *IEEE Journal of Selected Areas in Communications*, 13(7):2796–2815, September 1995.

[67] S. V. Hanly. Congestion measures in DS-CDMA networks. *IEEE Transactions on Communications*, 47(3):426–437, March 1999.

[68] T. Heikkinen. A minimax game of power control in a wireless network under incomplete information. DIMACS Technical Report 99-43, August 1999.

[69] J. D. Herdtner and E. K. P. Chong. Analysis of a class of distributed asynchronous power controlalgorithms for cellular wireless systems. *IEEE Journal of Selected Areas in Communications*, 18(3):436–446, March 2000.

[70] C. J. Ho, J. A. Copeland, C. T. Lea, and G. L. Stuber. On call admission control in DS/CDMA cellular networks. *IEEE Transactions on Vehicular Technology*, 50(6):1328–1343, November 2001.

[71] B. Hochwald and S. Vishwanath. Space-time multiple access: Linear growth in the sum rate. *Proceedings of Allerton Conference on Communication, Control and Computing*, October 2002.

[72] T. Holliday, N. Bambos, A. Goldsmith, and P. Glynn. Distributed power control for time varying wireless networks: optimality and convergence. *Proceedings of Allerton Conference on Communication, Control and Computing*, October 2003.

[73] T. Holliday, A. Goldsmith, P. Glynn, and N. Bambos. Distributed power and admission control for time varying wireless networks. *Proceedings of IEEE Globecom*, November 2004.

[74] M. Hu, J. Zhang, and J. Sadowsky. Traffic aided opportunistic scheduling for downlink transmissions: Algorithms and performance bounds. *Proceedings of IEEE Infocom*, March 2004.

[75] C. Y. Huang and R. Yates. Rate of convergence for minimum power assignment algorithms in cellular radio systems. *Wireless Networks*, 4(4):223–231, June 1998.

[76] J. Huang, R. Berry, and M. L. Honig. A game theoretic analysis of distributed power control for spread spectrum ad hoc networks. *Proceedings of IEEE ISIT*, September 2005.

[77] J. Huang, R. Berry, and M. L. Honig. Performance of distributed utility-based power control for wireless ad hoc networks. *Proceedings of IEEE Milcom*, October 2005.

[78] K. Huang, R. W. Heath, and J. G. Andrews. Joint beamforming and scheduling for sdma systems with limited feedback. *submitted to IEEE Transactions on Communications*, 2007.

[79] M. Huang, R. P. Malhame, and P. E. Caines. Uplink power adjustment in wireless communication systems: a stochastic control analysis. *IEEE Transactions on Automatic Control*, 49(10):1693–1708, October 2004.

[80] M. Huang, R. P. Malhame, and P. E. Caines. Computationally tractable stochastic power control laws in wireless communications. *IEEE Transactions on Automatic Control*, 50(2):263– 268, February 2005.

[81] L. A. Imhof and R. Mathar. The geometry of the capacity region for CDMA systems with general power constraints. *IEEE Transactions on Wireless Communications*, 4(5):2040–2044, September 2005.

[82] S. Jagannathan, M. Zawodniok, and Q. Shang. Distributed power control for cellular networks in the presence of channel uncertainties. *IEEE Transactions on Wireless Communications*, 5(3):540–549, March 2006.

[83] T. Javidi. Decentralized rate assignments in a multi-sector CDMA network. *Proceedings of IEEE Globecom*, December 2003.

[84] H. Ji and C. Huang. Non-cooperative uplink power control in cellular radio systems. *Wireless Networks*, 4(3):233–240, March 1998.

[85] T. Jiang, N. D. Sidiropoulos, and G. B. Giannakis. Kalman filtering for power estimation in mobile communications. *IEEE Transactions on Wireless Communications*, 2(1):151–161, January 2003.

[86] N. Jindal. MIMO broadcast channels with finite rate feedback. *IEEE Transactions on Information Theory*, 52(11):5045–5059, November 2006.

[87] N. Jindal and A. Goldsmith. Dirty paper coding vs. TDMA for MIMO broadcast channels. *Proceedings of IEEE ICC*, June 2004.

[88] N. Jindal, S. Vishwanath, and A. Goldsmith. On the duality of gaussian multiple-access and broadcast channels. *IEEE Transactions on Information Theory*, 50(5):68–78, May 2004.

[89] E. S. Jung and N. H. Vaidya. A power control MAC protocol for ad hoc networks. *Proceedings of International Conference on Mobile Computing and Networking*, September 2002.

[90] D. Kim. On the convergence of fixed-step power control algorithms with binary feedback for mobile communicattion systems. *IEEE Transactions on Communications*, 49(2):249–252, February 2001.

[91] R. Knopp and P. A. Humblet. Information capacity and power control in single-cell multiuser communications. *Proceedings of IEEE ICC*, June 1995.

[92] H. J. Kushner and P. A. Whiting. Convergence of proportional-fair sharing algorithms under general conditions. *IEEE Transactions on Wireless Communications*, 3(4):1250–1259, 2004.

[93] T. Lan, P. Hande, and M. Chiang. Joint beamforming and power control for optimal sir assigment in cellular data networks. *Proceedings of IEEE ISIT*, June 2007.

[94] R. Laroia, S. Uppala, and J. Li. Designing a mobile broadband wireless access network. *IEEE Signal Processing Magazine*, 21:20–28, September 2004.

[95] B.-K. Lee, H.-W. Chen, and B.-S. Chen. Power control of cellular radio systems via robust smith prediction filter. *IEEE Transactions on Wireless Communications*, 3(5):1822–1831, September 2004.

[96] J. Lee, R. Mazumdar, and N. Shroff. Joint power allocation and base station assignment based on pricing for the downlink in multi-class CDMA networks. *Proceedings of IEEE VTC*, October 2003.

[97] J. Lee, R. Mazumdar, and N. Shroff. Joint resource allocation and base-station assignment for the downlink in CDMA networks. *IEEE/ACM Transactions on Networking*, 14(1):1–14, February 2006.

[98] J. W. Lee, R. R. Mazumdar, and N. B. Shroff. Opportunistic power scheduling for dynamic multi-server wireless systems. *IEEE Transactions on Wireless Communications*, 5(6):1506–1515, June 2006.

[99] J.-W. Lee, R. R. Mazumdar, and N. B. Shroff. Joint opportunistic power scheduling and rate control for wireless ad-hoc networks. *IEEE Transactions on Vehicular Technology*, 56(2):801–809, March 2007.

[100] K. K. Leung. Power control by interference prediction for broadband wireless packet networks. *IEEE Transactions on Wireless Communications*, 1(2):256–265, April 2002.

[101] K. K. Leung and C. W. Sung. An opportunistic power control algorithm for cellular network. *IEEE/ACM Transactions on Networking*, 14(3):470–478, June 2006.

[102] K. K. Leung, C. W. Sung, and V. K. Bhargava. An opportunistic power control algorithm with fairness. *Proceedings of IEEE ISIT*, September 2005.

[103] K. K. Leung, C. W. Sung, W. S. Wong, and T. Lok. Convergence theorem for a general class of power-control algorithms. *IEEE Transactions on Communications*, 52(9):1566–1574, September 2004.

[104] K. K. Leung and L. C. Wang. Integrated link adaptation and power control to improve error and throughput performance in broadband wireless packet networks. *IEEE Transactions on Wireless Communications*, 1(4):619–629, October 2002.

[105] X. Lin and N. Shroff. Joint rate control and scheduling in multihop wireless networks. *Proceedings of IEEE CDC*, December 2004.

[106] X. Lin and N. B. Shroff. The impact of imperfect scheduling on cross-layer rate control in wireless networks. *Proceedings of IEEE Infocom*, 2005.

[107] Y. Lin and R. L. Cruz. Power control and scheduling for interfering links. *Proceedings of IEEE ITW*, October 2004.

[108] D. Liu, Y. Zhang, and S. Hu. Call admission policies based on calculated power control setpoints in sir-based power-controlled DS-CDMA cellular networks. *Wireless Networks*, 10(4):473–483, October 2004.

[109] X. Liu, E. K. P. Chong, and N. B. Shroff. Opportunistic transmission scheduling with resource-sharing constraints in wireless networks. *IEEE Journal of Selected Areas in Communications*, 19(10):2053–2064, October 2001.

[110] Y. Liu and E. Knightly. Opportunistic fair scheduling over multiple wireless channels. *Proceedings of IEEE Infocom*, April 2003.

[111] J. Luo, S. Ukulus, and A. Ephremides. Standard and quasi-standard stochastic power control algorithms. *IEEE Transactions on Information Theory*, 51(7):2612–2624, July 2005.

[112] A. B. MacKenzie and S. B. Wicker. Game theory in communications: Motivation, explanation, and application to power control. *Proceedings of IEEE Globecom*, November 2001.

[113] M. Mahmoudi and E. Sousa. Joint power control, base station assignment and sectorization for CDMA cellular systems. *Proceedings of IEEE VTC*, October 2000.

[114] F. Meshkati, M. Chiang, H. V. Poor, and S. C. Schwartz. A game-theoretic approach to energy-efficient power control in multi-carrier CDMA systems. *IEEE Journal of Selected Areas in Communications*, 24(6):1115–1129, June 2006.

[115] F. Meshkati, A. Goldsmith, H. V. Poor, and S. C. Schwartz. A game theoretic approach to energy-efficient modulation in CDMA networks with delay QoS constraints. *IEEE Journal of Selected Areas in Communications*, 25(6):1069–1078, August 2007.

[116] F. Meshkati, D. Guo, H. V. Poor, and S. C. Schwartz. A unified approach to energy-efficient power control in large cdma systems. *To appear in IEEE Transactions on Wireless Communications*, 2008.

[117] F. Meshkati, H. V. Poor, and S. C. Schwartz. Energy-efficient resource allocation in wireless networks. *IEEE Transaction on Signal Processing*, 24(3):58–68, May 2007.

[118] F. Meshkati, H. V. Poor, and S. C. Schwartz. Energy efficiency-delay tradeoffs in multiple-access networks. *To appear in IEEE Transactions on Information Theory*, 2008.

[119] F. Meshkati, H. V. Poor, S. C. Schwartz, and R. Balan. Energy-efficient resource allocation in wireless networks with quality-of-service constraints. *To appear in IEEE Transactions on Communications*, 2008.

[120] F. Meshkati, H. V. Poor, S. C. Schwartz, and N. B. Mandayam. An energy-efficient appraoch to power control and receiver design in wireless data net-

works. *IEEE Transactions on Communications*, 53(11):1885–1894, November 2005.

[121] J. Mo and J. Walrand. Fair end-to-end window-based congestion control. *IEEE/ACM Transactions on Networking*, 8(5):556–567, October 2000.

[122] K. Mukkavilli, A. Sabharwal, E. Erkip, and B. Aazhang. On beamforming with finite rate feedback in multiple-antenna systems. *IEEE Transactions on Information Theory*, 49(2):2562–2579, October 2003.

[123] A. F. Naguib, A. Paulraj, and T. Kailath. Capacity improvement with base-station antenna arrays in cellular CDMA. *IEEE Transactions on Vehicular Technology*, 43(2):691–698, August 1994.

[124] M. J. Neely, E. Modiano, and C. Li. Fairness and optimal stochastic control for heterogeneous networks. *Proceedings of IEEE Infocom*, 2005.

[125] L. Nuaymi and P. Godlewski. Association of uplink power control and base station assignment in cellular CDMA systems. *Proceedings of IEEE Symposium on Computers and Communications*, July 2000.

[126] M. M. Olama, S. M. Djouadi, C. D. Charalambous, and S. Sahyoun. Distributed stochastic power control for time-varying long-term and short-term fading wireless networks. *Proceedings of IEEE American Control Conference*, July 2007.

[127] D. O'Neill, D. Julian, and S. Boyd. Adaptive management of network resources. *Proceedings of IEEE VTC*, October 2003.

[128] S. Papavassiliou and L. Tassiulas. Joint optimal channel base station and power assignment for wireless access. *IEEE/ACM Transactions on Networking*, 4(6):857–872, December 1996.

[129] S. Papavassiliou and L. Tassiulus. Improving the capacity in wireless networks through integrated channel base station and power assignment. *IEEE Transactions on Vehicular Technology*, 47(2):417–427, May 1998.

[130] M. B. Pursley, H. B. Russell, and J. S. Wysocarski. Energy-efficient transmission and routing protocols for wireless multiple-hop networks and spread-spectrum radios. *Proceedings of IABC EuroComm Conference*, May 2000.

[131] L. Qian and Z. Gajic. Variance minimization stochastic power control in CDMA systems. *IEEE Transactions on Wireless Communications*, 5(1):193–202, January 2006.

[132] R. Ramjee, D. Towsley, and R. Nagarajan. On optimal call admission control in cellular networks. *Wireless Networks*, 3(2):29–41, March 1997.

[133] F. Rashid-Farrokhi, K. Liu, and L. Tassiulas. Downlink and uplink capacity enhancement in power controlled cellular systems. *Proceedings of IEEE VTC*, May 1997.

[134] F. Rashid-Farrokhi, K. Liu, and L. Tassiulas. Downlink power control and base station assignment. *IEEE Communications Letters*, 1(4):102–104, July 1997.

[135] F. Rashid-Farrokhi, K. J. R. Liu, and L. Tassiulas. Transmit beamforming and power control for cellular wireless systems. *IEEE Journal of Selected Areas in Communications*, 16(8):1437–1450, October 1998.

[136] F. Rashid-Farrokhi, L. Tassiulas, and K. J. R. Liu. Joint optimal power control and beamforming in wireless networks using antenna arrays. *IEEE Journal of Selected Areas in Communications*, 46(10):1313–1324, October 1998.

[137] R. T. Rockafellar. *Differential Games and Related Topics*. H. W. Kuhn and G. P. Szego, North-Holland, 1971.

[138] Z. Rosberg. Transmitter power control with adaptive safety margins based on duration outage. *IEEE Personal Communications*, 19(1):81–90, October 2004.

[139] Z. Rosberg and J. Zander. Toward a framework for power control in cellular systems. *Wireless Networks*, 4(4):215–222, June 1998.

[140] A. Sampath, P. S. Kumar, and J. M. Holtzman. Power control and resource management for a multimedia CDMA wireless system. *Proceedings of IEEE International Symposium on Personal, Indoor, Mobile Radio Communication*, September 1995.

[141] D. Samuelsson, M. Bengtsson, and B. Ottersten. An efficient algorithm for solving the downlink beamforming problem with indefinite constraints. *Proceedings of IEEE ICASSP*, March 2005.

[142] M. Saquib, R. Yates, and A. Ganti. Power control for an asynchronous multirate decorrelator. *IEEE Transactions on Communications*, 48(5):804–812, May 2000.

[143] C. Saraydar, N. Mandayam, and D. Goodman. Pareto efficiency of pricing-based power control in wireless data networks. *Proceedings of IEEE WCNC*, September 1999.

[144] C. Saraydar, N. Mandayam, and D. Goodman. Power control in a multicell CDMA data system using pricing. *Proceedings of IEEE VTC*, October 2000.

[145] C. U. Saraydar, N. B. Mandayam, and D. J. Goodman. Efficient power control via pricing in wireless data networks. *IEEE Transactions on Communications*, 50(2):291–303, February 2002.

[146] M. Schubert and H. Boche. Solution of the multi-user downlink beamforming problem with individual sir constraints. *IEEE Transactions on Vehicular Technology*, 53(1):18–28, January 2004.

[147] M. Schubert and H. Boche. Iterative multiuser uplink and downlink beamforming under individual sinr constraints. *IEEE Transaction on Signal Processing*, 53(7):2324–2334, July 2005.

[148] M. Sharif and B. Hassibi. On the capacity of MIMO broadcast channels with partial channel state information. *IEEE Transactions on Information Theory*, 51(2):506–522, February 2005.

[149] M. Sharif and B. Hassibi. A comparison of time-sharing, DPC, and bemforming for MIMO broadcast channels with many users. *IEEE Transactions on Communications*, 55(1):11–15, January 2007.

[150] S. Shen, C. J. Chang, C. Huang, and Q. Bi. Intelligent call admission control for wideband CDMA cellular systems. *IEEE Transactions on Wireless Communications*, 3(5):1810–1821, September 2004.

[151] E. H. Shin and D. Kim. Zero-forcing beamforming with semi-orthogonal user selection modified for reducing feedback information. *Asilomar Conference on Signals, Systems and Computers*, October 2006.

[152] V. A. Siris and C. Courcoubetis. Resource control for elastic traffic in CDMA networks. *Proceedings of ACM Mobicom*, September 2002.

[153] V. A. Siris and C. Courcoubetis. Resource control for loss-sensitive traffic in CDMA networks. *Proceedings of IEEE Infocom*, March 2004.

[154] S. Soliman, C. E. Wheatley, and R. Padovani. CDMA reverse link open loop power control. *Proceedings of IEEE Globecom*, December 1992.

[155] L. Song, N. B. Mandayam, and Z. Gajic. Analysis of an up/down power control algorithm for the CDMA reverse link under fading. *IEEE Journal of Selected Areas in Communications*, 19(2):277–286, February 2001.

[156] S. Sorooshyari and Z. Gajic. A robust kalman filtering approach to stochastic power control for time varying wireless networks. *Proceedings of IEEE ICC*, May 2005.

[157] S. Sorooshyari, C. W. Tan, and M. Chiang. Interference-awarepower control for cognitive radio networks. *Submitted to IEEE/ACM Transactions on Networking*, 2007.

[158] Q. Spencer, A. L. Swindlehurst, and M. Haardt. Zero-forcing methods for downlink spatial multiplexing in multiuser MIMO channels. *IEEE Transaction on Signal Processing*, 52(2):461–471, February 2004.

[159] S. Srinivasa and S. A. Jafar. The optimality of transmit beamforming: A unified view. *IEEE Transactions on Information Theory*, 52(4):1558–1564, April 2007.

[160] A. Stolyar. Maximizing queueing network utility subject to stability: Greedy primal-dual algorithm. *Queuing Systems*, 50(4):40–57, August 2005.

[161] A. Subramanian and A. H. Sayed. Joint rate and power control algorithms for wireless networks. *IEEE Transaction on Signal Processing*, 53(11):4204–4214, November 2005.

[162] C. Sung and W. Wong. *Mathematical Aspects of The Power Control Problem in Mobile Communication Systems*. ACM/International Press, New York, 2000.

[163] C. W. Sung. Log-convexity property of the feasible sir region in power-controlled cellular systems. *IEEE Transactions on Communications*, 6(6):248–249, June 2002.

[164] C. W. Sung and W. S. Wong. A distributed fixedstep power control algorithm with quantization and active link quality protection. *IEEE Transactions on Vehicular Technology*, 48(2):553–562, March 1999.

[165] C. W. Sung and W. S. Wong. A noncooperative power control game for multirate CDMA data networks. *IEEE Transactions on Wireless Communications*, 2(1):186–194, January 2003.

[166] T.Alpcan and T.Basar. A hybrid systems model for power control in a multicell wireless data network. *Proceedings of IEEE WiOpt*, March 2003.

[167] C. W. Tan, D. P. Palomar, and M. Chiang. Energy-robustness tradeoff in cellular network power control. *Submitted to IEEE/ACM Transactions on Networking*, 2007.

[168] C. W. Tan, D. P. Palomar, and M. Chiang. Exploiting hidden convexity for flexible and robust resource allocation in cellular networks. *Proceedings of IEEE Infocom*, May 2007.

[169] I. TINEINIS-95. *Mobile Station-base Station Compatibility Standard for Dual-Mode Wideband Spread Spectrum Cellular System*. Telecommunication Industry Association, 1993.

[170] D. M. Topkis. Equilibrium points in nonzero-sum N-person submodular games. *Journal of Control and Optimization*, 17(6):773–778, 1979.

[171] D. Tse and P. Viswanath. *Fundamentals of Wireless Communications*. Cambridge University Press, 2005.

[172] S. Ulukus and R. Yates. Stochastic power control for cellular radio systems. *IEEE Transactions on Communications*, 46(6):784–798, June 1998.

[173] A. Urpi, M. Bonuccelli, and S. Giordano. Modeling cooperation in mobile ad hoc networks: a formal description of selfishness. *Proceedings of IEEE WiOpt*, March 2003.

[174] D. Vengerov, N. Bambos, and H. R. Berenji. A fuzzy reinforcement learning approach to power control in wireless transmitters. *IEEE Transactions on Systems, Man and Cybernetics, Part B*, 35(4):768–778, August 2005.

[175] S. Vishwanath, N. Jindal, and A. Goldsmith. Duality, achievable rates, and sum-rate capacity of gaussian MIMO broadcast channels. *IEEE Transactions on Information Theory*, 49(10):2658–2668, October 2003.

[176] E. Visotsky and U. Madhow. Optimum beamforming using transmit antenna arrays. *Proceedings of IEEE VTC*, May 1999.

[177] P. Viswanath and D. Tse. Sum capacity of the multiple antenna gaussian broadcast channel and uplink-downlink duality. *IEEE Transactions on Information Theory*, 49(8):1912–1921, August 2003.

[178] P. Viswanath, D. N. C. Tse, and R. Laroia. Opportunistic beamforming using dumb antennas. *IEEE Transactions on Information Theory*, 48(6):1277–1293, June 2002.

[179] H. Viswanathan, S. Venkatesan, and H. Huang. Downlink capacity evaluation of cellular networks with known-interference cancellation. *IEEE Journal of Selected Areas in Communications*, 21(6):802–811, June 2003.

[180] B. R. Vojcic and W. M. Jang. Transmitter precoding in synchronous multiuser communication. *IEEE Transactions on Communications*, 46(10):1346–1355, October 1998.

[181] W. Wang, Y. Cui, T. Peng, and W. Wang. Noncooperative power control game with exponential pricing for cognitive radio network. *Proceedings of IEEE VTC*, April 2007.

[182] W. Wang, T. Peng, and W. Wang. Game theoretic analysis of power control for cognitive network in licensed spectrum. *Proceedings of IEEE ChinaCom*, October 2006.

[183] A. Wiesel, Y. C. Eldar, and S. Shamai. Linear precoding via conic optimization for fixed MIMO receivers. *IEEE Transaction on Signal Processing*, 54(3):161–176, January 2006.

[184] C. Wu and D. P. Bertsekas. Distributed power control algorithms for wireless networks. *IEEE Transactions on Vehicular Technology*, 50(2):504–514, March 2001.

[185] Y. Xi and E. M. Yeh. Throughput optimal distributed control of stochastic wireless networks. *Submitted to IEEE/ACM Transactions on Networking*, September 2006.

[186] M. Xiao, N. B. Shroff, and E. K. Chong. Distributed admission control for power-controlled cellular wireless systems. *IEEE/ACM Transactions on Networking*, 9(6):790–800, December 2001.

[187] M. Xiao, N. B. Shroff, and E. K. P. Chong. A utility-based power-control scheme in wireless cellular systems. *IEEE/ACM Transactions on Networking*, 11(2):210–221, April 2003.

[188] W. Yang and G. Xu. Optimal downlink power assignment for smart antenna systems. *Proceedings of IEEE ICASSP*, May 1998.

[189] R. D. Yates. A framework for uplink power control in cellular radio systems. *IEEE Journal of Selected Areas in Communications*, 13(7):1341–1347, September 1995.

[190] T. Yoo and A. Goldsmith. On the optimality of multiantenna broadcast scheduling using zero-forcing beamforming. *IEEE Journal of Selected Areas in Communications*, 24(3):528–541, March 2006.

[191] T. Yoo, N. Jindal, and A. Goldsmith. Finite-rate feedback MIMO broadcast channels with a large number of users. *Proceedings of IEEE ISIT*, July 2006.

[192] T. Yoo, N. Jindal, and A. Goldsmith. Multi-antenna downlink channels with limited feedback and user selection. *IEEE Journal of Selected Areas in Communications*, 25(7):1478–1491, September 2007.

[193] W. Yu. Uplink-downlink duality via minimax duality. *IEEE Transactions on Information Theory*, 52(2):361–374, February 2006.

[194] W. Yu and T. L. and. Transmitter optimization for the multi-antenna downlink with per-antenna power constraints. *IEEE Transaction on Signal Processing*, 55(6):2646–2660, June 2007.

[195] W. Yu, G. Ginis, and J. Cioffi. Distributed multiuser power control for digital subscriber lines. *IEEE Journal of Selected Areas in Communications*, 20(5):1105–115, June 2002.

[196] W. Yu and R. Lui. Dual methods for nonconvex spectrum optimization of multicarrier systems. *IEEE Transactions on Communications*, 54(7):1310–1322, July 2006.

[197] J. Zander. Distributed cochannel interference control in cellular radio systems. *IEEE Transactions on Vehicular Technology*, 41(3):305–311, August 1992.

[198] J. Zander. Performance of optimum transmitter power control in cellular radio systems. *IEEE Transactions on Vehicular Technology*, (1):57–62, February 1992.

[199] H. Zhang, C. S. Chen, and W. S. Wong. Distributed power control for time varying systems: performance and convergence analysis. *IEEE Transactions on Vehicular Technology*, 54(5):1896–1904, September 2005.

[200] J. Zhang and E. Chong. CDMA systems in fading channels: Admissibility, network capacity, and power control. *IEEE Transactions on Information Theory*, 46(3):962–981, May 2000.

[201] T. Zhang, Z. Zeng, C. Feng, J. Zheng, and D. Ma. Utility fair resource allocation based on game theory in ofdm systems. *Proceedings of IEEE International Conference on Computer Communications and Networks*, August 2007.

[202] W. Zhong, Y. Xu, and Y. Cai. Distributed game-theoretic power control for wireless data over MIMO CDMA systems. *Proceedings of IEEE International Conference on Communications, Circuits and Systems*, May 2005.

[203] S. Zhou, Z. Wang, and G. Giannakis. Quantifying the power loss when transmit beamforming relies on finite rate feedback. *IEEE Transactions on Wireless Communications*, 4(4):1948–1957, July 2005.